NONLINEAR INTERACTION OF A SHORT PULSE LASER WITH PLASMAS AND CLUSTERS

A THESIS SUBMITTED TO THE LOVELY PROFESSIONAL UNIVERSITY

FOR THE AWARD OF

DOCTOR OF PHILOSOPHY

IN

PHYSICS

BY

VIKAS NANDA

GUIDE

DR. NITI KANT

DEPARTMENT OF STUDIES IN PHYSICS

LOVELY PROFESSIONAL UNIVERSITY

JANUARY 2015

DECLARATION

I declare that the thesis entitled, NONLINEAR INTERACTION OF A SHORT PULSE LASER WITH PLASMAS AND CLUSTERS, has been prepared by me under the guidance of Dr. Niti Kant, Associate Professor of Physics, Lovely Professional University. No part of the thesis has formed the basis for the award of any degree or fellowship previously.

Vikas Nanda

Department of Physics,
Lovely Professional University,
Phagwara, (Punjab)

DATE:

CERTIFICATE

I certify that Vikas Nanda has prepared his thesis entitled, NONLINEAR INTERACTION OF A SHORT PULSE LASER WITH PLASMAS AND CLUSTERS, for the award of Ph. D. degree of the Lovely Professional University under my guidance. He has carried out the work at the Department of Physics, Lovely Professional University.

Dr. Niti Kant
Department of Physics,
Lovely Professional University,
Phagwara, (Punjab)

DATE:

ABSTRACT

The nonlinear interaction of cosh-Gaussian laser beam and Hermite-cosh-Gaussian laser beam with plasmas and clusters have been studied using WKB and paraxial ray approximations. In chapter-3, sensitiveness of the decentered parameter for relativistic self-focusing of HChG beam in the plasma has been investigated theoretically for mode indices 0, 1 and 2.The results obtained indicate the dependency of the self-focusing of the laser beam on the decentered parameter. The selection of decentered parameter is more sensitive to self-focusing. For the mode indices m=0 & 1, self-focusing becomes stronger and for m=2, self-focusing becomes weaker as the diffraction term becomes more dominant.

In chapter-4, self-focusing of a Hermite-cosh-Gaussian laser beam in magnetoplasma in the presence of density ramp has been observed. Focusing and de-focusing nature of the Hermite-cosh-Gaussian laser beam with decentered parameter and magnetic field has been studied and strong self-focusing is reported. It is investigated that decentered parameter '*b*' plays a significant role for the self-focusing of the laser beam and is very sensitive as in case of extraordinary mode. For mode indices $m = 0, 1 \text{ and } 2$, diffraction term becomes more dominant over nonlinear term for decentered parameter $b = 0$. Also, increase in the value of magnetic field, enhances the self-focusing ability of the laser beam.

In chapter-5, relativistic self-focusing of Hermite-cosh-Gaussian laser beam in plasma under density transition has been studied and enhancement in self-focusing has been observed. It is observed that strong self-focusing occurs as the HChG beam propagates deeper inside the non linear medium as spot size shrinks due to highly dense plasmas. In this chapter, a comparative study between self-focusing of HChG beam in the presence and absence of plasmas density transition is reported.

In chapter-6, self-focusing of a cosh-Gaussian laser beam in collisionless magneto-plasma under plasma density ramp has been studied. The focusing and de-focusing nature of the cosh-Gaussian laser beam with decentered parameter, intensity

parameter, magnetic field, and relative density parameter has been studied and strong self-focusing is reported. Also, a comparative study between Gaussian and cosh-Gaussian beam profile has been reported.

In chapter-7, relativistic self-focusing of cosh-Gaussian laser beam in the cold quantum plasma has been investigated. The comparative study between self-focusing of cosh-Gaussian laser beam in cold quantum case and classical relativistic case has been made for decentered parameter $b = 0$ and it is observed that as the beam propagates deeper inside the cold quantum plasma, the self-focusing ability of the laser beam enhances and shifted towards lower value of normalized propagation distance due to quantum contribution.

In chapter-8, propagation of cosh-Gaussian laser beam in an argon gas embedded with clusters is studied. This laser beam converts the clusters to plasma balls which expand rapidly under Coulomb explosion and hydrodynamic expansion. The dependency of self-focusing on decentered parameter and normalized time has been studied. The present research might be very useful in the applications like the generation of inertial fusion energy driven by lasers, laser driven accelerators, scribing type of applications in electronics etc.

PREFACE

The nonlinear interaction of Hermite-cosh-Gaussian laser beam and cosh-Gaussian laser beam with the plasmas and clusters is studied. In this work, we apply plasma density ramp and the affects of density transition on self-focusing are investigated. Self-focusing ability of an energetic beam in the nonlinear medium is widely studied by researchers and scientists as the converged beam have lot of energy focused at a point. It is very well known that a small convex lens (due to nonlinearity) can focuses the sun light at a point and this energy is sufficient to burn a piece of paper. In the present study an energetic beam gets focused as it propagates deeper into the nonlinear medium and one may have the idea of amount of energy generated in this process. In many socially useful applications like laser driven accelerators, scribing type of applications in electronics, the generation of inertial fusion energy driven by lasers, generation of x-rays etc., high energy is required and hence, self-focusing effect is very useful in these cases. We have focused our attention on enhancing self-focusing effect by the proper selection of various parameters of laser-plasma/cluster interaction. The enhancement in self-focusing of laser beam has been observed and reported in the present study.

I am highly thankful to Dr. Niti Kant for valuable guidance to complete this work. I am highly thankful to my wife and family for their co-operative attitude during the entire period of this work.

Vikas Nanda

TABLE OF CONTENTS

LIST OF FIGURES

CHAPTER-1

INTRODUCTION AND OVERVIEW

1.1 INTRODUCTION

After the discovery of self-focusing of light by Askar'yan in 1962 [1], it become the most fascinating and interesting area of research. The interaction of light with plasma [2-4], cluster [5, 6], liquid [7] etc. has been widely studied by the researchers and scientist due to its socially useful applications like x-ray lasers and the laser driven accelerators [8], the generation of inertial fusion energy driven by laser [9-11], the production of quasi mono-energetic electron bunches [12], optical harmonic generation [13] etc. These applications need the laser pulse to propagate over several Rayleigh lengths in the plasma or cluster without loss of energy. Today, extremely high intensity of the order of 10^{20} W/cm^2 produced by short pulse laser technology enabled various high energy related experiments. Investigators choose the propagation of different kind of laser beams profile like Gaussian beams [4], cosh-Gaussian beams [14], Hermite-Gaussian beams [15], Hermite-cosh-Gaussian beams [16-18] etc. in the plasma.

The non-linearity is accountable for self-focusing of light propagating through the non-linear medium as the velocity of light varies in the non-linear medium which causes the self-focusing effect. The relation between velocity of light in the medium and index of refraction is given as $v = c/n$. where v is velocity of light in medium, c is velocity of light in vacuum and n is the refractive index of the medium. As the ray of light propagates from rarer medium to the denser medium, it bends towards the normal to the surface on which ray of light incident.

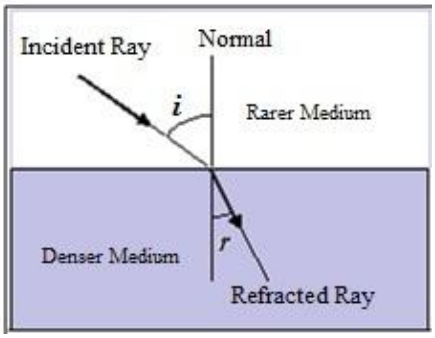

Figure1.1: Refraction of light

Figure1.1 represents the phenomenon of refraction of light as ray of light propagates from rarer medium to denser medium. Similarly, a ray of light propagating from denser to rarer medium bends away from the normal to the surface. This is the fundamental law of physics and is responsible for the converging or diverging of ray of light propagating from rarer to denser or denser to rarer medium respectively. When an intense laser pulse propagates through plasma, the relativistic nonlinearities or ponderomotive nonlinearities or thermal nonlinearities lead to self-focusing of the laser beam. This happens because the plasma density is perturbed by the highly energetic laser beam. Self-focusing/defocusing of laser pulse also occurs in clusters. The interaction of lasers with plasmas, clusters and semiconductors has been a charming field of research for more than fifty years.

Clusters are nanoscale solid density atomic aggregates bound by Vander Waals forces. Their size ranges from 10^2-10^6 atoms. The diameter of the clusters varies in size from a few angstroms to a 1000Å and their density in the gas ranges typically from 10^{11} to 10^{14} clusters/cm^3. Different atomic, molecular and hetero-nuclear species can clubbed together to form clusters. Clusters can be formed by solids, liquids or gaseous atoms, molecules or hetero-nuclear species.

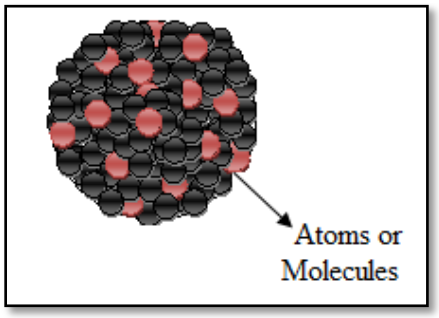

Figure1.2: Atoms or molecules clubbed together by Vander Waals forces to form cluster

Gas-atom clusters are formed when high-pressure flow of a cooled gas into vacuum results in adiabatic cooling and expansion of the gas and particle aggregation [19]. A clustered gas jet typically consists of solid density clusters and low-density background of un-clustered gas atoms. The characteristics of the clustered gas like the

size distribution, number density of clusters and the ratio of clustered to un-clustered atoms or molecules is determined by the backing temperature, pressure, nozzle geometry and other experimental factors. When clusters are irradiated by an intense laser pulse, it absorbs energy and explodes, leaving behind tenuous plasma. The clustered gas has low volume average density but the clusters themselves are at solid density. Due to this strong interaction of individual clusters with the incident laser beam is observed and it also allows the propagation of the laser beam through the clustered gas. The efficient blending of laser energy with the clustered gases [20] makes clustered gases as a unique medium for studying non-linear interaction with laser beams [21] and it can lead to numerous interesting applications.

The laser-heated clusters efficiently generate x-ray [22] and extreme ultraviolet (EUV) radiation [23-27]. Clusters are debris-free, which is an issue with solid targets and the system takes much less space than the conventional synchrotron radiation source. Hence clusters irradiated with strong laser pulses can be used as an easily-renewable, debris-free tabletop radiation source for many applications like X-ray lasers, X-ray and EUV lithography [24] and X-ray tomography [28]. Explosion of clusters in strong laser fields leads to ejection of high energy electrons and energetic charged ions [29, 30]. This opens up the possibility of using energetic particles from laser-irradiated clusters to seed particle accelerators and for proton beam radiation therapy in cancer treatment [31]. Collisions between energetic ions from exploding clusters can produce neutrons via thermonuclear fusion. Laser irradiated clusters can thus be a future tabletop source of thermonuclear neutrons for imaging purposes. The dynamics of exploding clusters gives rise to interesting nonlinear optical effects such as harmonic generation [32] and self-focusing [33]. Clustered gases are also proposed as targets for creating plasma waveguides and their ability of self-guiding of a laser pulse in plasma and plasma channel formation is the field of interest for laser-based particle acceleration schemes.

As the clusters are formed by the combination of atoms or molecules or hetero-nuclear species, so it become necessary and interesting to study the behaviour of these assemblies in strong electromagnetic field and investigating the dynamics of laser-clusters interaction and cluster explosion is always be a problem of great interest. Generally, clusters strongly absorb the energy from laser beams and this property of

clusters makes it useful for various applications as mentioned above. Clustered gases, having properties in between that of solid and gas phase, makes it better absorber of laser beams energy and laser beams propagating through clustered gases generates wonderful nonlinear optical effects like self-focusing of laser beams, modulation of pulse spectrum and higher harmonic generation. The present work is dedicated to the study of the effect of self-focusing in plasmas and clusters.

1.2 SELF-FOCUSING OF LASER BEAM IN PLASMA

When a Gaussian laser beam propagates in non-linear medium, the intensity would be the greatest on the axis of the medium and the index of refraction would be greater on the axis than off the axis of medium. Due to the induced refractive index variations the wave front of the laser acquires a curvature and laser tends to focus. The process is known as self focusing of the beam in a non-linear medium. Self focusing is frequently observed when the radiation produced by femtosecond laser transmits through a number of gases, liquids and solids.

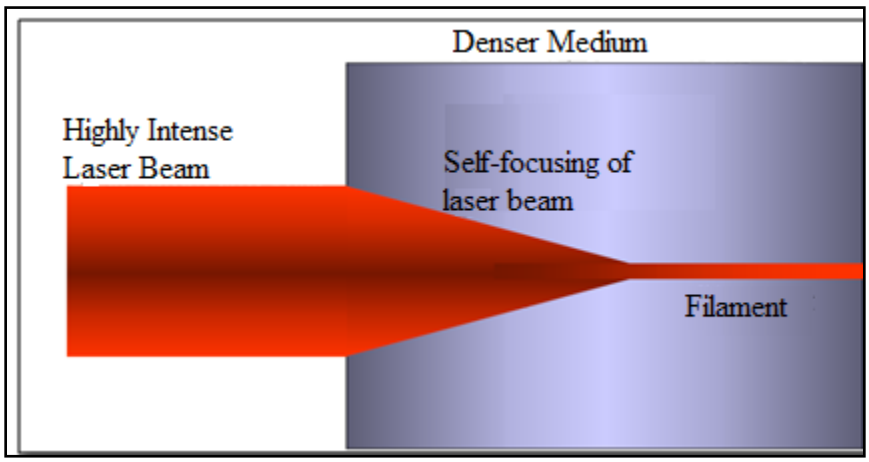

Figure1.3: Observation of self-focusing effect of laser beams propagating deeper into the denser medium

When an intense laser beam propagates through plasma, then the refractive index of the plasma is modified and is composed of a linear and an intensity dependent nonlinear component. Self focusing in plasma can occurs through thermal, relativistic and ponderomotive effects and correspondingly it is called thermal self focusing, relativistic self focusing and ponderomotive self focusing. The availability of high power lasers

attracts the attention and interest of the researcher towards nonlinear laser plasma interactions and harmonic generation. There are certain processes which are not assumed to be of great importance earlier because of low available powers of electromagnetic beams and now, these processes become very important in plasma and cluster and are studied by number of researchers. As a very high power laser beam propagates through the plasma, the electron velocity in plasma may become quite large comparable to the velocity of light in free space. Thus, the effect of variation of mass must be taken in to account and it gives rise to the effect of relativistic self-focusing. The relativistic effect of an intense laser pulse propagation through the plasma leads to self-focusing because the dielectric constant of plasma is an increasing function of the intensity and as the intensity of the pulse increases, the index of refraction of the medium also increases. Also, the ponderomotive force of the focussed laser beam pushes the electrons out of the region of high intensity. It decreases the local electron density and increases the plasma dielectric function and it leads to more self-focusing of the laser beams.

Now a day's researchers focus their attention on the medium with varying density profile. Such medium can be achieved by the application of plasma density ramp. The density of such medium can be assumed to enhance along the direction of propagation of the laser beam. The plasma density ramp plays a very significant role during laser-plasma interaction. A very high power laser beam transmitting through plasma with varying density profile shrinks and can attain a least spot size due to self-focusing effect. After the focusing of the beam, the nonlinear refraction starts dwindling and hence, the beam waist of the laser beam starts increasing. Thus one may observe the self-focusing and defocusing effect of the laser beam with the distance of propagation. In order to get rid from the defocusing of laser beam, one can apply localized upward plasma density ramp. Thus the laser beam obtains a least beam waist and maintains it till longer distance along the direction of propagation. The plasma density ramp could be very useful for the strong self-focusing of a high power laser by the proper selection of laser and plasma parameters. With the increase in plasma density, the self-focusing ability of laser beam becomes stronger because as the laser beam penetrates deeper into the density ramp region, it observes a slowly narrowing channel and thus, in this region, the fluctuating amplitude of the spot size contracts, while its energy enhances. Also, it is well known fact

that the equilibrium electron density is an increasing function of the distance of propagation of the laser beam so the plasma dielectric constant decreases quickly as the beam penetrates deeper inside the medium. Due to it, the self-focusing effect is enhanced and one may observe strong focusing of the laser beam. In case of underdense plasma, the minimum plasma density is chosen. The proper length of plasma density ramp is assumed to avoid the utmost defocusing of the laser beam. But the plasma density should not be considered to be much larger; otherwise, the laser beam can be reflected back and propagation of the laser beam become complicated. So, proper selection of plasma density ramp plays an significant role to make the self-focusing stronger.

The application of magnetic field in the plasma region can affect the self-focusing ability of the laser beam. Thus the study of the propagation of a high power laser beam through plasma with a density ramp where a magnetic field is also present becomes more important and interesting. The collective effect of the plasma density ramp and the magnetic field increases the self-focusing ability of the laser beam in plasma. The beam waist of the laser beam contracts as the beam propagates deeper inside the plasma due to the effect of the plasma density ramp.The application of magnetic field acts as a strong tool to enhance the self-focusing effect of the laser beam during propagation in a plasma density ramp. The simultaneous application of plasma density ramp and magnetic field converge the laser beam strongly. In this kind of experimental model, the laser beam can propagate over a long distance without divergence and hence, this scheme is useful in many laser-driven applications.

1.3 SELF-FOCUSING OF LASER BEAM IN CLUSTER

Self-focusing in clusters is also an important phenomenon to be studied numerically and analytically. If a gas expands out of a nozzle into vacuum, the expanding gas becomes supersaturated and forms condensed molecular beams or cluster beams where the atoms or molecules are held together by Vander Waals forces. An atomic cluster is an intermediate form of matter with particle densities comparable to that of bulk solids. As the highly intense laser beam propagates through the cluster, there occur many non-linear optical effects like self-focusing of laser beams, modulation of pulse spectrum and higher harmonic generation. Since the clusters strongly absorb the energy from laser

beams, so this property of cluster makes it useful for various applications. A highly intense laser converts the clusters into high electron density plasma balls which may expand quickly under hydrodynamic expansion or Coulomb explosion [34, 35]. The electron response to the laser increases in the expanding clusters due to decrease in electron density [36]. It give rise to many exciting phenomena's like self-focusing [33], generation of harmonics and x-rays [22], strong absorption of energy [37], production of energetic neutrons [38] etc. The electrons of each cluster undergo oscillatory displacement and these electrons execute large excursions in the laser and spend a considerable part of time outside the cluster and the cluster acquires a positive charge. Coulomb explosion of these clusters produces energetic ions. A gas containing clusters may also contain free atoms. Our emphasis will be on analytical and numerical study of self-focusing of a short pulse laser in plasmas and clusters.

1.4 TYPES OF SELF-FOCUSING

There are three kinds of self-focusing of light namely relativistic self-focusing, ponderomotive self-focusing and thermal self-focusing. These are briefly defined as below:

1.4.1 Relativistic Self-Focusing

Relativistic self-focusing effect arises due to the variation in the electron density in plasmas caused by the propagating laser pulse of extremely high intensities of the order ranging from 10^{17} - 10^{20} W/cm^2. The high intensity laser pulses provide sufficient energy to the constituents like electrons of the plasma or cluster which cause an electron oscillatory velocity comparable to the velocity of light. Thus the mass of electron, oscillating at relativistic velocities in laser field, increases by a factor given by $\gamma = 1/\sqrt{1-v^2/c^2}$ and give rise to non-linearity due to which the relativistic self-focusing effect occurs.

1.4.2 Ponderomotive Self-Focusing

This kind of self-focusing effect is caused by ponderomotive forces, $F = \left(\omega_p^2/\omega^2\right)\nabla\left(\varepsilon_0 E^2/2\right)$. The ponderomotive force acting on electrons takes place due to

the drifting of the electrons in an inhomogeneous field and the interaction of drift velocity of electron with the magnetic field. The electrons undergo strong repulsion from the region of maximum intensity to the region of minimum intensity due to the action of ponderomotive forces and it decreases the local concentration of electrons density in plasma. It increases the plasma dielectric function and laser beams become more self-focused in plasma.

1.4.3 Thermal Self-Focusing

Thermal self-focusing occurs due to the thermal heating of the medium. It occurs due to collisional heating of plasma exposed to high energy laser beams. The high energy laser beams increases the temperature and the increased temperature causes an expansion which causes to an increase of refraction index of the medium. The variation in refractive index of the medium gives rise to nonlinear effects. Thus a laser beam propagating through this medium undergoes strong self-focusing.

CHAPTER-2

REVIEW OF LITERATURE

2.1 LITERATURE REVIEW

The interaction of electromagnetic wave with matter has been extensively studied by researchers due to its socially useful applications. Self focusing of laser beams in plasmas and clusters have many useful applications in the field of science and technology viz laser fusion-schemes, laser driven plasma accelerators, x-rays productions etc. So from past few decades laser beam becomes interesting and fascinating area of research.

Askar'yan (1962) firstly predicted that a powerful radiation propagating through a medium converges or diverges due to different nonlinear processes occurring in the medium. Askar'yan observes the energy momentum flux density of the laser beam at self-focusing. At this location the whole plasma has been expelled and the pressure is balanced by the plasma pressure profile acting against the centre of the laser beam. He compares the necessary optical intensities for compensating the gas dynamic pressure.

Akhmanov et al. (1968) studied the self-focusing and diffraction of light in a nonlinear medium. They studied the concept of convergence of light and divergence of light in a nonlinear medium by applying geometic optics approach. Diffraction corrections to the self-focusing length, formation of proper optical waveguide, nonstationary processes, stimulated scattering in liquids, self-focusing and parametric amplification etc. are being studied by them in detail.

Hora (1969) worked on the self-focusing of laser beams in plasma by ponderomotive forces. He treated the process of self-focusing in plasma propagated by a laser beam at a time when the plasma has been produced. The ponderomotive forces accelerate the plasma in the radial direction of the beam and this creates a lower density in the centre regions. They use the condition of equilibrium between the ponderomotive and hydrostatic forces and evaluate a minimum laser power from the conditions of total reflection and diffraction. For cut-off density and a plasma temperature of about 10eV, the focusing of radiation within the first minima of diffraction sets a lower limit to the laser power which is of the order of 1MW for the usual lasers.

Litvak (1970) studied the self-focusing of electromagnetic beams in magnetoactive plasma for the case of longitudinal propagation. The nonlinearity mechanisms for the magnetoactive plasma have been studied and expressions are obtained for the nonlinear corrections to the refractive index due to the striction, heating, and nonlinear motion of a single electron. They have obtained the necessary condition for self-focusing and determined the characteristic parameters for self-focusing of the beam.

Sodha et al. (1971) studied the propagation and focusing of an electromagnetic wave in inhomogeneous dielectrics. They concluded that the focusing length is enhanced in a medium where the dielectric constant is a decreasing function of axial distance of propagation. Similarly, the focusing length is reduced in a medium where the dielectric constant is an increasing function of axial distance of propagation.

Ashkin et al. (1973) studied radiation pressure on a free liquid surface. They focused laser pulse on the free surface of a transparent liquid dielectric to study the force of radiation pressure. It is observed that light pulse entering or leaving the liquid surface exerts a net outward force and this force causes strong surface lens effect, surface scattering and nonlinear absorption.

Askar'yan (1973) studied the self-focusing effect of light propagating through a medium and reported that the self-focusing effect consists in a decrease of the divergence or to an increase in the convergence of powerful radiation in a medium, owing to different nonlinear processes. All the varieties of self-focusing are the consequences of such a change in the divergence or convergence.

Sodha et al. (1973) studied that as a strong Gaussian laser beam propagates through the medium, then the dielectric constant of the strongly ionized plasma varies and it give rise to nonlinearity. They concluded that this nonlinearity arises due to the heating and redistribution of the electrons. This self-induced non-linearity causes self-focusing and oscillatory waveguide propagation of the laser beam even when the non-linear dielectric constant does not fall in the saturating range. In a typical case of a 10^{10} W laser, the enhancement of axial intensity by a factor of 25 has been predicted in a length of 0.6cm.

Brueckner et al. (1974) studied the laser driven fusion. The intense laser light is used to bring about thermonuclear reactions in plasma. They reported the detailed analytical and computational results which show the possibility of laser-driven fusion.

Sodha et al. (1974) studied the self-focusing/defocusing of a laser beam in a non-linear dielectric. In this case, they assume that the laser is operating in the TEM_{01} doughnut mode. They concluded that the cylindrical symmetry of the irradiance distribution enhances inside the medium and the power gets concentrated around the points of maximum irradiance. The maximum irradiance in different directions occurs at different values of the distance from the z-axis.

Sodha et al. (1974) studied the self-focusing of a cylindrically symmetric Gaussian electromagnetic pulse in collision-less and collisional plasmas. They assumed that nonlinearity arises due to the ponderomotive force and the non-uniform heating of the medium. They considered that the duration of pulse is larger than the characteristic time of non-linearity and found that the beam is focused in a moving filament. Because of relaxation effects the peak of the pulse is shifted to higher values in case of collisional plasmas and the pulse is severely distorted because of self-focusing so the shift of peak in the case of collision-less plasmas is not significant.

Hora (1975) studied the theory of relativistic self-focusing of laser radiation in plasmas and reported that laser beam at irradiances higher than 1/500 of the relativistic threshold propagating through plasma undergoes self-focusing due to relativistic dependence of the optical constants on laser irradiance. Further, this self-focusing effect enhances the refractive index of the medium. In prepulsed plasmas, formed by Nd-glass laser pulses of $3\times10^{16} W/cm^2$, relativistic diffraction-limited self-focusing can generate relativistic electron oscillation energies and hence pair production.

Sodha et al. (1975) studied thermal self-focusing and defocusing of a laser beam in an absorbing dielectric. They considered that the laser is operating in the TEM_{01} mode and observed that when the refractive index decreases with increasing temperature, the electromagnetic energy converges in the x-direction and diverges in the y-direction. However reverse is the case when the refractive index increases with increasing temperature. Also, they observed that the energy of the beam concentrated around a circular ring of maximum irradiance in case of geometric-optics self-focusing of laser

beams operating in the doughnut mode and mixed TEM_{00} and TEM_{10} cylindrical modes oscillating in phase opposition.

Siegrist (1976) studied self-focusing in plasma due to ponderomotive forces and relativistic effects. The propagation of intense laser pulses in a plasma discussed in terms of a constant shape, paraxial-ray approximation. He investigated self-focusing due to ponderomotive forces and relativistic effects. It is found that the stationary self-focusing behaviour of each mechanism treated separately similar with several orders of magnitude difference in critical power. In stationary self-focusing due to the combined mechanisms, complete saturation of ponderomotive self-focusing prevents the occurrence of relativistic effects. Self focusing lengths and minimum radii are given for a large range of beam powers. A characteristic focal spot radius is found which depends only on the plasma density.

Nayyar (1978) studied the self focusing of a high power non-Gaussian laser beam operating in TEM_{01} mode in strongly ionized plasma. It is found that when the power of the beam exceeds the critical power, focusing effects are observed in Y-direction, whereas divergence of the beam takes place in the X-direction and in the reverse case the normalized beam width parameter f_2 first increases in Y-direction, after penetrating a certain depth it reaches a broadened maxima and then starts decreasing with the distance of propagation inside the medium. The beam continues diverging in the X-direction. Nayyar further found that absorption brings about a reduction in the extent of self focusing.

Nayyar et al. (1979) studied the self-focusing and defocusing of elliptically shaped Gaussian laser beams in collisional and collision-less plasmas. They found that the non-linear dependence of the dielectric constant inside a collision-less plasma is due to the ponderomotive force and inside a collisional plasma, it is due to inhomogeneous heating of energy carriers. Further they found that the beam gets focused at different points in different planes, exhibiting the effect of astigmatism. In certain power regions considered, the beam converges or diverges in both the directions, while in some other regions of the power spectrum one dimension of the beam converges while the other diverges.

Askar'yan et al. (1981) studied the nonlinear defocusing of a focused beam and observed a fine beam from the focus zone. They have used a single-mode, unmodulated neodymium laser with energy of 1J and with a millisecond pulse and a YAG-Nd laser in operating single and high frequency millisecond-pulse repetition modes and experimentally explained the defocusing nature of the beam in the weakly absorbing nonlinear medium.

Hegana (1981) studied the nucleation and growth of clusters in expanding nozzle flows. The nozzle flows have been used for many years both as a source to obtained microscopic clusters of some ten to some thousand molecules and as a test bed to study nucleation and growth of clusters. They summarize the experimental and theoretical knowledge of producing cluster beams. The gas dynamics of expanding nozzle flows and gives detailed formulas for the axisymmetric and plane free jets and for different ratios of specific heats. The conventional approach of condensation theory is shown not to give a self-consistent description of the condensation process in expanding flows, but progress in the direction of a rigorous theory is to be expected at least for Vander Waals molecules. Finally, a discussion of the kinetics of cluster growth is used to derive scaling laws which correlate the available cluster beam data and allow predicting results under different experimental conditions for pure gases and for gas mixtures.

Jones et al. (1982) studied density modification and energetic ion production at relativistic self-focusing of laser beams in plasmas. They have described a two dimensional time dependent laser plasma interaction code and used it to model the interaction between 5ps Nd glass laser beam of peak power 10^{13}W and a 35 times ionized tin target. They have observed that the nonlinear forces modified the plasma density. Further, highly accelerated tin ions having maximum energy of 5GeV are observed.

Mori et al. (1988) studied the self focusing of intense electromagnetic waves in a very under dense plasma in computer simulations. Mori *et al.* found that initially relativistic self focusing occurs and it is then followed by the ponderomotive blowout and filamentation at the edge of the channel walls. The self focusing is more intense for resonant double frequency than the single frequency illumination.

Kurki et al. (1989) studied the relativistic and ponderomotive self-focusing of an intense optical beam in plasma. They have obtained the steady-state asymptotic solution

of beam propagation in a localized solitary waveform in slab geometry and also presented the solutions for the beam profile where it is oscillatory in nature, which correspond to the presence of the steady-state solution of a multiple-beamlet profile.

Cicchitelli et al. (1990) studied the longitudinal field components for laser beams in vacuum. The discovery of Lax, Louisell, and Knight (LLK) that electromagnetic beams in vacuum do have a longitudinal component can be proved experimentally from the polarization independence of the energy of electrons from the focus of a laser. They have developed the LLK paraxial approximation to a Maxwellian exact solution for a Gaussian beam and included the exact longitudinal field components of the laser beam.

Brandi et al. (1993) studied the transmission of a high-irradiance laser beam in plasma whose optical index depends non-linearly on the light intensity. The relativistic decrease of the plasma frequency and the ponderomotive expelling of the electrons are the nonlinear effects studied by this group. The focusing and defocusing effects of a beam assumed to remain cylindrical and for plasma supposed homogeneous along the propagation direction but radially inhomogeneous with a parabolic density profile.

Chen et al. (1993) derived a set of three dimensional equations for the propagation of an intense laser pulse of arbitrary strength $a = eA/mc^2$ **(**where A is the magnetic vector potential of the laser pulse**)** in cold underdense plasma. In different limits, these equations can be reduced to certain previous one dimensional model. Chen *et al.* found that for $|a| < 1$, an approximate set of equations from the averaged Lagrangian is obtained. They solved the axisymmetric two dimensional model equations numerically to show the effect of dispersion in the self focusing process.

Chen et al. (1993) studied the propagation of a short intense laser pulse in underdense cold plasma. When no electron cavitation is present, a global invariant '*H*' is obtained and Chen et al. studied its relation with self-focusing of laser pulse. For relativistic self-focusing, $H<0$ is a sufficient and necessary condition. For relativistic and ponderomotive self-focusing, $H<0$ is a sufficient but not necessary. Chen et al. have performed the numerical simulations to confirm these conditions.

Bulanov et al. (1995) studied that an ultra-short, relativistically strong pulse can be self-focused in plasma with strong magnification of its amplitude and channelling in a

narrow channel shaped like a "bullet". Plasma turbulence occurs in the region occupied by the pulse and behind it and leads to electron heating. It is found that a regular longitudinal electric field is produced in the wake of a wide pulse shorter than the plasma wave period and behind the shape edge of a long pulse. The transverse nonuniformity of the pulse causes the formation of horseshoe structures that can be used to focus and accelerate electrons and protons. Hence fast and strong modulation of the pulse occurs by the induced focusing of the EM radiation.

Ditmire et al. (1995) observed the strong x-ray emission from high-temperature plasmas produced by intense irradiation of clusters. They observed that enhanced absorption of the laser light by the dense cluster results in the production of high ion charge states and hence it give rise to the emission of strong x-ray from the hot plasma.

Feng et al. (1995) produced plasmas using a target consists of an in-vacuum flowing stream of liquid water droplets and then measured its extreme ultraviolet (EUV) emission spectrum. Using such kind of target, no debris related effects are observed. They have reported a new type of target for laser plasma x-ray generation.

Ditmire et al. (1996) concluded that large clusters produced in expanding gas jets can be used to produce hot, moderate density plasmas with intense, short pulse laser. This group investigated that thermal plasmas created by the enlightenment of clusters by femtosecond pulses of 10^{16}-10^{17} W/cm^2 dominates the plasma kinetics, generating emission from high charge states that can last for several nanoseconds. They found that cluster-heated plasma acts as a source of x-ray radiation.

Donnelly et al. (1996) studied high order harmonic generation in atom clusters. In this study they used high pressure gas jet to produce clusters containing about 1000 atoms. They reported the generation of short-wavelength, high-order harmonics of intense laser radiation from atom clusters.

Gibbon et al. (1996) experimentally studied the relativistic self-focusing and self-channeling of a terawatt laser pulse $(0.7TW \le P \le 15TW)$ in underdense plasma. The results are obtained with picosecond $(\tau = 1ps)$ and $(\tau = 0.4ps)$ subpicosecond pulses and self-guiding of subpicosecond pulses is observed for $P \approx P_c$, where P_c is the critical power for self-focusing. Using a paraxial envelope model describing the laser propagation and taking account the plasma response to the ponderomotive force, it is shown that a

maximum laser intensity of $5-15$ times that reached in vacuum may be achieved when P is in the $(1.25-4)\times P_c$ range.

Shao et al. (1996) studied multi-keV electron generation in the interaction of intense laser pulses with Xe clusters. They have observed the generation of multi-keV electrons as intense femtosecond laser pulse propagates through the Xe clusters. They have also observed electron kinetic energy distribution consists of a warm peak of energy between 0.1 and 1keV and a hot peak of energy between 2 and 3 keV.

Ditmire et al. (1997) studied the atomic clusters in ultrahigh intensity light fields. He explained the theory of laser cluster interaction and observes that the cluster starts to expand on the time scale of the laser. Due to this expansion, the electron density of the medium is supposed to decrease. Ditmire found that Xe cluster microplasma with a temperature of $\approx 2keV$ and an average charge state $Z=20,$ will expand with a kinetic energy of around $50keV$. This observed energy value is found to be agreeing with the average ion energy observed in the experiments. He also explained the generation of high order harmonics in gases of clusters.

Ditmire et al. (1999) studied the nuclear fusion from explosions of femtosecond laser heated deuterium clusters. They have reported that interaction of intense laser beams with clusters can produce superheated microplasma that ejects high energy ions having energy of the order of 1MeV. They have observed 10^5 fusion neutrons per joule of incident laser energy. They have reported the nuclear fusion from the explosions of deuterium clusters heated with a laser pulse.

Glenn et al. (1999) reported a high average power extreme UV source based on a laser plasma cluster jet that can be used for EUV lithography. A cooled supersonic nozzle expansion is used to produce a dense beam of Xe-cluster which will act as a plasma target. A highly intense laser beam interacts with this cluster beam.In the firet phase of EUV power scale-up, the continuous cluster jet has been integrated with a 200W laser driver operating at repetition rates upto 500Hz. In the second phase, the jet is being integrated with a 1700W diode-pumped solid state laser driver operating at repetition rates up to 6000Hz.

Asthana et al. (2000) studied the relativistic self-focusing of a Gaussian laser beam propagating through a non linear medium with intensity dependent dielectric constant. They have studied self-focusing of the propagated laser beam using Wentzel-Kramers-Brillouin (WKB) approximation and Paraxial approximation and the numerical calculations for various parameters of laser plasma interaction suggests that self-focusing of the laser beam occurs strongly.

Belafhal et al. (2000) studied the propagation properties of Hermite-cosh-Gaussian laser beams through an aperture lens and free space. They have studied the relative intensity allocation of the Hermite-cosh-Gaussian beams propagating through the free space for different values of the decentered parameter and also reported the normalised intensity plots of the Hermite-cosh-Gaussian beam profiles for the propagation through an aperture lens for various values of the truncation parameter for mode indices $m = 1$ and 2.

Hafizi et al. (2000) studied that a powerful laser beam focused on plasma can be stably guided by a combination of relativistic focusing and ponderomotive channeling over extended distances. Hafizi *et al.* described an envelope equation for the laser spot size that can be used to describe the axial evolution of the spot size as a function of the ratio of laser power P to the critical power for relativistic focusing P_c and depending on the initial beam spot size and divergence, the envelope or radius of a laser beam that is incident on a plasma will oscillate with propagation distance provided that P/P_c should be more than one. This envelop equation is valid for arbitrary laser intensity within the long pulse, quasi-static approximation and neglects instabilities. They analyzed that a significant contraction of the spot size is possible for laser powers exceeding the critical power for relativistic self-focusing and hence it leads to corresponding increase in intensity of laser beam. Thus ponderomotive channeling can significantly lead to enhancement of the focusing effect.

Liu et al. (2000) studied the laser frequency up-shift, self-defocusing and ring formation in tunnel ionizing gases and plasmas. In their work the collective effects of tunnel ionization of gases on laser frequency up-shift, defocusing and ring formation are considered self-consistently. A high intensity laser beam causes quick tunnel ionization of a gas and the plasma density is found to be enhanced. The high intensity laser beam

decreases the refractive index near the axis of the beam and due to this the laser beam gets defocused. The defocusing of the beam decreases the ionization rate and frequency up-shift. They found that the trailing portion of the propagating beam forms ring shape distribution due to stronger defocusing of the on axis part of the laser beams than the off-axis part of the laser beams.

Osman et al. (2000) presented the numerical programming of self-focusing at laser plasma interaction. They have studied the forces and optical properties causing self-focusing of the laser beam. They have developed a numerical program in $C++$ that incorporates the ponderomotive force and relativistic effects which cause self-focusing of the laser beam. This devolped programme has been used to explore the self-focusing over a wide range of parameters.

Springate et al. (2000) studied the explosion of atomic clusters irradiated by a sequence of two high-intensity laser pulses. It is observed by experiments and numerical calculations that heating efficiency of atomic clusters can be increased by using two high intensity laser beams of different frequencies. They have calculated the ion energies from Xe clusters irradiated with two high intensity femtosecond laser beams of frequencies 780nm and 390nm (second harmonic) respectively.

Feit et al. (2001) studied the description of powerful beam self focusing in underdense plasma. They emphasized on the total electron evacuation under the effect of ponderomotive forces. Feit *et al.* demonstrated that a laser beam can be self channeled by underdense plasma if the laser intensity is high enough to produce electron cavitations. It is studied that cavitation results in suppression of filamentation and the possibility to channel power well above the nominal critical power of self focusing for a distance of many Rayleigh lengths.

Krainov et al. (2002) studied the interaction of the super intense femtosecond laser beam with clusters. They investigated multiple inner and outer ionization and X-ray emission followed by explosion in clusters irradiated by a laser field. They have analyzed the increase in temperature of the electron in this process and also, of the charge of the ionized cluster. They have also analyzed the expansion and decay of the cluster during the propagation of laser beam as well as after the propagation of the laser beam.

Zweiback et al. (2002) studied the nuclear fusion from femtosecond laser-driven explosions of deuterium clusters. They irradiate deuterium clusters with a $35\,fs$ laser pulse and found that the fusion neutron yield is strongly dependent on such factors as cluster size, laser focal geometry and deuterium gas jet parameters. They found that the various measured scalings indicate that a Coulomb explosion model of the ion energy is a good description of the ion explosion. Further, from the experiments they give the detailed understanding of how the laser deposits its energy and heats the deuterium cluster plasma.

Weaver et al. (2003) used a spectrometer to study the spatial distribution of soft x-ray radiation from low atomic number elements like carbon. Weaver *et al.* recorded the soft x-ray emission as a function of the target material and target orientation with respect to the incident laser beam and line of sight of the spectrometer. Weaver *et al.* found that inferred plasma expansion velocities are slightly higher than those previously reported.

Zharova et al. (2003) studied analytically and numerically the self-focusing of laser radiation in plasma with ionized gaseous clusters and proposed an electrodynamic model for cluster plasma in a field of ultra-short laser pulse. It is shown that, for a laser power exceeding the self-focusing critical power, the wave field self-compression occurs in a medium with dispersion of any type (normal, anomalous, or combined). Further, due to the dependence of the characteristic nonlinear field on the size of ionized cluster, the corresponding processes occur faster than in a homogenous medium and it give rise to the ultra-short pulses.

Issac et al (2004) studied the interaction of ultrashort laser pulses with krypton clusters at intensity up to 1.3×10^{18} Wcm^{-2}. Intense Kα and Kβ emission from krypton at 12.66 and 14.1 KeV, respectively, has been observed using conventional solid state x-ray detectors. The measured x-ray spectra have broad bremsstrahlung continuum reaching to photon energies up to 45 KeV, with evidence that approximately 10% of electrons that are heated to very high electron temperatures, which is consistent with a two-temperature electron distribution. This is ascribed to the presence of a hot electron population, similar to that found in laser–solid interactions. Issac *et al.* observed that the highest laser energy to x-ray conversion efficiency is 9.2×10^{-7}, which is equivalent to 45 nJ x-ray pulse energy from the 12.66 KeV krypton Kα transition.

Jha et al. (2004) investigated the relativistic and ponderomotive effects on laser plasma interaction dynamics. They studied the combined effect of relativistic and ponderomotive nonlinearities on the propagation characteristics and modulation instability of a laser beam propagating through partially stripped plasma. Further, they found that the non linearity arising due to ponderomotive force tends to defocus the laser beam as against the nonlinear relativistic self-focusing phenomenon. Also the current density perturbation arising due to ponderomotive nonlinearity combined with relativistic nonlinearity tends to increase the modulation instability of the laser beam.

Kant et al. (2004) studied that second harmonic in plasma is generated by a Gaussian laser beam in the presence of a magnetic wiggler of suitable period. The phase matching conditions for the process of satisfied for a specific value of the Wiggler period. The intensity of the second harmonic pulse is enhanced by self-focusing of the fundamental pulse. The harmonic undergoes periodic focusing in the plasma channel formed by the fundamental wave. The normalized second harmonic amplitude changes periodically with distance with successive maxima acquiring higher values.

Sharma et al. (2004) studied the self-focusing of electromagnetic beams in collisional plasmas in the presence of nonlinear absorption. They considered the nonlinear absorption by the medium to observe the effect of self-focusing of electromagnetic waves. Further they employed a complex eikonal which does not need any approximation about the relative magnitudes of the real and imaginary parts of the dielectric constant or their dependence on the irradiance of the beam. They found that the nonlinearity in absorption tends to cancel the effect of divergence due to diffraction effect. They found that the beam-width and attenuation of the laser beam depends on distance of propagation of the laser beam in the medium considered.

Kant et al. (2005) studied that a plane parallel laser beam incident on a cylindrical dielectric fibre perpendicular to the axis of the fibre, focuses to small dimension as it approaches the axis. The focusing effect is enhanced by nonlinear self-focusing in the dielectric. For a specific laser intensity and for given radius of the fibre, the beam focuses on the axis of the fibre. In the axial region however, the high intensity of the laser leads to tunnel ionization and optical breakdown of the dielectric which causes electron-hole pair

production and plasma formation in the form of capillary and the plasma tends to self-defocus the laser.

Prakash et al. (2005) studied the focusing of an intense Gaussian laser beam in a radially inhomogeneous medium and investigated the steady-state focusing and defocusing of the laser beam. They have discussed the nonlinear refractive index in detail and obtained the coupled differential equation for beam width parameter, absorption parameter and nonlinearity parameter. The numerical solution of these equations for a typical set of values of various parameters yields the dependence of the beam width and axial irradiance on the distance of propagation.

Varsheney et al. (2005) studied the relativistic self-focusing of a laser beam in inhomogeneous plasma. The nonlinearity in the dielectric constant arises due to the relativistic variation of mass for an arbitrary magnitude of intensity. They have evaluated the variations of the beam width parameter with the propagation distance, the self-trapping condition and the critical power of the beam. It was seen that the laser beam width tends to attain a constant value depending upon the plasma inhomogeneity and the initial laser intensity. Numerical estimates are made for typical values of the laser–plasma interaction applicable for underdense and overdense plasmas.

Kumar et al. (2006) studied the self focusing of laser pulse through a tunnel ionizing helium gas in both relativistic and non-relativistic regimes, relaxing the near-axis approximation. In the non-relativistic regime, the laser pulse produces multiple ionization of the gas and faces strong defocusing due to the steep radial density gradient caused by the same. The uneven defocusing of paraxial and marginal rays leads to a beam acquiring a ring shaped intensity distribution. In the relativistic regime, the laser pulse produces fully ionized plasma within a few wave periods, subsequently the relativistic mass effect and the ponderomotive force induced electron cavitation cause periodic self-focusing.

Shukla et al. (2006) studied nonlinear wave interactions in quantum magnetoplasma. They have considered nonlinear interactions involving electrostatic upper-hybrid, ion-cyclotron, lower-hybrid and Alfven waves in quantum magnetoplasmas. The quantum hydrodynamical equations are used to find the coupled equations for nonlinearity. The equations are then Fourier analyzed to obtain the nonlinear dispersion relations.

Sodha et al. (2006) studied the mutual focusing/defocusing of Gaussian electromagnetic beams in collisional plasma. They have considered the mutual focusing/defocusing of a number of coaxial Gaussian electromagnetic beams in singly ionized collisional plasma which is initially in thermal equilibrium. They started from the expression of the electron temperature in terms of the irradiance of the waves and derived expressions for the electron density and the dielectric function. The coupled wave equations corresponding to different beams have been solved in the paraxial approximation to obtain a system of coupled second-order differential equations for the beam width parameters. They also solved coupled equations for the widths of two beams numerically for some typical cases and correspondingly the critical curves for the two beams have also been obtained. They published the results for plasmas in thermal equilibrium and also for day-time mid-latitude ionosphere at a height of 150 km.

Gupta et al. (2007) introduced upward density ramp in underdence plasma. It is found that as a result of relativistic mass nonlinearity and wake field generation, the laser becomes self-focused in the underdense plasma and attains a minimum spot size. If there is no density ramp, the laser is defocused beyond this distance due to the dominance of the diffraction effect. To reduce this defocusing, an upward density ramp is introduced.

Gupta et al. (2007) studied the additional focusing of a high-intensity laser beam in a plasma with a density ramp and a magnetic field and investigated that the spot size of the beam decreases as the beam penetrates into the plasma due to the presence of density ramp and magnetic field. Further, they reported that density ramp and magnetic field not only reduce the spot size of the laser beam but also maintain it with only a mild ripple over several Rayleigh lengths.

Hora (2007) studied new aspects for fusion energy using inertial con-finement. H. Hora has reported very high ion current density space charge neutral plasma blocks interacting as pistons to ignite DT may lead to a new scheme of laser fusion with low cost energy generation.

Konar et al. (2007) investigated the propagation characteristics of a cosh-Gaussian laser beam both in Kerr and cubic quintic nonlinear media. It is found that these beams are unstable and convert into sech/Gaussian type beam. At high power cosh-Gaussian laser beam form flat top beam and the length of the flat top and sharpness of

flatness increase with the increase in power. It is observed that at very high power, the beam first splits into two and then again combines to form a single beam. This process continues repeatedly.

Liu et al. (2007) studied the laser self-focusing and nonlinear absorption in expanding clusters. An intense laser beam propagating through clustered gas converts the clusters into plasma balls. The cluster expands under hydrodynamic pressure and it leads to non uniform refractive index profile. The variation in refractive index leads to self-focusing of laser beams.

Misra et al. (2007) studied the nonplanar ion-acoustic waves in quantum plasma. The nonlinear properties of ion-acoustic waves in electron–ion quantum plasma with the effects of quantum corrections are studied in a nonplanar spherical geometry. For this purpose Misra *et al*. have applied quantum hydrodynamic model.

Wei et al. (2007) studied quantum ion-acoustic waves in single-walled carbon nanotubes applying quantum hydrodynamic model. Wei *et al.* have considered the electrons and ion components of the nanotubes as two species quantum plasma system. The quantum hydrodynamic model is used by Wei *et al.*

Zhang et al. (2007) identified the virtual sources for a cosh-Gaussian beam. On the basis of superposition of beams, they have identified a group of virtual sources that generate a cosh-Gaussian wave. A closed-form expression is derived for this cosh-Gaussian wave, which, in the appropriate limit, yields the paraxial approximation for the cosh-Gaussian beam. From this expression, the paraxial approximation and the nonparaxial corrections of all orders for the corresponding paraxial cosh-Gaussian beam are determined.

Crouseilles et al. (2008) studied quantum hydrodynamic model for the nonlinear electron dynamics in thin metal films. They have applied Wigner-Poisson equations to derive quantum hydrodynamic model to investigate the ultrafast electron dynamics in thin metal films. The ultrafast nonlinear electron dynamics is investigated and the results so obtained are then compared to recent semiclassical results obtained with a Vlasov-Poisson approach.

Patil et al. (2008) studied the propagation of Hermite-cosh-Gaussian laser beams in a non-degenerate germanium having space charge neutrality for the first three mode

indices. They have obtained the differential equation for beam width parameters by applying parabolic wave equation approach under paraxial approximation and analytical solutions are obtained under the condition $R_n < R_d$, where R_n and R_d are the self-focusing length and diffraction length respectively. They examined the behaviour of beam width parameter with normalized propagation distance numerically for various values of decentered parameter.

Jung et al. (2009) studied the quantum effects on magnetization due to ponderomotive force in cold plasmas. It is shown that the ponderomotive force of the electromagnetic wave induces the magnetization and cyclotron motion in quantum plasmas and the magnetic field would not be induced without the quantum effects in plasmas. It is also found that the quantum effect enhances the cyclotron frequency due to the ponderomotive force related to the time variation of the field intensity.

Parashar (2009) studied the effect of self-focusing on laser third harmonic generation in a clustered gas. The propagation of intense Gaussian laser beam through a gas embedded with atomic clusters produces nanoplasma medium which causes self-focusing of laser beam. This propagating laser beam produces third harmonic due to nonlinear response of electron. The hydrodynamic model of cluster expansion is applied. It is observed that self-focusing of the laser increases the efficiency of harmonic generation by ten times.

Patil et al. (2009) studied the self-focusing of cosh-Gaussian laser beams in a parabolic medium with linear absorption and reported the field distribution in the medium in terms of beam width parameter, decentered parameter and absorption coefficient. The differential equation for beam width parameter has been developed by using WKB approximation and paraxial approximation. The behaviour of beam width parameter with normalized propagation distance is studied at various values of decentered parameter with different absorption levels in the medium.

Sadighi-Bonabi et al. (2009) introduced the ellipsoid model to describe bubble acceleration of electrons. In the experimental work, they have focused a 20TW power and 30fs laser pulse on a pulsed He-gas jet. They have focused the laser pulse in the best matched point above the nozzle gas to obtain a stable ellipsoid bubble. They have found that in the ellipsoid cavity regime, the quality of the electron beam is improved as

compared to other methods like plasma channel guided acceleration, periodic plasma wakefield, spherical cavity regime. Further, it is observed that the trajectory of electron motion can be hyperbola, parabola or ellipsoid and is influenced by the position and energy of the electrons and electrostatic potential of the cavity.

Yazdani et al. (2009) studied the interaction of terawatt, higher power and picoseconds laser pulses with plasmas. They have studied, numerically, how the necessary nonlinear force accelerated plasma blocks may reach the highest possible thickness by using optimized dielectric properties of the irradiated plasma. The use of double Rayleigh initial density profiles results in many wavelength thick low reflectivity directed plasma blocks of modest temperatures. The results of computations with the genuine two-fluid model are presented.

Patil et al. (2010) studied the focusing of Hermite-cosh-Gaussian laser beam in collisionless magnetoplasma considering the ponderomotive nonlinearity. They have presented the dynamics of the combined effects of nonlinearity and spatial diffraction and to highlight the nature of focusing, plot between beam-width parameter and dimensionless distance of propagation has been obtained. The effect of mode index and decentered parameter on the self-focusing of the beams has been discussed.

Singh et al. (2010) studied the relativistic self-focusing and self-channeling of Gaussian laser beam in plasma. They have solved the non-linear differential equation for the beam width parameter of the main beam by using moment theory approach and solved it numerically by using Runge-Kutta method and reported strong self-focusing of laser beam for different values of intensity parameter and relative density parameter.

Shukla et al. (2010) studied the nonlinear aspects of quantum plasma physics. The nonlinear aspects of wave-wave and wave-electron ineractions in dense quantum plasma are studied theoretically. They have studied nonlinear electrostatic electron and ion plasma waves, novel aspects of 3D quantum electron fluid turbulence, nonlinearly coupled intense electromagnetic waves, localized plasma wave structures and phase space kinetic structures and mechanisms that can generate quasi-stationary magnetic fields in dense quantum plasmas. They have discussed the influence of the external magnetic field and the electron angular momentum spin on the electromagnetic wave dynamics.

Thakur et al. (2010) studied self-focusing and defocusing of twisted light in non linear medium. A light beam carrying angular momentum is called as twisted light. The differential equation for beam width parameter is obtained by applying the Wentzel-Kramers-Brillouin and the paraxial approximations. The focusing of beam and its dependence on beam's parameters is studied analytically with the help of numerical calculations.

Xiong et al. (2010) studied the influence of arbitrary outside magnetic field on self-focusing of short intense laser pulse propagating in underdense and magnetized cold plasma. Xiong *et al.* set the outside magnetic field in yz-plane and used the angle between y-axis and outside magnetic field. Xiong *et al.* reported that larger the angle between y-axis and outside magnetic field, weaker is the effect of self-focusing. The strengthening of the outside magnetic field enhances the relevant effect of self-focusing.

Bergamin et al. (2011) studied the kerr nonlinearity in detail and the concept of transformation optics is applied to solve the problem in nonlinear electrodynamics. The transformation optics based engineering of self-interaction effects is studied in detail by Bergamin *et al.* They applied the transformation optics on self-focusing effect of laser beam.

Gill et al. (2011) studied the propagation characteristics of cosh-Gaussian laser beam in magnetoplasma using relativistic nonlinearity and expressed the field distribution in the medium in terms of beam width parameter and decentered parameter. They have studied the self-phase modulation and self-trapping of the laser beam under variety of parameters. Further, effect of magnetic field on the self-focusing of the laser has also been reported.

Kant et al. (2011) studied the ponderomotive self-focusing of a short pulse in underdense plasma under a plasma density ramp. The pulse may acquire a minimum spot size due to the ponderomotive self-focusing and then defocusing of the beam starts. They have applied the upward plasma density ramp to overcome the defocusing of the beam and so that the minimum spot size may be maintained to longer distance of propagation of the laser beam.

Kim et al. (2011) studied the effect of the density ramp structure on the electron energy in laser wakefield acceleration. They have reported that with a downward density

ramp, the electron energy decreased due to a lag in the acceleration region and to the acceleration field strength being lower than that with a uniform density, but with an upward ramp, the energy increased because of the higher acceleration field and the position of the acceleration region. These effects were studied by using simulations with a 2-dimensional particle-in-cell code and by experiments using a 20TW laser.

Patil et al. (2011) studied the relativistic self-focusing of cosh-Gaussian laser beams in a plasma. The differential equation for beam width parameter is obtained by using WKB and paraxial approximations. They have studied the effect of decentered parameter of the laser pulse on self-focusing of the beam and reported strong self-focusing of the laser beam.

Yang et al. (2011) studied the energy enhancement for deuteron beam driven fast ignition of a precompressed inertial confinement fusion target. The deuteron beam driven fast ignition is considered by Yang *et al.* because it provides hot spot ignition spark and also provides bonus fusion energy through reactions in the targets. It is observed that 30% of extra energy can be obtained from deuterons with 1MeV initial energy and 12% from deuterons with 3MeV initial energy. The focused beam helps in energy gain.

Habibi et al. (2012) applied density ramp profile in the medium and study stationary self-focusing of intense laser beam in cold plasma. They have found that presence of upward ramp density profile and quantum effects causes better focusing of laser beam in cold plasma than that of for classical relativistic case. It is observed that after initial focusing of laser beam, the relativistic effect and quantum effect becomes more dominant in the medium of increasing density and enhances the self-focusing effect.

Kant et al. (2012) studied the self-focusing of Hermite-Gaussian laser beams in plasma. They have applied the plasma density ramp to overcome the defocusing and to enhance the self-focusing of the laser beam and reported stronger self-focusing of the laser beam with propagation distance by choosing the appropriate laser and plasma parameters. Further, the laser beam attains a minimum spot size and maintains it with only a mild ripple.

Nanda et al. (2013) studied the sensitiveness of decentered parameter for relativistic self-focusing of Hermite-cosh Gaussian laser beam in plasma and reported

that the selection of decentered parameter is very sensitive as small change in its value greatly changes the self-focusing ability of the laser beam. Further, self-focusing of laser beam is found to be stronger for mode indices $m=0$ and 1 than that of for $m=2$ due to the dominance of diffraction term over focusing term in the beam width parameter equation.

Nanda et al. (2013) applied density ramp to study the self-focusing of Hermite-cosh Gaussian laser beam in the presence of magnetic field. The application of density ramp profile in the medium and presence of magnetic field increases the self-focusing ability of the laser beam greatly. Also, they have reported that decentered parameter plays a vital role to enhance the self-focusing effect of the laser beam.

Patil et al. (2013) studied the self-focusing of Gaussian laser beam in relativistic cold quantum plasma. The beam width parameter equation is obtained by applying WKB and paraxial approximation. In the present case, expression for dielectric constant is taken to be $\varepsilon = 1 - \omega_p^2 \left(1 - \partial q / \gamma\right)^{-1} / \gamma\omega^2$. It is observed from the results reported by them that quantum effect enhances the self-focusing ability of the laser beam significantly than classical relativistic case.

CHAPTER-3

SENSITIVENESS OF DECENTERED PARAMETER FOR RELATIVISTIC SELF-FOCUSING OF HERMITE-COSH-GAUSSIAN LASER BEAM IN PLASMA

3.1 INTRODUCTION

The interaction of light with matter is one of the basic phenomena in nature. The advancement in the short pulse laser technology have enabled experiments using laser pulses focused to extremely high intensity of the order of 10^{20} W/cm^2. Self-focusing of laser beams in plasmas [2, 3, 16, 58, 61, 88] becomes one of the most interesting and fascinating field of research for several decades due to its various applications like the generation of inertial fusion energy driven by lasers [9, 10, 11], optical harmonic generation [13], the production of quasi mono-energetic electron bunches [12], x-ray lasers and the laser driven accelerators [8]. These applications need the laser pulse to propagate over several Rayleigh lengths in the plasmas without loss of energy.

In the plasma three types of self-focusing mechanism occur namely Relativistic, ponderomotive and thermal self-focusing as the laser pulse propagate through it. The dielectric constant of plasma changes greatly with the increase in intensity of the laser beam and it leads to the self-focusing of the beam [15, 85]. The variation in the electron density [89] in plasmas is caused by the propagating laser pulse of extremely high intensities of the order ranging from 10^{17} - 10^{20} W/cm^2. These high intensity laser pulses provide sufficient energy to the constituents like ions, electrons etc. of the plasmas which causes an electron oscillatory velocity comparable to the velocity of light. Thus the mass of electron, oscillating at relativistic velocities in laser field, increases and give rise to non-linearity due to which the relativistic self-focusing effect occurs. The theory of relativistic self-focusing of laser radiation in plasmas has been studied by Hora [88]. Self-focusing in a plasma due to ponderomotive forces and relativistic effects has been studied by Siegrist [3]. Relativistic self-focusing and self-channeling of Gaussian laser beam has been, recently, reported by Singh *et al.* by applying moment theory approach to solve the

non-linear differential equation for beam width parameter and then solved it numerically by Runge-Kutta method [82].

Recently, theoretical investigators focus their attention on paraxial wave family of laser beams. Hermite-cosh-Gaussian beam is one of the solutions of paraxial wave equation and such HChG beam can be obtained in the laboratory by the superposition of two decentered Hermite-Gaussian beams as Cosh-Gaussian ones. Propagation of Hermite-cosh-Gaussian beams in plasmas has been studied theoretically earlier by Belafhal *et al.* [16]; Patil *et al.* [17, 18]. The focusing of HChG laser beams in magneto-plasma by considering ponderomotive nonlinearity has been theoretically examined by Patil *et al.* [81] and reported the effect of mode index and decentered parameter on the self-focusing of the beams.

The present work is dedicated to the study of the sensitiveness of decentered parameter for relativistic self-focusing of HChG beams in plasmas. We derive the equations for beam width parameter for HChG beam and solve them numerically by applying Wentzel-Kramers-Brillouin (WKB) approximation and Paraxial approximation [4, 90] for mode index 0, 1 and 2 and observed the enhancement in the self-focusing of the laser beams as the beam width parameter decreases with the normalized distance for the optimum sensitive values of decentered parameter. For the sake of simplicity only the transversal components of laser field are evaluated and longitudinal components are not taken in to consideration in the present paper. However, longitudinal components should be taken for an exact formulation, while dealing with nonlinear phenomenon [52].

3.2 FIELD DISTRIBUTION OF HCHG LASER BEAMS

The field distribution of HChG laser beams propagating in the plasma along z-axis is of the following form:

$$E(r,z)=\frac{E_0}{f(z)}\left[H_m\left(\frac{\sqrt{2}r}{r_0 f(z)}\right)\right]Exp\left[\frac{b^2}{4}\right]\left\{Exp\left[-\left(\frac{r}{r_0 f(z)}+\frac{b}{2}\right)^2\right]+Exp\left[-\left(\frac{r}{r_0 f(z)}-\frac{b}{2}\right)^2\right]\right\} \quad \ldots (3.1)$$

Here $E(r,z)$ is the amplitude of HChG laser beam for the central position at $r = z = 0$. $f(z)$ is the dimensionless beam width parameters, H_m is the Hermite polynomial of m^{th} order, r_0 is the spot size of the beam and b is the decentered parameter of the beam.

3.3 NON-LINEAR DIELECTRIC CONSTANT

The dielectric constant for the non-linear medium (collision-less plasma) is obtained by applying the approach given by Sodha *et al.* [4]:

$$\varepsilon = \varepsilon_0 + \phi\left(EE^*\right) \quad \ldots (3.2)$$

With $\varepsilon_0 = 1 - \omega_P^2/\omega^2$, $\omega_P^2 = 4\pi\, n_0 e^2/m$, $m = m_0\gamma$, $\omega_P^2 = \omega_{P0}^2/\gamma$, $\omega_{P0}^2 = 4\pi\, n_0 e^2/m_0$ and $\gamma = 1/\sqrt{1 - v^2/c^2}$

here 'ε_0' and 'ϕ' represent the linear and non-linear parts of the dielectric constant respectively, 'ω_{P0}' is the plasma frequency, 'e' is the electronic charge, 'm' is the rest mass of the electron, 'ω' is the frequency of the incidents laser beam and 'n_0' is the equilibrium electron density.

In case of collision-less plasma, ponderomotive force causes the non-linearity in the dielectric constant and hence non-linear part of the dielectric constant can be written as [4]:

$$\phi\left(EE^*\right) = \frac{\omega_{P0}^2}{\gamma\omega^2}\left(1 - Exp\left[-\frac{3m_0\gamma\alpha_1 EE^*}{4M}\right]\right) \quad \ldots (3.3)$$

With $\alpha_1 = e^2 M/6m_0^2\gamma^2\omega^2 k_b T_0$, here '$M$' is the mass of the scatterer in the plasma, 'k_b' is the Boltzmann constant and 'T_0' is the equilibrium plasma temperature.

3.4 EVOLUTION OF BEAM WIDTH PARAMETER

For isotropic, non-conducting and non-absorbing medium with $\mu = 1$, Maxwell's equation are:

$$\vec{\nabla} \times \vec{H} = \frac{1}{c}\frac{\partial \vec{D}}{\partial t} \quad \ldots (3.4a)$$

$$\vec{\nabla} \times \vec{E} = -\frac{1}{c}\frac{\partial \vec{H}}{\partial t} \quad \ldots (3.4b)$$

$$\vec{\nabla} \cdot \vec{D} = 0 \quad \ldots (3.4c)$$

$$\vec{\nabla} \cdot \vec{B} = 0 \quad \ldots (3.4d)$$

Taking curl of equation (3.4b),

$$\vec{\nabla} \times \vec{\nabla} \times \vec{E} = -\frac{1}{c}\frac{\partial}{\partial t}\left(\vec{\nabla} \times \vec{H}\right)$$

Substituting the value of $(\vec{\nabla} \times \vec{H})$ from equation (3.4a) and applying vector identity, $\vec{A} \times \vec{B} \times \vec{C}$, we get

$$\vec{\nabla}\left(\vec{\nabla} \cdot \vec{E}\right) - \vec{E}\left(\vec{\nabla} \cdot \vec{\nabla}\right) = -\frac{1}{c}\frac{\partial}{\partial t}\left(\frac{1}{c}\frac{\partial \vec{D}}{\partial t}\right)$$

$$\vec{\nabla}\left(\vec{\nabla} \cdot \vec{E}\right) - \nabla^2 \vec{E} = -\frac{1}{c^2}\frac{\partial^2 \vec{D}}{\partial t^2}$$

$$-\nabla^2 \vec{E} + \frac{1}{c^2}\frac{\partial^2 \vec{D}}{\partial t^2} + \vec{\nabla}\left(\vec{\nabla} \cdot \vec{E}\right) = 0 \quad \ldots (3.5)$$

From equation (3.4c),

$$\vec{\nabla} \cdot \vec{D} = 0$$

$$\vec{\nabla}\left(\varepsilon \vec{E}\right) = 0$$

Here 'ε' is a variable quantity, thus we have,

$$\varepsilon \vec{\nabla} \cdot \vec{E} + \vec{E}\vec{\nabla} \cdot \varepsilon = 0$$

$$\vec{\nabla} \cdot \vec{E} = -\frac{\vec{E}\vec{\nabla} \cdot \varepsilon}{\varepsilon}$$

Thus equation (3.5) becomes,

$$-\nabla^2 \vec{E} + \frac{1}{c^2}\frac{\partial^2 \vec{D}}{\partial t^2} + \vec{\nabla}\left(-\frac{\vec{E}\vec{\nabla} \cdot \varepsilon}{\varepsilon}\right) = 0$$

$$\nabla^2\vec{E} - \frac{\varepsilon}{c^2}\frac{\partial^2\vec{E}}{\partial t^2} + \vec{\nabla}\left(\frac{\vec{E}\vec{\nabla}\cdot\varepsilon}{\varepsilon}\right) = 0 \qquad \ldots (3.6)$$

Consider a plane polarized wave with electric field vector along y-axis, propagating in the z-direction, the solution of equation (3.6) is given by,

$$\vec{E} = \hat{j}E_0 Exp\left[i(\omega t - kz)\right] \qquad \ldots (3.7)$$

where $\hat{j}$ is the unit vector along y-direction.

Differentiating equation (3.7) twice, w. r. t. 't' , we get

$$\frac{\partial\vec{E}}{\partial t} = i\omega\ \hat{j}E_0 Exp\left[i(\omega t - kz)\right]$$

$$\frac{\partial^2\vec{E}}{\partial t^2} = -\omega^2\,\hat{j}E_0 Exp\left[i(\omega t - kz)\right]$$

$$\frac{\partial^2\vec{E}}{\partial t^2} = -\omega^2\vec{E} \qquad \ldots (3.8)$$

Thus equation (3.6) becomes,

$$\nabla^2\vec{E} - \frac{\varepsilon}{c^2}\left(-\omega^2\vec{E}\right) + \vec{\nabla}\left(\frac{\vec{E}\vec{\nabla}\cdot\varepsilon}{\varepsilon}\right) = 0$$

$$\nabla^2\vec{E} + \frac{\varepsilon}{c^2}\omega^2\vec{E} + \vec{\nabla}\left(\frac{\vec{E}\vec{\nabla}\cdot\varepsilon}{\varepsilon}\right) = 0$$

$$\nabla^2\vec{E} + k^2\vec{E} + \vec{\nabla}\left(\frac{\vec{E}\vec{\nabla}\cdot\varepsilon}{\varepsilon}\right) = 0 \qquad \left(\because k^2 = \varepsilon\frac{\omega^2}{c^2}\right)$$

$$\nabla^2\vec{E} + k^2\vec{E} + \left[-\vec{E}\left(\frac{\vec{\nabla}\varepsilon}{\varepsilon}\right)^2 + \vec{E}\left(\frac{\nabla^2\varepsilon}{\varepsilon}\right)\right] = 0$$

$$\nabla^2\vec{E} + \left[k^2 - \left(\frac{\vec{\nabla}\varepsilon}{\varepsilon}\right)^2 + \left(\frac{\nabla^2\varepsilon}{\varepsilon}\right)\right]\vec{E} = 0$$

$$\nabla^2\vec{E} + \left[k^2 + \vec{\nabla}\left(\frac{\vec{\nabla}\varepsilon}{\varepsilon}\right)\right]\vec{E} = 0$$

$$\nabla^2\vec{E} + \left[k^2 + \nabla^2(\ln\varepsilon)\right]\vec{E} = 0$$

$$\nabla^2\vec{E} + k^2\left[1 + \frac{1}{k^2}\nabla^2(\ln\varepsilon)\right]\vec{E} = 0 \qquad \ldots (3.9)$$

If $\left(1/k^2\right)\nabla^2(\ln\varepsilon) << 1$, then,

$$\nabla^2\vec{E} + k^2\vec{E} = 0$$

In cylindrical co-ordinate system, we can write this equation as

$$\frac{\partial^2\vec{E}}{\partial z^2} + \frac{\partial^2\vec{E}}{\partial r^2} + \frac{1}{r}\frac{\partial\vec{E}}{\partial r} + \varepsilon\frac{\omega^2}{c^2}\vec{E} = 0 \qquad \ldots (3.10)$$

For slowly converging or diverging cylindrically symmetric beam, the solution of equation (3.10) is of the following form,

$$\vec{E} = A(r,z)Exp[i(\omega t - kz)] \qquad \ldots (3.11)$$

with $k^2 = \varepsilon_0\,\omega^2/c^2 = \omega^2/c^2\left(1 - \omega_{P0}^2/\gamma\omega^2\right)$.

Differentiating equation (3.11) twice w. r. t. 'r' and 'z', we get

$$\frac{\partial\vec{E}}{\partial r} = Exp[i(\omega t - kz)]\frac{\partial A(r,z)}{\partial r}$$

$$\frac{\partial^2\vec{E}}{\partial r^2} = Exp[i(\omega t - kz)]\frac{\partial^2 A(r,z)}{\partial r^2}$$

And

$$\frac{\partial\vec{E}}{\partial z} = -ikA(r,z)Exp[i(\omega t - kz)] + Exp[i(\omega t - kz)]\frac{\partial A(r,z)}{\partial z}$$

$$\frac{\partial^2\vec{E}}{\partial z^2} = -k^2A(r,z)Exp[i(\omega t - kz)] - 2ikExp[i(\omega t - kz)]\frac{\partial A(r,z)}{\partial z} + Exp[i(\omega t - kz)]\frac{\partial^2 A(r,z)}{\partial z^2}$$

Substituting these values in equation (3.10), we get

$$-k^2A(r,z)Exp[i(\omega t - kz)] - 2ikExp[i(\omega t - kz)]\frac{\partial A(r,z)}{\partial z} + Exp[i(\omega t - kz)]\frac{\partial^2 A(r,z)}{\partial z^2} +$$

$$Exp[i(\omega t - kz)]\frac{\partial^2 A(r,z)}{\partial r^2} + \frac{1}{r}Exp[i(\omega t - kz)]\frac{\partial A(r,z)}{\partial r} + \left(\varepsilon_0 + \phi\left(AA^*\right)\right)\times$$

$$\frac{\omega^2}{c^2}A(r,z)Exp[i(\omega t - kz)] = 0$$

$$-k^2 A(r,z) - 2ik\frac{\partial A(r,z)}{\partial z} + \frac{\partial^2 A(r,z)}{\partial z^2} + \frac{\partial^2 A(r,z)}{\partial r^2} + \frac{1}{r}\frac{\partial A(r,z)}{\partial r} + \varepsilon_0 \frac{\omega^2}{c^2} A(r,z) +$$

$$\phi\left(AA^*\right)\frac{\omega^2}{c^2} A(r,z) = 0$$

$$-k^2 A(r,z) - 2ik\frac{\partial A(r,z)}{\partial z} + \frac{\partial^2 A(r,z)}{\partial z^2} + \frac{\partial^2 A(r,z)}{\partial r^2} + \frac{1}{r}\frac{\partial A(r,z)}{\partial r} + k^2 A(r,z) +$$

$$\phi\left(AA^*\right)\frac{\omega^2}{c^2} A(r,z) = 0$$

Neglecting $\frac{\partial^2 A(r,z)}{\partial z^2}$, we get

$$-2ik\frac{\partial A(r,z)}{\partial z} + \frac{\partial^2 A(r,z)}{\partial r^2} + \frac{1}{r}\frac{\partial A(r,z)}{\partial r} + \frac{\phi\left(AA^*\right)}{\varepsilon_0} k^2 A(r,z) = 0 \qquad \ldots (3.12)$$

To solve equation (3.12), we express

$$A(r,z) = A_{0p}(r,z) Exp\left[-ikS(r,z)\right] \qquad \ldots (3.13)$$

Here A_{0p} and S are the real functions of $'r'$ and $'z'$.

Differentiating equation (3.13) twice, w. r. t. $'r'$, we get

$$\frac{\partial A(r,z)}{\partial r} = A_{0p} Exp\left[-ikS(r,z)\right](-ik)\frac{\partial S(r,z)}{\partial r} + Exp\left[-ikS(r,z)\right]\frac{\partial A_{0p}}{\partial r}$$

$$\frac{\partial^2 A(r,z)}{\partial r^2} = -ikA_{0p} Exp\left[-ikS(r,z)\right]\frac{\partial^2 S(r,z)}{\partial r^2} - k^2 A_{0p} Exp\left[-ikS(r,z)\right]\left(\frac{\partial S(r,z)}{\partial r}\right)^2 -$$

$$2ikExp\left[-ikS(r,z)\right]\frac{\partial S(r,z)}{\partial r}\frac{\partial A_{0p}}{\partial r} + Exp\left[-ikS(r,z)\right]\frac{\partial^2 A_{0p}}{\partial r^2}$$

Now differentiating equation (3.13) w. r. t. $'z'$,

$$\frac{\partial A(r,z)}{\partial z} = -ikA_{0p} Exp\left[-ikS(r,z)\right]\frac{\partial S(r,z)}{\partial z} + Exp\left[-ikS(r,z)\right]\frac{\partial A_{0p}}{\partial z}$$

Thus equation (3.12) becomes,

$$2ik\left(-ikA_{0p}Exp\left[-ikS(r,z)\right]\frac{\partial S(r,z)}{\partial z}+Exp\left[-ikS(r,z)\right]\frac{\partial A_{0p}}{\partial z}\right)$$

$$=Exp\left[-ikS(r,z)\right]\left(\begin{array}{l}-ikA_{0p}\dfrac{\partial^2 S(r,z)}{\partial r^2}-k^2A_{0p}\left(\dfrac{\partial S(r,z)}{\partial r}\right)^2-2ik\dfrac{\partial S(r,z)}{\partial r}\dfrac{\partial A_{0p}}{\partial r}\\ +\dfrac{\partial^2 A_{0p}}{\partial r^2}-i\dfrac{kA_{0p}}{r}\dfrac{\partial S(r,z)}{\partial r}+\dfrac{1}{r}\dfrac{\partial A_{0p}}{\partial r}+\dfrac{k^2A_{0p}\phi\left(A_{0p}^2\right)}{\varepsilon_0}\end{array}\right)$$

$$2k^2A_{0p}\frac{\partial S(r,z)}{\partial z}+2ik\frac{\partial A_{0p}}{\partial z}$$

$$=-ikA_{0p}\frac{\partial^2 S(r,z)}{\partial r^2}-k^2A_{0p}\left(\frac{\partial S(r,z)}{\partial r}\right)^2-2ik\frac{\partial S(r,z)}{\partial r}\frac{\partial A_{0p}}{\partial r}+\frac{\partial^2 A_{0p}}{\partial r^2}$$

$$-i\frac{kA_{0p}}{r}\frac{\partial S(r,z)}{\partial r}+\frac{1}{r}\frac{\partial A_{0p}}{\partial r}+\frac{k^2A_{0p}\phi\left(A_{0p}^2\right)}{\varepsilon_0}$$

$$\frac{\partial^2 A_{0p}}{\partial r^2}+\frac{k^2A_{0p}\phi\left(A_{0p}^2\right)}{\varepsilon_0}-k^2A_{0p}\left(\frac{\partial S(r,z)}{\partial r}\right)^2-ik\left(A_{0p}\frac{\partial^2 S(r,z)}{\partial r^2}+2\frac{\partial S(r,z)}{\partial r}\frac{\partial A_{0p}}{\partial r}\right)$$

$$=2k^2A_{0p}\frac{\partial S(r,z)}{\partial z}+2ik\frac{\partial A_{0p}}{\partial z}+i\frac{kA_{0p}}{r}\frac{\partial S(r,z)}{\partial r}-\frac{1}{r}\frac{\partial A_{0p}}{\partial r}$$

Comparing real and imaginary parts of equation (3.14), we get

Real part equation is

$$\frac{\partial^2 A_{0p}}{\partial r^2}+\frac{k^2A_{0p}\phi\left(A_{0p}^2\right)}{\varepsilon_0}-k^2A_{0p}\left(\frac{\partial S(r,z)}{\partial r}\right)^2=2k^2A_{0p}\frac{\partial S(r,z)}{\partial z}-\frac{1}{r}\frac{\partial A_{0p}}{\partial r}\qquad\ldots(3.14)$$

$$2\frac{\partial S(r,z)}{\partial z}+\left(\frac{\partial S(r,z)}{\partial r}\right)^2$$

$$=\frac{1}{k^2}\left[\frac{1}{2A_{0p}^2}\frac{\partial^2 A_{0p}^2}{\partial r^2}-\frac{1}{4A_{0p}^4}\left(\frac{\partial A_{0p}^2}{\partial r}\right)^2+\frac{1}{2A_{0p}^2r}\frac{\partial A_{0p}^2}{\partial r}\right]+\frac{\phi\left(A_{0p}^2\right)}{\varepsilon_0}\qquad\ldots(3.15)$$

Imaginary part equation is

$$-k\left(A_{0p}\frac{\partial^2 S(r,z)}{\partial r^2}-2\frac{\partial S(r,z)}{\partial r}\frac{\partial A_{0p}}{\partial r}\right)=2k\frac{\partial A_{0p}}{\partial z}+\frac{kA_{0p}}{r}\frac{\partial S(r,z)}{\partial r}$$

$$2\frac{\partial A_{0p}}{\partial z}+\frac{A_{0p}}{r}\frac{\partial S(r,z)}{\partial r}+A_{0p}\frac{\partial^2 S(r,z)}{\partial r^2}+2\frac{\partial S(r,z)}{\partial r}\frac{\partial A_{0p}}{\partial r}=0$$

Multiplying by A_{0p}

$$2A_{0p}\frac{\partial A_{0p}}{\partial z}+\frac{A_{0p}^2}{r}\frac{\partial S(r,z)}{\partial r}+A_{0p}^2\frac{\partial^2 S(r,z)}{\partial r^2}+2A_{0p}\frac{\partial S(r,z)}{\partial r}\frac{\partial A_{0p}}{\partial r}=0$$

$$\frac{\partial A_{0p}^2}{\partial z}+\frac{\partial S(r,z)}{\partial r}\frac{\partial A_{0p}^2}{\partial r}+A_{0p}^2\left[\frac{\partial^2 S(r,z)}{\partial r^2}+\frac{1}{r}\frac{\partial S(r,z)}{\partial r}\right]=0 \qquad \ldots (3.16)$$

For initially Hermite-cosh-Gaussian beam, the solution of equation (3.15) and (3.16) are of the form

$$A_{0p}^2=\frac{E_0^2}{f^2(z)}\left[H_m\left(\frac{\sqrt{2}r}{r_0 f(z)}\right)\right]^2 Exp\left[\frac{b^2}{2}\right]$$

$$\left\{Exp\left[-2\left(\frac{r}{r_0 f(z)}+\frac{b}{2}\right)\right]+Exp\left[-2\left(\frac{r}{r_0 f(z)}-\frac{b}{2}\right)\right]+2Exp\left[-\left(\frac{2r^2}{r_0^2 f^2(z)}+\frac{b^2}{2}\right)\right]\right\} \qquad \ldots (3.17)$$

And

$$S(r,z)=\frac{r^2}{2}\beta(z)+\varphi(z) \qquad \ldots (3.18)$$

with, $\beta(z)=\left(1/f(z)\right)\partial f/\partial z.$ where $'\varphi(z)'$ is an arbitrary function of $'z'$.

For $m=0$, $\left[H_m\left(\frac{\sqrt{2}r}{r_0 f(z)}\right)\right]^2=1$

$$\therefore\ A_{0p}^2=\frac{E_0^2}{f^2(z)}Exp\left[\frac{b^2}{2}\right]$$

$$\left\{Exp\left[-2\left(\frac{r}{r_0 f(z)}+\frac{b}{2}\right)^2\right]+Exp\left[-2\left(\frac{r}{r_0 f(z)}-\frac{b}{2}\right)^2\right]+2Exp\left[-\left(\frac{2r^2}{r_0^2 f^2(z)}+\frac{b^2}{2}\right)\right]\right\} \qquad \ldots (3.19)$$

Differentiating equation (3.18) w. r. t. $'z'$ and $'r'$ respectively,

$$\frac{\partial S(r,z)}{\partial z}=\frac{r^2}{2}\frac{\partial \beta}{\partial z}+\frac{\partial \varphi}{\partial z}$$

$$\frac{\partial S(r,z)}{\partial z} = \frac{r^2}{2f(z)}\frac{\partial^2 \beta}{\partial z^2} - \frac{r^2}{2f^2(z)}\left(\frac{\partial f(z)}{\partial z}\right)^2 + \frac{\partial \varphi}{\partial z}$$

$$\frac{\partial S(r,z)}{\partial r} = 2r\frac{\beta}{2} = r\beta = \frac{r}{f(z)}\frac{\partial f(z)}{\partial z}$$

Differentiating equation (3.19) twice w. r. t. 'r', we get

$$\frac{\partial A_{0p}^2}{\partial r} = \frac{-4rA_{0p}^2}{r_0^2 f^2(z)} + \frac{E_0^2}{f^2(z)}Exp\left[\frac{b^2}{2}\right]\left(\frac{-2b}{r_0 f(z)}\right)Exp\left[-2\left(\frac{r}{r_0 f(z)} + \frac{b}{2}\right)^2\right]$$

$$+ \frac{E_0^2}{f^2(z)}Exp\left[\frac{b^2}{2}\right]\left(\frac{2b}{r_0 f(z)}\right)Exp\left[-2\left(\frac{r}{r_0 f(z)} - \frac{b}{2}\right)^2\right]$$

Similarly,

$$\frac{\partial^2 A_{0p}^2}{\partial r^2} = \frac{E_0^2}{f^2(z)}Exp\left[\frac{b^2}{2}\right]\left(\frac{16r^2}{f^4(z)r_0^4} + \frac{16rb}{r_0^3 f^3(z)} - \frac{4}{r_0^2 f^2(z)}\right)Exp\left[-2\left(\frac{r}{r_0 f(z)} + \frac{b}{2}\right)^2\right]$$

$$+ \frac{E_0^2}{f^2(z)}Exp\left[\frac{b^2}{2}\right]\left(\frac{16r^2}{f^4(z)r_0^4} - \frac{16rb}{r_0^3 f^3(z)} - \frac{4}{r_0^2 f^2(z)}\right)Exp\left[-2\left(\frac{r}{r_0 f(z)} - \frac{b}{2}\right)^2\right]$$

$$+ \frac{E_0^2}{f^2(z)}Exp\left[\frac{b^2}{2}\right]\left(\frac{32r^2}{r_0^4 f^4(z)} - \frac{8}{r_0^2 f^2(z)}\right)Exp\left[-\left(\frac{2r^2}{r_0^2 f^2(z)} + \frac{b^2}{2}\right)\right]$$

$$+ \frac{E_0^2}{f^2(z)}Exp\left[\frac{b^2}{2}\right]\left(\frac{4b^2}{r_0^2 f^2(z)}\right)Exp\left[-2\left(\frac{r}{r_0 f(z)} + \frac{b}{2}\right)^2\right]$$

$$- \frac{E_0^2}{f^2(z)}Exp\left[\frac{b^2}{2}\right]\left(\frac{4b^2}{r_0^2 f^2(z)}\right)Exp\left[-2\left(\frac{r}{r_0 f(z)} - \frac{b}{2}\right)^2\right]$$

$$\frac{\partial^2 A_{0p}^2}{\partial r^2} = \frac{16r^2 A_{0p}^2}{f^4(z)r_0^4} + \frac{E_0^2}{f^2(z)}Exp\left[\frac{b^2}{2}\right]\left(\frac{16rb}{r_0^3 f^3(z)} + \frac{4b^2}{r_0^2 f^2(z)}\right)Exp\left[-2\left(\frac{r}{r_0 f(z)} + \frac{b}{2}\right)^2\right]$$

$$- \frac{4A_{0p}^2}{r_0^2 f^2(z)} + \frac{E_0^2}{f^2(z)}Exp\left[\frac{b^2}{2}\right]\left(-\frac{16rb}{r_0^3 f^3(z)} + \frac{4b^2}{r_0^2 f^2(z)}\right)Exp\left[-2\left(\frac{r}{r_0 f(z)} - \frac{b}{2}\right)^2\right]$$

Substituting the values of $\partial S(r,z)/\partial z$, $\partial S(r,z)/\partial r$, $\partial A_{0p}^2/\partial r$, $\partial^2 A_{0p}^2/\partial r^2$ and A_{0p}^2 in equation (3.15) and solving, we get

$$\frac{\partial^2 f(z)}{\partial \xi^2} = \left[4 - 4b^2 - \frac{6\alpha E_0^2 \omega^2 r_0^2 m_0 \omega_{p0}^2}{\omega^2 \gamma c^2 M} Exp\left[\frac{b^2}{2} \right] \right] \frac{1}{f^3(z)} \qquad \ldots (3.20)$$

For $m = 1$, $\left[H_m\left(\frac{\sqrt{2}r}{r_0 f(z)} \right) \right]^2 = \frac{8r^2}{r_0^2 f^2(z)}$

$$A_{0p}^2 = \frac{E_0^2}{f^2(z)} Exp\left[\frac{b^2}{2} \right] \left(\frac{8r^2}{r_0^2 f^2(z)} \right) \left\{ Exp\left[-2\left(\frac{r}{r_0 f(z)} + \frac{b}{2} \right)^2 \right] + Exp\left[-2\left(\frac{r}{r_0 f(z)} - \frac{b}{2} \right)^2 \right] + 2Exp\left[-\left(\frac{2r^2}{r_0^2 f^2(z)} + \frac{b^2}{2} \right) \right] \right\} \qquad \ldots (3.21)$$

Differentiating equation (3.21) twice w. r. t. 'r', we get

$$\frac{\partial A_{0p}^2}{\partial r} = \frac{-4rA_{0p}^2}{r_0^2 f^2(z)} + \frac{2A_{0p}^2}{r} + \frac{8}{r_0^2 f^2(z)} \frac{E_0^2}{f^2(z)} Exp\left[\frac{b^2}{2} \right] \left(\frac{-2br^2}{r_0 f(z)} \right) Exp\left[-2\left(\frac{r}{r_0 f(z)} + \frac{b}{2} \right)^2 \right] + \frac{8}{r_0^2 f^2(z)} \frac{E_0^2}{f^2(z)} Exp\left[\frac{b^2}{2} \right] \left(\frac{2br^2}{r_0 f(z)} \right) Exp\left[-2\left(\frac{r}{r_0 f(z)} - \frac{b}{2} \right)^2 \right]$$

Similarly,

$$\frac{\partial^2 A_{0p}^2}{\partial r^2} = \frac{\partial}{\partial r}\left(\frac{-4rA_{0p}^2}{r_0^2 f^2(z)} + \left(\frac{8}{r_0^2 f^2(z)} \right) \frac{E_0^2}{f^2(z)} Exp\left[\frac{b^2}{2} \right] \left(\frac{-2br^2}{r_0 f(z)} \right) Exp\left[-2\left(\frac{r}{r_0 f(z)} + \frac{b}{2} \right)^2 \right] \right) + \frac{\partial}{\partial r}\left(\frac{2A_{0p}^2}{r} + \left(\frac{8}{r_0^2 f^2(z)} \right) \frac{E_0^2}{f^2(z)} Exp\left[\frac{b^2}{2} \right] \left(\frac{2br^2}{r_0 f(z)} \right) Exp\left[-2\left(\frac{r}{r_0 f(z)} - \frac{b}{2} \right)^2 \right] \right)$$

Substituting the values of $\partial S(r,z)/\partial z$, $\partial S(r,z)/\partial r$, $\partial A_{0p}^2/\partial r$, $\partial^2 A_{0p}^2/\partial r^2$ and A_{0p}^2 in equation (3.13) and solving, we get

$$\frac{\partial^2 f(z)}{\partial \xi^2} = \left[4 - 4b^2 - \frac{12\alpha E_0^2 \omega^2 r_0^2 m_0 \omega_{p0}^2}{\omega^2 \gamma c^2 M} Exp\left[\frac{b^2}{2} \right] \left(b^2 - 2 \right) \right] \frac{1}{f^3(z)} \qquad \ldots (3.22)$$

For $m=2$, $\left[H_m\left(\frac{\sqrt{2}r}{r_0 f(z)}\right)\right]^2 = \frac{64r^4}{r_0^4 f^4(z)} - \frac{32r^2}{r_0^2 f^2(z)} + 4$

$$A_{0p}^2 = \frac{E_0^2}{f^2(z)} Exp\left[\frac{b^2}{2}\right]\left(\frac{64r^4}{r_0^4 f^4(z)} - \frac{32r^2}{r_0^2 f^2(z)} + 4\right)$$

$$\left\{Exp\left[-2\left(\frac{r}{r_0 f(z)} + \frac{b}{2}\right)^2\right] + Exp\left[-2\left(\frac{r}{r_0 f(z)} - \frac{b}{2}\right)^2\right] + 2Exp\left[-\left(\frac{2r^2}{r_0^2 f^2(z)} + \frac{b^2}{2}\right)\right]\right\}$$

… (3.23)

Substituting the value of equation (3.18) and (3.23) in equation (3.15), we get

$$\frac{\partial^2 f(z)}{\partial \xi^2} = \left[-8b^2 - \frac{24\alpha E_0^2 \omega^2 r_0^2 m_0 \omega_{p0}^2}{\omega^2 \gamma c^2 M} Exp\left[\frac{b^2}{2}\right]\left(5-2b^2\right)\right]\frac{1}{f^3(z)} \qquad \text{… (3.24)}$$

where $\xi = z/R_d$, similarly Eq. (3.16) gives the condition, $\partial f/\partial \xi = 0$, f =constant.

3.5 RESULTS AND DISCUSSION

We have solved the Eqs. (3.20), (3.22) and (3.24) numerically and analyze the sensitiveness of decentered parameter for relativistic self-focusing of HChG beams in plasmas for first three mode indices. The variation of beam width parameter f with the normalized propagation distance ξ for mode indices m = 0, 1 & 2, for different intensity parameters $\alpha E_0^2 = 3, 5 \text{ and } 7$ (corresponding intensities are $2.2\times10^{17} W/cm^2$, $3.7\times10^{17} W/cm^2$ and $5.2\times10^{17} W/cm^2$ respectively) has been analyzed for different parameters given as $\omega r_0/c = 3$, $r_0 = 3\times10^{-6} m$, $\omega = 3\times10^{14} rad/s$, $m_0/M = 0.02$ and $\omega_{p0}/\omega = 0.4$. From figure 3.1(a), it is clear that with the little increase in the value of the decentered parameter *b*, the beam width parameter *f* decreases greatly for $\alpha E_0^2 = 3$. Hence self-focusing of laser beam becomes more and more strong and it is obvious from the figure that small decimal change in the value of the decentered parameter greatly affects the beam width parameter. Moreover, decentered parameter is very sensitive and its proper selection decides the focusing or the defocusing effect at different intensities. In figure 3.1(b) and 3.1(c), the variation of beam width parameter *f* with normalized

propagation distance ξ for intensity parameters $\alpha E_0^2 = 5, 7$ has been observed for various parameters taken to be similar as that in figure 3.1(a). The plot obtained clarifies that for mode index, m=0, the beam gets more and more focused due to the dominance of the non-linear self-focusing term. For the values of the intensity parameters $\alpha E_0^2 = 3, 5$ and 7, self-focusing becomes stronger for decentered parameter b=0.92, 0.74 and 0.52 respectively. Hence, for the laser of high intensity, self-focusing occurs at low values of the decentered parameter.

Figure 3.2 represents the variation of the beam width parameter *f* with the normalized propagation distance ξ, for mode index m=1, at different values of various parameter taken similar to previous values as taken in case of mode index m=0. From fig. 3.2(a), it is concluded that for certain values of the decentered parameter *b*, focusing of laser beam occurs. These selected values of decentered parameter depend on initial intensity of laser beam. From figure 3.1 & 3.2, it is clear that in case of mode index m=0, for intensity parameter $\alpha E_0^2 = 3$, self-focusing is stronger at b=0.92, however, in case of mode index m=1, for intensity parameter $\alpha E_0^2 = 3$, self-focusing of beam becomes stronger at *b* =1.287. In comparison with the results obtained for m=0 & 1, it is clear that for m=1, self-focusing occurs at higher values of decentered parameter. From figure 3.1 & 3.2, one can clearly see the sensitiveness of the decentered parameter on self-focusing. Thus, self-focusing of Hermite-cosh-Gaussian laser beam can be controlled by mode indices and decentered parameter as the decentered parameter is more sensitive to self-focusing. These results support the results obtained by Patil *et al.* [18, 81]. For m=1, with the increase in value of decentered parameter *b*, focusing term becomes dominant for all taken values of intensity. It would be quite interesting to see the effect of decentered parameter on the focusing/de-focusing nature of HChG beam for higher values of mode indices.

Figure 3.3, represents the variation of beam width parameter *f* with the normalized propagation distance ξ for m=2 and other parameters are same as taken previously. From the plot it is concluded that for mode index m=2, self-focusing effect of laser beam reduces greatly with the increase in the value of the decentered parameter and the defocusing term in Eq. (3.24) becomes dominant over non-linear self-focusing term.

Again the selection of values of the decentered parameter plays a very crucial role by virtue of which at least weak self-focusing effect is observed and thereafter beam get defocused. Here, we observed that for m=2, self-focusing is weak for intensity parameters $\alpha E_0^2 = 3, 5 \text{ and } 7$ as compared to that in case of mode indices m=0 & 1 for the same parameters.

3.6 CONCLUSION

In the present investigation we have studied the sensitivity of decentered parameter for relativistic self-focusing of HChG laser beam in plasma. We have derived the equation of beam width parameter using paraxial ray approach and investigated the sensitiveness of the decentered parameter on the self-focusing. The focusing/ defocusing phenomena of HChG laser beam in plasma for mode indices m=0, 1 and 2, can be controlled and made stronger with the decentered parameter *b*, as the value of *b* is more sensitive to self-focusing. Moreover, self-focusing becomes stronger with the increase in selected values of the decentered parameter at a particular intensity for mode indices m=0 & 1. For m=2, we observe opposite results indicating that self-focusing effect becomes weaker. Thus for m=2, Hermite-Cosh-Gaussian beam exhibits diffraction effect and self-focusing effect is weaker for all taken values of laser intensity. The results obtained in this study add to the sensitiveness of decentered parameter to self-focusing. We report the selection of decentered parameter as decentered parameter is more sensitive to self-focusing. The present study helps the investigators to choose the intensity parameter as per their requirement by the proper selection of the decentered parameter leads to substantial improvement in the focusing quality which may be useful in inertial fusion energy driven by lasers.

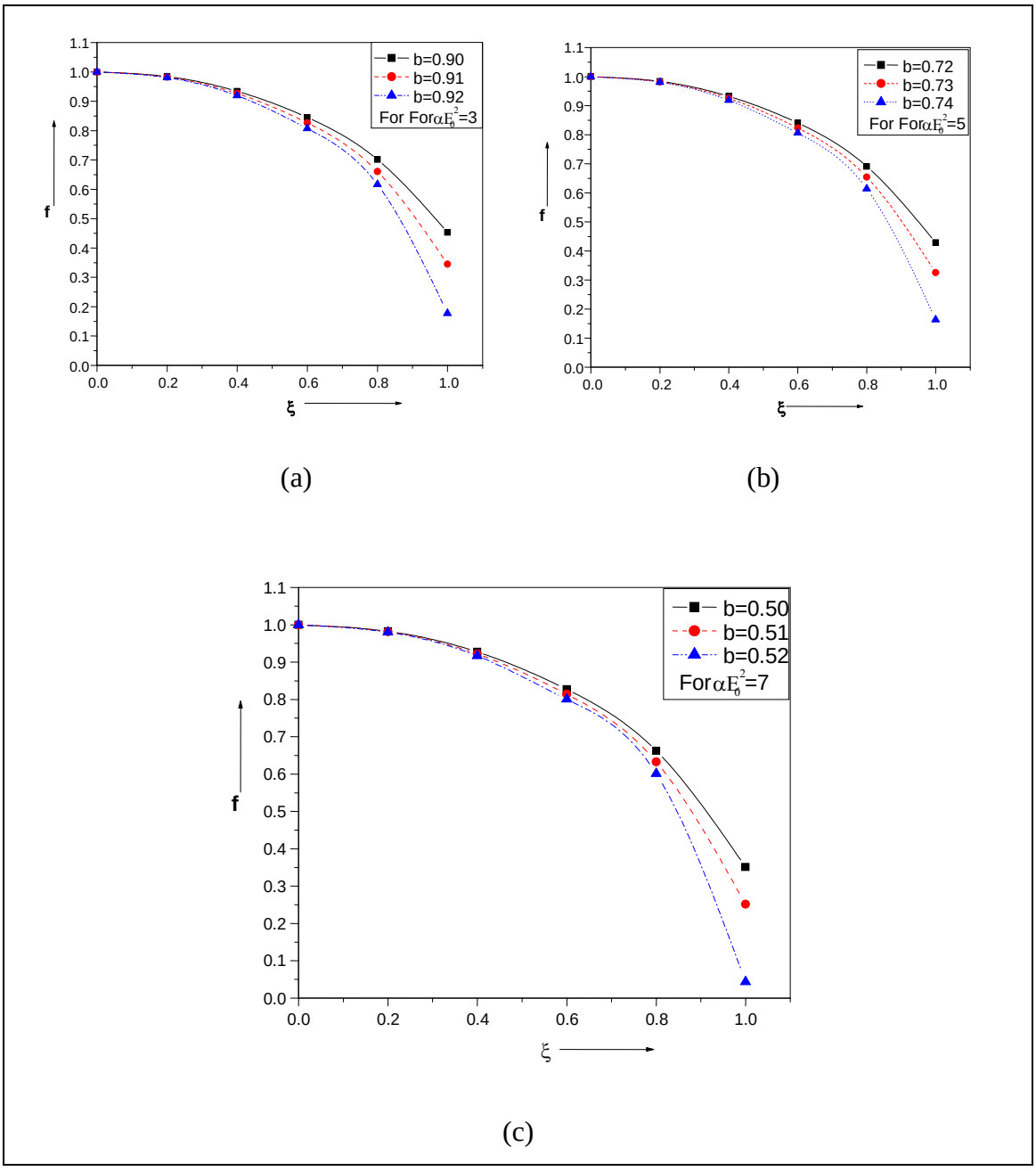

Figure 3.1: Variation of beam width parameter $'f(\xi)'$ with normalized propagation distance $'\xi'$ for different values of dcentered parameters. The other parameters are taken as $m=0$, $\omega r_0/c=3$, $m_0/M=0.02$ and $\omega_{P0}/\omega=0.4$.

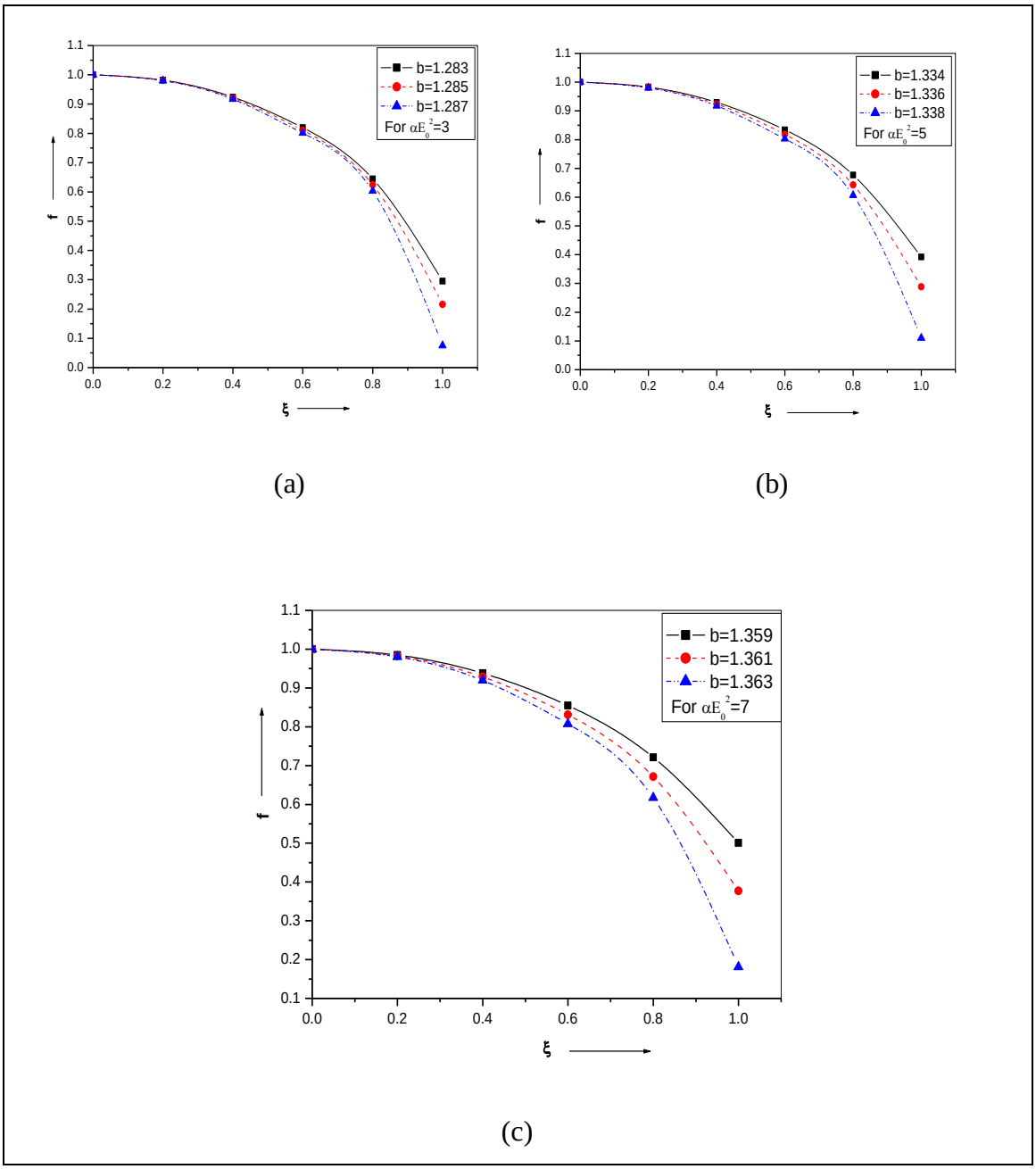

Figure 3.2: Variation of beam width parameter (f) with normalized propagation distance (ξ) for different values of decentered parameter. The other parameters are taken as $m = 1,\ \omega r_0 / c = 3,\ m_0 / M = 0.02$ **and** $\omega_{P0} / \omega = 0.4.$

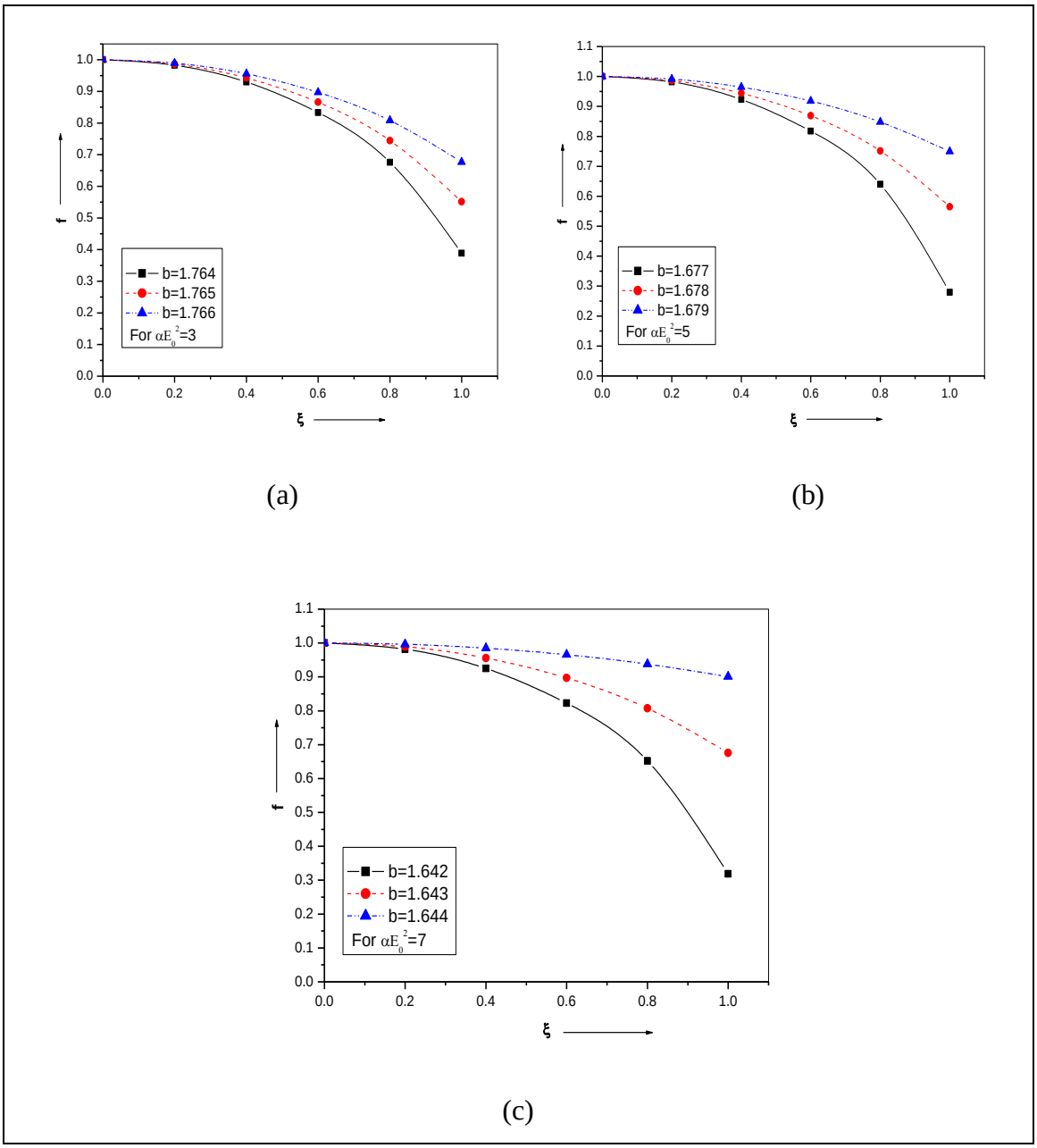

Figure 3.3: Variation of beam width parameter (f) with normalized propagation distance (ξ) for different values of decentered parameter. The other parameters are taken as $m = 2,\ \omega r_0/c = 3,\ m_0/M = 0.02$ **and** $\omega_{P0}/\omega = 0.4.$

CHAPTER-4

SELF-FOCUSING OF A HERMITE-COSH GAUSSIAN LASER BEAM IN A MAGNETOPLASMA WITH RAMP DENSITY PROFILE

4.1 INTRODUCTION

The interaction of light with solids, liquids, gases and plasmas occurs very frequently in nature. For over more than four decades, the nonlinear interaction of laser beams with matter has been studied intensively by researchers. Development of short-pulse high intensity lasers of the order of 10^{20} W/cm^2 make it possible to investigate the nonlinear interaction of strong electromagnetic waves with plasmas. A series of applications of self-focusing of laser beams in plasmas [2, 3] like optical harmonic generation [13], laser driven fusion [11], x-ray lasers and the laser driven accelerators [8], the production of quasi mono-energetic electron bunches [8] etc. creates a center of attention of many researchers and scientists. These applications need the laser beams to propagate over several Rayleigh lengths in the plasmas without loss of the energy. The propagation of different kind of laser beams profile like Gaussian beams [4], Cosh-Gaussian beams [14, 84, 91], Hermite-cosh-Gaussian beams [16], Elliptic Gaussian beams [92], Bessel beams [93], Leguerre-Gaussiaon beams [94] etc. in the plasmas attracts the attention of the researchers.

Recently, theoretical investigators focus their attention on paraxial wave family of laser beams. Hermite-cosh-Gaussian beam is one of the solutions of paraxial wave equation and such HChG beam can be obtained in the laboratory by the superposition of two decentered Hermite-Gaussian beams as Cosh-Gaussian ones. Propagation of Hermite-cosh-Gaussian beams in plasmas has been studied theoretically earlier by Belafhal *et al.* [19], and Patil *et al.* [17, 18]. The focusing of HChG laser beams in magneto-plasma by considering ponderomotive nonlinearity has been theoretically examined by Patil *et al.* [81] and reported the effect of mode index and decentered parameter on the self-focusing of the beams. Gill *et al.* [84] has recently studied the relativistic self-focusing and self-phase modulation of cosh-Gaussian laser beam in magnetoplasma in the absence of plasma density ramp and reported strong self-focusing

of the laser beams. Gupta *et al.* [78] in 2007, has investigated the addition focusing of a high intensity laser beams in a plasma with a density ramp and a magnetic field and reported the strong self-focusing of the laser beams. Again density ramp has also been applied by Kant *et al.* [85, 87] to study the Ponderomotive self-focusing of a short laser pulse and self-focusing of Hermite-Gaussian laser beams in plasma. In both the cases Kant *et al.* [85, 87] reported strong self-focusing of the laser beams.

The present work is dedicated to the study of self-focusing of Hermite-cosh-Gaussian laser beams in collisionless magneto-plasma under plasma density ramp in applied magnetic field. We derive the equations for beam width parameter for Hermite-cosh-Gaussian beam profile propagating in the plasmas in the presence of magnetic field and plasma density ramp, by applying Wentzel-Kramers-Brillouin (WKB) approximation and Paraxial approximation [4, 90] and hence, solve them numerically by using Mathematica software. The sensitiveness of decentered parameter [95] is observed and small increase in its value enhances greatly the self-focusing ability of the beam. In order to simplify mathematical calculation, only the transversal components of laser field are evaluated and longitudinal components are not taken in to consideration in the present paper. However, while dealing with nonlinear phenomenon, longitudinal components should be considered for an exact formulation [52].

4.2 NON-LINEAR DIELECTRIC CONSTANT

The dielectric constant for the non-linear medium (collisionless magnetoplasma) with density ramp profile is obtained by applying the approach as applied by Sodha *et al.* [4]:

$$\varepsilon_{\pm} = \varepsilon_{\pm 0} + \phi_{\pm}(EE^{*}) \qquad \ldots (4.1)$$

with $\varepsilon_{\pm 0} = 1 - \omega_P^2 / \omega(\omega \mp \omega_c)$, $\phi_{\pm}(EE^{*}) = \varepsilon_{\pm 2} A_0^2 / (1 - \omega_c / \omega)^2$, $\omega_P^2 = 4\pi\, e^2 n(\xi) / m$

$$n(\xi) = n_0 \tan(\xi / d), \quad \omega_{P0}^2 = 4\pi e^2 n_0 / m, \quad \omega_c = eB_0 / mc, \quad \alpha = e^2 M / 6m^2 \omega^2 k_B T_0$$

$$\varepsilon_{\pm 2} = 3m\alpha\omega_P^2 (1 \mp \omega_c / 2\omega) / 8M\omega(\omega \mp \omega_c)$$

here $\varepsilon_{\pm 0}$ and $\phi_{\pm}(EE^{*})$ represent the linear and non-linear parts of the dielectric constant respectively. ω_P and ω_c are the plasma frequency and electron cyclotron frequency respectively. e, m and n_0 are the magnitude of the electronic charge, mass and electron

density, ' M ' is the mass of scatterer in the plasma, ' ω ' is the frequency of laser used, ' $\xi = z/R_d$ ' is the normalized propagation distance, ' R_d ' is the diffraction length, ' d ' is a dimensionless adjustable parameter, ' k_B ' is the Boltzmann constant and ' T_0 ' is the equilibrium plasma temperature.

4.3 SELF-FOCUSING EQUATIONS

Consider the Hermite-cosh-Gaussian laser beam is propagating along the z-direction with the field distribution in the following form:

$$E(r,z) = \frac{E_0}{f_+(z)} e^{\frac{b^2}{4}} H_m\left(\frac{\sqrt{2}r}{r_0 f_+(z)}\right)\left(Exp\left[-\left(\frac{r}{f_+(z)r_0}+\frac{b}{2}\right)^2\right]+Exp\left[-\left(\frac{r}{f_+(z)r_0}-\frac{b}{2}\right)^2\right]\right) \quad \ldots (4.2)$$

'E_0' is the amplitude of Hermite-cosh-Gaussian laser beam for the central position at $r = z = 0$, $'f_+(z)'$ is the dimensionless beam width parameter, H_m is the Hermite polynomial and 'm' is the mode index associated with Hermite polynomial, ' r_0 ' is the initial spot size of the laser beam.

The general form of wave equation for exponentially varying field obtained from Maxwell's equation is given by

$$\nabla^2\vec{E} - \nabla(\nabla.\vec{E}) = -\frac{\omega^2}{c^2}\varepsilon.\vec{E} \quad \ldots (4.3)$$

In components form this equation can be written as

$$\frac{\partial^2 E_x}{\partial z^2}+\frac{\partial^2 E_x}{\partial y^2}-\frac{\partial}{\partial x}\left(\frac{\partial E_y}{\partial y}+\frac{\partial E_z}{\partial z}\right) = -\frac{\omega^2}{c^2}\left(\varepsilon.\vec{E}\right)_x \quad \ldots (4.4a)$$

$$\frac{\partial^2 E_y}{\partial z^2}+\frac{\partial^2 E_y}{\partial x^2}-\frac{\partial}{\partial y}\left(\frac{\partial E_x}{\partial x}+\frac{\partial E_z}{\partial z}\right) = -\frac{\omega^2}{c^2}\left(\varepsilon.\vec{E}\right)_y \quad \ldots (4.4b)$$

$$\frac{\partial^2 E_z}{\partial x^2}+\frac{\partial^2 E_z}{\partial y^2}-\frac{\partial}{\partial z}\left(\frac{\partial E_x}{\partial x}+\frac{\partial E_y}{\partial y}\right) = -\frac{\omega^2}{c^2}\left(\varepsilon.\vec{E}\right)_z \quad \ldots (4.4c)$$

In the present case, the variation of magnetic field ($\vec{B} = B_0\hat{k}$) is assumed to be very strong along z-direction of the co-ordinate system than x-y plane. Thus the propagating

wave is considered to be transverse in nature in zero order approximation. This assumption gives rise to the condition $\nabla.\vec{D}=0$ or,

$$\frac{\partial E_z}{\partial z} \approx -\frac{1}{\varepsilon_{zz}}\left(\varepsilon_{xx}\frac{\partial E_x}{\partial x}+\varepsilon_{xy}\frac{\partial E_y}{\partial x}+\varepsilon_{yx}\frac{\partial E_x}{\partial y}+\varepsilon_{yy}\frac{\partial E_y}{\partial y}\right) \qquad \ldots (4.5)$$

The equations (4.4a), (4.4b) & (4.4c) are coupled and one cannot define the propagation vectors which describe the independent propagation of E_x , E_y and E_z.

To investigate the independent modes of propagation, we multiply equation (4.4b) by '*i*' and adding so obtained equation to equation (4.4a), we get,

$$\frac{\partial^2 E_x}{\partial z^2}+\frac{\partial^2 E_x}{\partial y^2}-\frac{\partial}{\partial x}\left(\frac{\partial E_y}{\partial y}+\frac{\partial E_z}{\partial z}\right)+i\left(\frac{\partial^2 E_y}{\partial z^2}+\frac{\partial^2 E_y}{\partial x^2}-\frac{\partial}{\partial y}\left(\frac{\partial E_x}{\partial x}+\frac{\partial E_z}{\partial z}\right)\right)$$

$$=-\frac{\omega^2}{c^2}\left(\varepsilon.\vec{E}\right)_x-i\frac{\omega^2}{c^2}\left(\varepsilon.\vec{E}\right)_y$$

Using the value of $\frac{\partial E_z}{\partial z}$, $A_1=E_x+iE_y$ and $A_2=E_x-iE_y$, we get

$$\frac{\partial^2 A_1}{\partial z^2}+\frac{\partial^2 E_x}{\partial y^2}+i\frac{\partial^2 E_y}{\partial x^2}-i\frac{\partial^2 A_2}{\partial x\partial y}-\frac{\partial}{\partial x}\left[-\frac{1}{\varepsilon_{zz}}\left(\varepsilon_{xx}\frac{\partial E_x}{\partial x}+\varepsilon_{xy}\frac{\partial E_y}{\partial x}+\varepsilon_{yx}\frac{\partial E_x}{\partial y}+\varepsilon_{yy}\frac{\partial E_y}{\partial y}\right)\right]$$

$$-i\frac{\partial}{\partial y}\left[-\frac{1}{\varepsilon_{zz}}\left(\varepsilon_{xx}\frac{\partial E_x}{\partial x}+\varepsilon_{xy}\frac{\partial E_y}{\partial x}+\varepsilon_{yx}\frac{\partial E_x}{\partial y}+\varepsilon_{yy}\frac{\partial E_y}{\partial y}\right)\right]=-\frac{\omega^2}{c^2}\left[\left(\varepsilon.\vec{E}\right)_x+i\left(\varepsilon.\vec{E}\right)_y\right]$$

Solving this equation and using $\varepsilon_{xx}=\varepsilon_{yy}$ and $\varepsilon_{yx}=-\varepsilon_{xy}$, we get,

$$\frac{\partial^2 A_1}{\partial z^2}+\frac{1}{2}\left(1+\frac{\varepsilon_{+0}}{\varepsilon_{0zz}}\right)\left(\frac{\partial^2 A_1}{\partial x^2}+\frac{\partial^2 A_1}{\partial y^2}\right)+\frac{1}{2}\left(\frac{\varepsilon_{-0}}{\varepsilon_{0zz}}-1\right)\left(\frac{\partial^2 A_2}{\partial x^2}-\frac{\partial^2 A_2}{\partial y^2}\right)-i\left(1-\frac{\varepsilon_{-0}}{\varepsilon_{0zz}}\right)\frac{\partial^2 A_2}{\partial x\partial y}$$

$$+\frac{\omega^2}{c^2}\left[\varepsilon_{+0}+\varepsilon_{+2}\left\{\frac{A_1A_1^*}{\left(1-\frac{\omega_c}{\omega}\right)^2}+\frac{A_2A_2^*}{\left(1+\frac{\omega_c}{\omega}\right)^2}\right\}\right]A_1=0 \qquad \ldots(4.6)$$

Similarly for ordinary mode of propagation,

$$\frac{\partial^2 A_2}{\partial z^2}+\frac{1}{2}\left(1+\frac{\varepsilon_{-0}}{\varepsilon_{0zz}}\right)\left(\frac{\partial^2 A_2}{\partial x^2}+\frac{\partial^2 A_2}{\partial y^2}\right)+\frac{1}{2}\left(\frac{\varepsilon_{+0}}{\varepsilon_{0zz}}-1\right)\left(\frac{\partial^2 A_1}{\partial x^2}-\frac{\partial^2 A_1}{\partial y^2}\right)+i\left(1-\frac{\varepsilon_{+0}}{\varepsilon_{0zz}}\right)\frac{\partial^2 A_1}{\partial x\partial y}$$

$$+\frac{\omega^2}{c^2}\left[\varepsilon_{-0}+\varepsilon_{-2}\left\{\frac{A_1A_1^*}{\left(1-\frac{\omega_c}{\omega}\right)^2}+\frac{A_2A_2^*}{\left(1+\frac{\omega_c}{\omega}\right)^2}\right\}\right]A_2=0 \qquad \text{... (4.7)}$$

with, $\varepsilon_{0zz}=1-\omega_P^2/\omega^2$

The functions A_1 and A_2, having propagation vectors k_+ and k_- respectively, represent the extraordinary and ordinary modes of propagation of a magnetoplasma. The variation of equation (4.6) and (4.7) is very slow along x and y-direction as compared to z-direction. It indicates the weak coupling of these two equations. In order to study the behavior of one of the mode other mode can be considered to be zero. Let us assume $A_2\approx 0$, then equation (4.6) becomes,

$$\frac{\partial^2 A_1}{\partial z^2}+\frac{1}{2}\left(1+\frac{\varepsilon_{+0}}{\varepsilon_{0zz}}\right)\left(\frac{\partial^2 A_1}{\partial x^2}+\frac{\partial^2 A_1}{\partial y^2}\right)+\frac{\omega^2}{c^2}\left[\varepsilon_{+0}+\varepsilon_{+2}\left\{\frac{A_1A_1^*}{\left(1-\frac{\omega_c}{\omega}\right)^2}\right\}\right]A_1=0 \qquad \text{… (4.8a)}$$

Similarly for considering $A_1\approx 0$, equation (4.7) becomes,

$$\frac{\partial^2 A_2}{\partial z^2}+\frac{1}{2}\left(1+\frac{\varepsilon_{-0}}{\varepsilon_{0zz}}\right)\left(\frac{\partial^2 A_2}{\partial x^2}+\frac{\partial^2 A_2}{\partial y^2}\right)+\frac{\omega^2}{c^2}\left[\varepsilon_{-0}+\varepsilon_{-2}\left\{\frac{A_2A_2^*}{\left(1+\frac{\omega_c}{\omega}\right)^2}\right\}\right]A_2=0 \qquad \text{… (4.8b)}$$

The solution of equation (a) is of the form

$$A_1=A\exp[i(\omega t-k_+z)] \qquad \text{… (4.9)}$$

where $k_+=(\omega/c)\varepsilon_{+0}^{1/2}$ and A is the complex amplitude.

Differentiating eq. (4.9) twice w. r. t. x, we get,

$$\frac{\partial A_1}{\partial x}=\exp[i(\omega t-k_+z)]\frac{\partial A}{\partial x}$$

$$\frac{\partial^2 A_1}{\partial x^2} = \exp[i(\omega t - k_+ z)]\frac{\partial^2 A}{\partial x^2}$$

Similarly, differentiating eq. (4.9) twice w. r. t. y, we get,

$$\frac{\partial A_1}{\partial y} = \exp[i(\omega t - k_+ z)]\frac{\partial A}{\partial y}$$

$$\frac{\partial^2 A_1}{\partial y^2} = \exp[i(\omega t - k_+ z)]\frac{\partial^2 A}{\partial y^2}$$

Now, differentiating eq. (4.9) twice w. r. t. z, we get,

$$\frac{\partial A_1}{\partial z} = -iA\exp[i(\omega t - k_+ z)]k_+ - iAZ\exp[i(\omega t - k_+ z)]\frac{\partial k_+}{\partial z} + \exp[i(\omega t - k_+ z)]\frac{\partial A}{\partial z}$$

$$\frac{\partial^2 A_1}{\partial z^2} = -2iA\exp[i(\omega t - k_+ z)]\frac{\partial k_+}{\partial z} - ik_+\frac{\partial A_1}{\partial z} - iAZ\exp[i(\omega t - k_+ z)]\frac{\partial^2 k_+}{\partial z^2} - iz\frac{\partial A_1}{\partial z}\frac{\partial k_+}{\partial z}$$

$$+\exp[i(\omega t - k_+ z)]\frac{\partial^2 A}{\partial z^2} - ik_+\exp[i(\omega t - k_+ z)]\frac{\partial A}{\partial z} - iz\exp[i(\omega t - k_+ z)]\frac{\partial A}{\partial z}\frac{\partial k_+}{\partial z}$$

Substituting these values in equation (4.8a) and neglecting $\partial^2 A/\partial z^2 = 0$, we get

$$\frac{iA\omega^2\omega_s Sec^2\left(\frac{z}{dR_d}\right)}{k_+ c^2 dR_d} + \frac{Az\omega^2\omega_s Sec^2\left(\frac{z}{dR_d}\right)}{2c^2 dR_d} - 2ik_+\frac{\partial A}{\partial z} + \frac{iAz\omega^2\omega_s Sec^2\left(\frac{z}{dR_d}\right)\tan\left(\frac{z}{dR_d}\right)}{k_+ c^2 d^2 R_d^2}$$

$$+\frac{iAz\omega^4\omega_s^2 Sec^4\left(\frac{z}{dR_d}\right)}{4k_+^3 c^4 d^2 R_d^2} + \frac{Az\omega^2\omega_s Sec^2\left(\frac{z}{dR_d}\right)}{2c^2 dR_d} - \frac{Az\omega^4\omega_s^2 Sec^4\left(\frac{z}{dR_d}\right)}{4k_+^3 c^4 d^2 R_d^2}$$

$$+\frac{iz\omega^2\omega_s Sec^2\left(\frac{z}{dR_d}\right)}{2k_+ c^2 dR_d}\frac{\partial A}{\partial z} + \frac{iz\omega^2\omega_s Sec^2\left(\frac{z}{dR_d}\right)}{2k_+ c^2 dR_d}\frac{\partial A}{\partial z} + \frac{1}{2}\left(1+\frac{\varepsilon_{+0}}{\varepsilon_{0zz}}\right)\left(\frac{\partial^2 A}{\partial x^2} + \frac{\partial^2 A}{\partial y^2}\right)$$

$$+\frac{\omega^2}{c^2}\varepsilon_{+2}\left(\frac{AA^*}{\left(1-\frac{\omega_c}{\omega}\right)^2}\right)A = 0$$

$$i\frac{A\omega^2\omega_s Sec^2\left(\frac{z}{dR_d}\right)}{k_+c^2dR_d}-2ik_+\frac{\partial A}{\partial z}+\frac{Az\omega^2\omega_s Sec^2\left(\frac{z}{dR_d}\right)\tan\left(\frac{z}{dR_d}\right)}{k_+c^2d^2R_d^2}i+\frac{Az\omega^4\omega_s^2 Sec^4\left(\frac{z}{dR_d}\right)}{4k_+^3c^4d^2R_d^2}i$$

$$+\frac{z\omega^2\omega_s Sec^2\left(\frac{z}{dR_d}\right)}{k_+c^2dR_d}\frac{\partial A}{\partial z}i+\frac{Az\omega^2\omega_s Sec^2\left(\frac{z}{dR_d}\right)}{c^2dR_d}-\frac{Az\omega^4\omega_s^2 Sec^4\left(\frac{z}{dR_d}\right)}{4k_+^3c^4d^2R_d^2}$$

$$+\frac{1}{2}\left(1+\frac{\varepsilon_{+0}}{\varepsilon_{0zz}}\right)\left(\frac{\partial^2 A}{\partial x^2}+\frac{\partial^2 A}{\partial y^2}\right)+\frac{\omega^2}{c^2}\varepsilon_{+2}\left(\frac{AA^*}{\left(1-\frac{\omega_c}{\omega}\right)^2}\right)A=0$$

where $\omega_s=\omega_{P0}^2/\omega(\omega-\omega_c)$

The solution of this equation is of the form

$$A=A_0(x,y,z)Exp[-ik_+(z)S(x,y,z)] \qquad \ldots (4.10)$$

Substituting this value in equation, we get

$$\frac{A_0\omega^2\omega_s Sec^2\left(\frac{z}{dR_d}\right)}{k_+c^2dR_d}i-2ik_+\frac{\partial A_0}{\partial z}+\frac{A_0z\omega^2\omega_s Sec^2\left(\frac{z}{dR_d}\right)\tan\left(\frac{z}{dR_d}\right)}{k_+c^2d^2R_d^2}i$$

$$+i\frac{A_0z\omega^4\omega_s^2 Sec^4\left(\frac{z}{dR_d}\right)}{4k_+^3c^4d^2R_d^2}+i\frac{z\omega^2\omega_s Sec^2\left(\frac{z}{dR_d}\right)}{k_+c^2dR_d}\frac{\partial A_0}{\partial z}-\frac{i}{2}\left(1+\frac{\varepsilon_{+0}}{\varepsilon_{0zz}}\right)$$

$$\left[A_0k_+\frac{\partial^2 S}{\partial x^2}+2k_+\frac{\partial S}{\partial x}\frac{\partial A_0}{\partial x}+A_0k_+\frac{\partial^2 S}{\partial y^2}+2k_+\frac{\partial S}{\partial y}\frac{\partial A_0}{\partial y}\right]-2A_0k_+^2\frac{\partial S}{\partial z}$$

$$+\frac{A_0S\omega^2\omega_s Sec^2\left(\frac{z}{dR_d}\right)}{c^2dR_d}+\frac{A_0z\omega^2\omega_s Sec^2\left(\frac{z}{dR_d}\right)}{c^2dR_d}\frac{\partial S}{\partial z}-\frac{A_0Sz\omega^4\omega_s^2 Sec^4\left(\frac{z}{dR_d}\right)}{2k_+^3c^4d^2R_d^2}$$

$$+\frac{A_0z\omega^2\omega_s Sec^2\left(\frac{z}{dR_d}\right)}{c^2dR_d}-\frac{A_0z^2\omega^4\omega_s^2 Sec^4\left(\frac{z}{dR_d}\right)}{4k_+^2c^4d^2R_d^2}-\frac{1}{2}\left(1+\frac{\varepsilon_{+0}}{\varepsilon_{0zz}}\right)$$

$$\left[A_0k_+^2\left(\frac{\partial S}{\partial x}\right)^2-\frac{\partial^2 A_0}{\partial x^2}+A_0k_+^2\left(\frac{\partial S}{\partial y}\right)^2-\frac{\partial^2 A_0}{\partial y^2}\right]+\frac{\omega^2}{c^2}\varepsilon_{+2}\left(\frac{A_0^2}{\left(1-\frac{\omega_c}{\omega}\right)^2}\right)A_0=0$$

Now separating real and imaginary parts, we get

Real part

$$\left[\frac{z\omega^2\omega_s\sec^2\left(\frac{z}{dR_d}\right)}{k_+^2c^2dR_d}-2\right]\frac{\partial S}{\partial z}-\frac{1}{2}\left(1+\frac{\varepsilon_{+0}}{\varepsilon_{0zz}}\right)\left[\left(\frac{\partial S}{\partial x}\right)^2+\left(\frac{\partial S}{\partial y}\right)^2\right]+\frac{1}{4A_0^2k_+^2}\left(1+\frac{\varepsilon_{+0}}{\varepsilon_{0zz}}\right)$$

$$\left[\left(\frac{\partial^2A_0^2}{\partial x^2}+\frac{\partial^2A_0^2}{\partial y^2}\right)-\frac{1}{2A_0^2}\left\{\left(\frac{\partial A_0^2}{\partial x}\right)^2+\left(\frac{\partial A_0^2}{\partial y}\right)^2\right\}\right]-\frac{S\omega^2\omega_s\sec^2\left(\frac{z}{dR_d}\right)}{k_+^2c^2dR_d}-\frac{Sz\omega^4\omega_s^2\sec^4\left(\frac{z}{dR_d}\right)}{2k_+^4c^4d^2R_d^2}$$

$$+\frac{z\omega^2\omega_s\sec^2\left(\frac{z}{dR_d}\right)}{k_+^2c^2dR_d}-\frac{z^2\omega^4\omega_s^2\sec^4\left(\frac{z}{dR_d}\right)}{4k_+^4c^4d^2R_d^2}+\frac{\omega^2}{k_+^2c^2}\varepsilon_{+2}\left(\frac{A_0^2}{\left(1-\frac{\omega_c}{\omega}\right)^2}\right)=0 \qquad ...(4.11)$$

Imaginary part

$$\frac{\omega^2\omega_s\sec^2\left(\frac{z}{dR_d}\right)}{k_+^3c^2dR_d}+\frac{z\omega^2\omega_s\sec^2\left(\frac{z}{dR_d}\right)\tan\left(\frac{z}{dR_d}\right)}{k_+^3c^2dR_d}+\frac{z\omega^4\omega_s^2\sec^4\left(\frac{z}{dR_d}\right)}{4k_+^5c^4d^2R_d^2}$$

$$+\left(\frac{z\omega^2\omega_s\sec^2\left(\frac{z}{dR_d}\right)}{2A_0^2k_+^3c^2dR_d}-\frac{1}{k_+A_0^2}\right)\frac{\partial A_0^2}{\partial z}-\frac{1}{2k_+}\left(1+\frac{\varepsilon_{+0}}{\varepsilon_{0zz}}\right)\left(\frac{\partial^2S}{\partial x^2}+\frac{\partial^2S}{\partial y^2}\right)$$

$$+\frac{1}{2k_+A_0^2}\left(1+\frac{\varepsilon_{+0}}{\varepsilon_{0zz}}\right)\left[\left(\frac{\partial S}{\partial x}\right)\left(\frac{\partial A_0^2}{\partial x}\right)+\left(\frac{\partial S}{\partial y}\right)\left(\frac{\partial A_0^2}{\partial y}\right)\right]=0. \qquad ...(4.12)$$

The solution of equation (4.11) & (4.12) for initially Hermite-cosh-Gaussian beam is of the following form,

$$A_0^2=\frac{E_0^2}{f_+^2(z)}e^{\frac{b^2}{2}}\left[H_m\left(\frac{\sqrt{2}r}{r_0f_+(z)}\right)\right]^2$$

$$\left(Exp\left[-2\left(\frac{r}{f_+(z)r_0}+\frac{b}{2}\right)^2\right]+Exp\left[-2\left(\frac{r}{f_+(z)r_0}-\frac{b}{2}\right)^2\right]+2Exp\left[-\left(\frac{2r}{f_+(z)r_0}+\frac{b^2}{2}\right)\right]\right)$$

… (4.13)

and

$$S = \frac{x^2}{2}\beta(z) + \frac{y^2}{2}\beta(z) + \phi(z) \qquad \ldots (4.14)$$

where $\beta(z) = 2/f_+(z)\left(1+\varepsilon_{+0}/\varepsilon_{0zz}\right)\partial f_+(z)/\partial z$, is the curvature of the wave front and $r^2 = \left(x^2 + y^2\right)$. '$E_0$'is the amplitude of Hermite-cosh-Gaussian laser beam for the central position at $r = z = 0$, '$f_+(z)$' is the dimensionless beam width parameter; 'r_0' is the spot size of the beam.

For m=0

$$\left[H_0\left(\frac{\sqrt{2}r}{r_0 f_+(z)}\right)\right]^2 = 1$$

Thus,

$$A_0^2 = \frac{E_0^2}{f_+^2(z)} e^{\frac{b^2}{2}}\left(Exp\left[-2\left(\frac{r}{f_+(z)r_0} + \frac{b}{2}\right)^2\right] + Exp\left[-2\left(\frac{r}{f_+(z)r_0} - \frac{b}{2}\right)^2\right] + 2Exp\left[\left(\frac{-2r}{f_+(z)r_0} + \frac{b^2}{2}\right)\right]\right)$$

Substituting this value in equation (4.11) and simplifying the equation, we get

$$\left\{\frac{\xi\omega_s \sec^2\left(\frac{\xi}{d}\right)}{d} - 2\left(1-\omega_s \tan\left(\frac{\xi}{d}\right)\right)\right\}\frac{\partial^2 f_+}{\partial\xi^2} - \frac{\xi\omega_s \sec^2\left(\frac{\xi}{d}\right)}{d}\frac{1}{f_+}\left(\frac{\partial f_+}{\partial\xi}\right)^2 - \frac{\xi\omega_s \sec^4\left(\frac{\xi}{d}\right)\omega_{P0}^2\varepsilon_{+0}}{d^2\omega^2\varepsilon_{0zz}^2\left(1+\frac{\varepsilon_{+0}}{\varepsilon_{0zz}}\right)}\frac{\partial f_+}{\partial\xi}$$

$$+\frac{\xi\omega_s^2 \sec^4\left(\frac{\xi}{d}\right)}{d^2\varepsilon_{0zz}\left(1+\frac{\varepsilon_{+0}}{\varepsilon_{0zz}}\right)}\frac{\partial f_+}{\partial\xi} + \frac{2\sec^2\left(\frac{\xi}{d}\right)\left(1-\omega_s \tan\left(\frac{\xi}{d}\right)\right)\omega_{P0}^2\varepsilon_{+0}}{d\omega^2\varepsilon_{0zz}^2\left(1+\frac{\varepsilon_{+0}}{\varepsilon_{0zz}}\right)}\frac{\partial f_+}{\partial\xi}$$

$$-\frac{2\omega_s \sec^2\left(\frac{\xi}{d}\right)\left(1-\omega_s \tan\left(\frac{\xi}{d}\right)\right)}{d\,\varepsilon_{0zz}\left(1+\frac{\varepsilon_{+0}}{\varepsilon_{0zz}}\right)}\frac{\partial f_+}{\partial\xi} + \frac{\left(1+\frac{\varepsilon_{+0}}{\varepsilon_{0zz}}\right)^2\left(1-\frac{\omega_{P0}^2}{\omega^2}\tan\left(\frac{\xi}{d}\right)\right)}{f_+^3}\left(2-2b^2\right)$$

$$-\frac{8R_{d1}^2 e^{\frac{b^2}{2}}\left(1-\frac{\omega_{P0}^2}{\omega^2}\tan\left(\frac{\xi}{d}\right)\right)}{R_{nl1}^2 f_+^3}\left(1+\frac{\varepsilon_{+0}}{\varepsilon_{0zz}}\right) = 0 \qquad \ldots (4.15)$$

where $R_{nl1}^2 = (1-\omega_c/\omega)^2 r_0^2 \left(\varepsilon_{+0}/\varepsilon_{+2}\, E_0^2\right)$ and $R_{d1} = k_+ r_0^2$

For m=1

$$\left[H_1\left(\frac{\sqrt{2}r}{r_0 f_+(z)}\right)\right]^2 = \frac{8r^2}{f_+^2(z) r_0^2}$$

$$A_0^2 = \frac{E_0^2}{f_+^2(z)} e^{\frac{b^2}{2}\left(\frac{8r^2}{f_+^2(z) r_0^2}\right)}$$

$$\left(Exp\left[-2\left(\frac{r}{f_+(z)r_0}+\frac{b}{2}\right)^2\right]+Exp\left[-2\left(\frac{r}{f_+(z)r_0}-\frac{b}{2}\right)^2\right]+2Exp\left[\left(\frac{-2r}{f_+(z)r_0}+\frac{b^2}{2}\right)\right]\right)$$

Substituting this value in equation (4.11) and simplifying the equation, we get

$$\left\{\frac{\xi\omega_s \sec^2\left(\frac{\xi}{d}\right)}{d}-2\left(1-\omega_s \tan\left(\frac{\xi}{d}\right)\right)\right\}\frac{\partial^2 f_+}{\partial\xi^2}-\frac{\xi\omega_s \sec^2\left(\frac{\xi}{d}\right)}{d}\frac{1}{f_+}\left(\frac{\partial f_+}{\partial\xi}\right)^2-\frac{\xi\omega_s \sec^4\left(\frac{\xi}{d}\right)\omega_{P0}^2\varepsilon_{+0}}{d^2\omega^2\varepsilon_{0zz}^2\left(1+\frac{\varepsilon_{+0}}{\varepsilon_{0zz}}\right)}\frac{\partial f_+}{\partial\xi}$$

$$+\frac{\xi\omega_s^2 \sec^4\left(\frac{\xi}{d}\right)}{d^2\varepsilon_{0zz}\left(1+\frac{\varepsilon_{+0}}{\varepsilon_{0zz}}\right)}\frac{\partial f_+}{\partial\xi}+\frac{2\sec^2\left(\frac{\xi}{d}\right)\left(1-\omega_s \tan\left(\frac{\xi}{d}\right)\right)\omega_{P0}^2\varepsilon_{+0}}{d\omega^2\varepsilon_{0zz}^2\left(1+\frac{\varepsilon_{+0}}{\varepsilon_{0zz}}\right)}\frac{\partial f_+}{\partial\xi}$$

$$-\frac{2\omega_s \sec^2\left(\frac{\xi}{d}\right)\left(1-\omega_s \tan\left(\frac{\xi}{d}\right)\right)}{d\,\varepsilon_{0zz}\left(1+\frac{\varepsilon_{+0}}{\varepsilon_{0zz}}\right)}\frac{\partial f_+}{\partial\xi}+\frac{\left(1+\frac{\varepsilon_{+0}}{\varepsilon_{0zz}}\right)^2\left(1-\frac{\omega_{P0}^2}{\omega^2}\tan\left(\frac{\xi}{d}\right)\right)}{f_+^3}\left(2-2b^2\right)$$

$$+\frac{16R_{d1}^2 e^{\frac{b^2}{2}}\left(1-\frac{\omega_{P0}^2}{\omega^2}\tan\left(\frac{\xi}{d}\right)\right)}{R_{nl1}^2 f_+^3}\left(2-2b^2\right)\left(1+\frac{\varepsilon_{+0}}{\varepsilon_{0zz}}\right)=0 \qquad \ldots(4.16)$$

For m=2

$$H_2\left(\frac{\sqrt{2}r}{r_0 f_+(z)}\right)^2 = \frac{64r^4}{f_+^4(z) r_0^4}-\frac{32r^2}{f_+^2(z) r_0^2}+4$$

$$A_0^2 = \frac{E_0^2}{f_+^2(z)} e^{\frac{b^2}{2}} \left\{ \frac{64r^4}{f_+^4(z)r_0^4} - \frac{32r^2}{f_+^2(z)r_0^2} + 4 \right\}$$

$$\left(Exp\left[-2\left(\frac{r}{f_+(z)r_0} + \frac{b}{2} \right)^2 \right] + Exp\left[-2\left(\frac{r}{f_+(z)r_0} - \frac{b}{2} \right)^2 \right] + 2Exp\left[-\left(\frac{2r}{f_+(z)r_0} + \frac{b^2}{2} \right) \right] \right)$$

Substituting this value in equation (4.11) and simplifying the equation, we get

$$\left\{ \frac{\xi\omega_s \sec^2\left(\frac{\xi}{d}\right)}{d} - 2\left(1 - \omega_s \tan\left(\frac{\xi}{d}\right)\right) \right\} \frac{\partial^2 f_+}{\partial \xi^2} - \frac{\xi\omega_s \sec^2\left(\frac{\xi}{d}\right)}{d} \frac{1}{f_+} \left(\frac{\partial f_+}{\partial \xi} \right)^2 - \frac{\xi\omega_s \sec^4\left(\frac{\xi}{d}\right) \omega_{P0}^2 \varepsilon_{+0}}{d^2\omega^2\varepsilon_{0zz}^2 \left(1 + \frac{\varepsilon_{+0}}{\varepsilon_{0zz}}\right)} \frac{\partial f_+}{\partial \xi}$$

$$+ \frac{\xi\omega_s^2 \sec^4\left(\frac{\xi}{d}\right)}{d^2\varepsilon_{0zz} \left(1 + \frac{\varepsilon_{+0}}{\varepsilon_{0zz}}\right)} \frac{\partial f_+}{\partial \xi} + \frac{2\sec^2\left(\frac{\xi}{d}\right)\left(1 - \omega_s \tan\left(\frac{\xi}{d}\right)\right)\omega_{P0}^2 \varepsilon_{+0}}{d\omega^2\varepsilon_{0zz}^2 \left(1 + \frac{\varepsilon_{+0}}{\varepsilon_{0zz}}\right)}$$

$$- \frac{2\omega_s \sec^2\left(\frac{\xi}{d}\right)\left(1 - \omega_s \tan\left(\frac{\xi}{d}\right)\right)}{d\ \varepsilon_{0zz} \left(1 + \frac{\varepsilon_{+0}}{\varepsilon_{0zz}}\right)} - 12b^2 \frac{\left(1 + \frac{\varepsilon_{+0}}{\varepsilon_{0zz}}\right)^2 \left(1 - \frac{\omega_{P0}^2}{\omega^2} \tan\left(\frac{\xi}{d}\right)\right)}{f_+^3}$$

$$- \frac{32R_{d1}^2 e^{\frac{b^2}{2}} \left(1 - \frac{\omega_{P0}^2}{\omega^2} \tan\left(\frac{\xi}{d}\right)\right)}{R_{nl1}^2 f_+^3} \left(5 - 2b^2\right) \left(1 + \frac{\varepsilon_{+0}}{\varepsilon_{0zz}}\right) = 0 \qquad \text{... (4.17)}$$

Equation (4.15), (4.16) & (4.17) are the required equations for beam width parameter for extraordinary modes of propagation of magnetoplasma. Similarly the equations for beam width parameter for ordinary mode of propagation can be obtained by replacing ω_c by $-\omega_c$ and +ve sign by –ve sign in the subscript of f.

Similarly on solving imaginary part we get the condition $\partial f_\pm / \partial z = 0$ and $f_\pm$ = Constant, for extraordinary and ordinary modes.

4.4 RESULTS AND DISCUSSION

The various parameters taken for numerical calculation are:

$\omega = 1.778X10^{14}$ rad/s, $r_0 = 253\,\mu$m, $e = 1.6X10^{-19}$C, $m = 9.1X10^{-31}$Kg, $c = 3X10^{8}$m/s

The value of the intensity in the present case is $I_0 = 1.84X10^{14}\,W/cm^2$.

Figure 4.1 represents the variation of beam width parameter $(f_{\pm})$ with the normalized propagation distance (ξ) for different values of decentered parameter, $b = 0.00, 3.90, 3.95$ and 4.00 for m=0. The sensitiveness of decentered parameter is also observed in the present case and it supports the previous work of Nanda *et al.* [95]. It is clear from the plot that for extraordinary mode, Fig 4.1(a), beam width parameter decreases with increase in the values of decentered parameter. For $b = 4.00$, beam width parameter falls abruptly at normalized propagation distance, $\xi = 0.10$ and hence self-focusing become strong. In case of ordinary mode same patterns are observed but self-focusing is weak as compare to extraordinary mode of propagation. Gill *et al.* [14] has studied self-focusing and self-phase modulation as well as self-trapping of cosh-Gaussian beam at various values of decentered parameter (b) and concluded that self-focusing become sharper for $b = 2$ and occurs at $\xi = 1.45$ and the value of beam width parameter is nearly 0.91(approximately). In another work Gill *et al.* [84] reported strong self-focusing effect nearly at $\xi = 0.65$. Patil *et al.* [18] has reported strong self-focusing for $m = 0, b = 2$ nearly at $\xi = 0.21$. In the present work, in the presence of density ramp, we report very strong self-focusing which occurs at $\xi = 0.10$ for $b = 4.00$. In case of ordinary mode, Fig 4.1(b), the self-focusing of beam occurs for $b = 0.00, 3.90, 3.95$ and 4.00. For $b = 4.00$, self-focusing effect is very strong; however, it is weaker as compared to extraordinary mode. In the absence of decentered parameter no self-focusing is observed in both the cases.

Figure 4.2 represents the variation of beam width parameter $(f_{\pm})$ with the normalized propagation distance (ξ) for different values of decentered parameter, $b = 0.00, 3.04, 3.09$ and 3.14 for m=1. It is clear from the plot fig. 4.2(a), that with the increase in the values of decentered parameter beam width parameter decreases and hence self-focusing effect is observed. However, for $b = 0$, diffraction term become more dominant over focusing term and causes the defocusing of beam. Fig. 4.2(b), describes the same pattern as that in fig. 4.2(a), however; self-focusing is weaker in this

case. Patil *et al.* [81] has reported strong self-focusing for $m = 1, b = 2$ nearly at $\xi = 1.9$ (approximately) and for $b = 0$ and 1, diffraction effect becomes dominant, both for extraordinary and ordinary modes of propagation. In the present work, in the presence of density ramp, we report very strong self-focusing which occurs at $\xi = 0.10$ for $b = 3.14$ and only for $b = 0$ defocusing of beam occurs while for $b = 1, 2$ and 3, self-focusing of beam occurs and is very strong for $b = 3.14$.

Figure 4.3, represents the variation of beam width parameter with the normalized propagation distance for different values of decentered parameter, $b = 0.00, 1.95, 2.00$ and 2.05 for m=2 for extraordinary mode of propagation. In this case for $b = 1.95, 2.00$ and 2.05, beam exhibit self-focusing effect for both extraordinary and ordinary modes, however, relatively self-focusing is weaker in case of ordinary mode as compared to that in case of extraordinary mode of propagation. While for $b = 0.00$ beam gets defocused both for extraordinary and ordinary mode of propagation. Patil *et al.* [81] has reported strong self-focusing for $m = 2, b = 0$ and 1 nearly at $\xi = 2.3$ (approximately) and for $b = 2$, diffraction effect becomes dominant, both for extraordinary and ordinary modes of propagation. In the present work, in the presence of density ramp, we report very strong self-focusing which occurs at $\xi = 0.10$ for $b = 2.05$, in case of extraordinary mode, fig. 4.3(a) and for $b = 2.049$, in case of ordinary mode of propagation, fig. 4.3(b).

Figure 4.4, represents the variation of beam width parameter with the normalized propagation distance for mode indices $m = 0, 1, 2$ and decentered parameter $b = 3.29$, both for extraordinary, fig. 4.4(a) and ordinary mode of propagation of beam, fig. 4.4(b). It is reported that in case of extraordinary mode, for $m = 2$, self-focusing occurs earlier at $\xi = 0.07$. While for mode indices $m = 0$ and 1, self-focusing occurs at $\xi = 0.16$ and 0.11 respectively. In case of ordinary mode, self-focusing is strong for $m = 2, b = 3.29$ and occurs at $\xi = 0.08$ and thereafter beams starts defocusing for higher values of decentered parameter.

Figure 4.5(a), represents the variation of beam width parameter with normalised propagation distance for extraordinary mode for different values of magnetic field parameter given as $\omega_c / \omega = 0.05, 0.10$ and 0.15. It is investigated that for $m = 0$ and

$b = 3.95$, with the increase in the values of magnetic field parameter, beam width parameter decreases and hence self-focusing ability of beam enhances to greater extent. For $\omega_c / \omega = 0.15$, strong self-focusing is observed than for $\omega_c / \omega = 0.05$, and 0.10. Gupta *et al.* [78] has investigated the addition focusing of a high intensity laser beam in a plasma with density ramp and a magnetic field and reported strong focusing which occur at $\xi = 0.8$ for magnetic field 45MG. However, in our case self-focusing occurs at $\xi = 0.1$ for $\omega_c / \omega = 0.15$. Similar patterns are observed in case of mode indices $m = 1$ and 2, for optimized values of other parameter as taken in case of $m = 0$. Whereas, in case of ordinary mode of propagation, fig. 4.5(b), beam width parameter increases with the increase in the value of magnetic field parameter and hence decreases self-focusing of laser beams.

4.5 CONCLUSION

From the above results, we conclude that the presence of density ramp enhances the self-focusing effect to greater extent and also it occurs earlier with normalized propagation distance. For mode indices $m = 0, 1$ and 2, self-focusing is more commonly observed for higher values of decentered parameter b viz. 4.00, 3.14 and 2.05 respectively both for ordinary and extraordinary mode of propagation of laser beams. However, for ordinary mode, self-focusing is a little bit weaker than extraordinary mode. Decentered parameter decides the focusing/ defocusing nature of Hermite-cosh-Gaussian beam as for b=0, defocusing of beam occurs and for $m = 1$, weaker self-focusing effect is observed. The dependence of beam width parameter on decentered parameter is previously also investigated by Patil *et al.* [81]. For $b = 3.29$, self-focusing of Hermite-cosh-Gaussian laser beam is found to be occurs earlier at $\xi = 0.07$ for mode index $m = 2$ for both modes of propagation. Further, sensitiveness of decentered parameter is observed which strongly supports our previous work [95]. Also with the increase in the value of magnetic field parameter, self-focusing ability of the laser beam increases abruptly. All this happens due to the presence of plasma density ramp and magnetic field. Thus plasma density ramp plays a very vital role to the self-focusing of the Hermite-cosh-Gaussian laser beam and it enhances the self-focusing effect. Present study may be useful for the scientist working on laser-induced fusion.

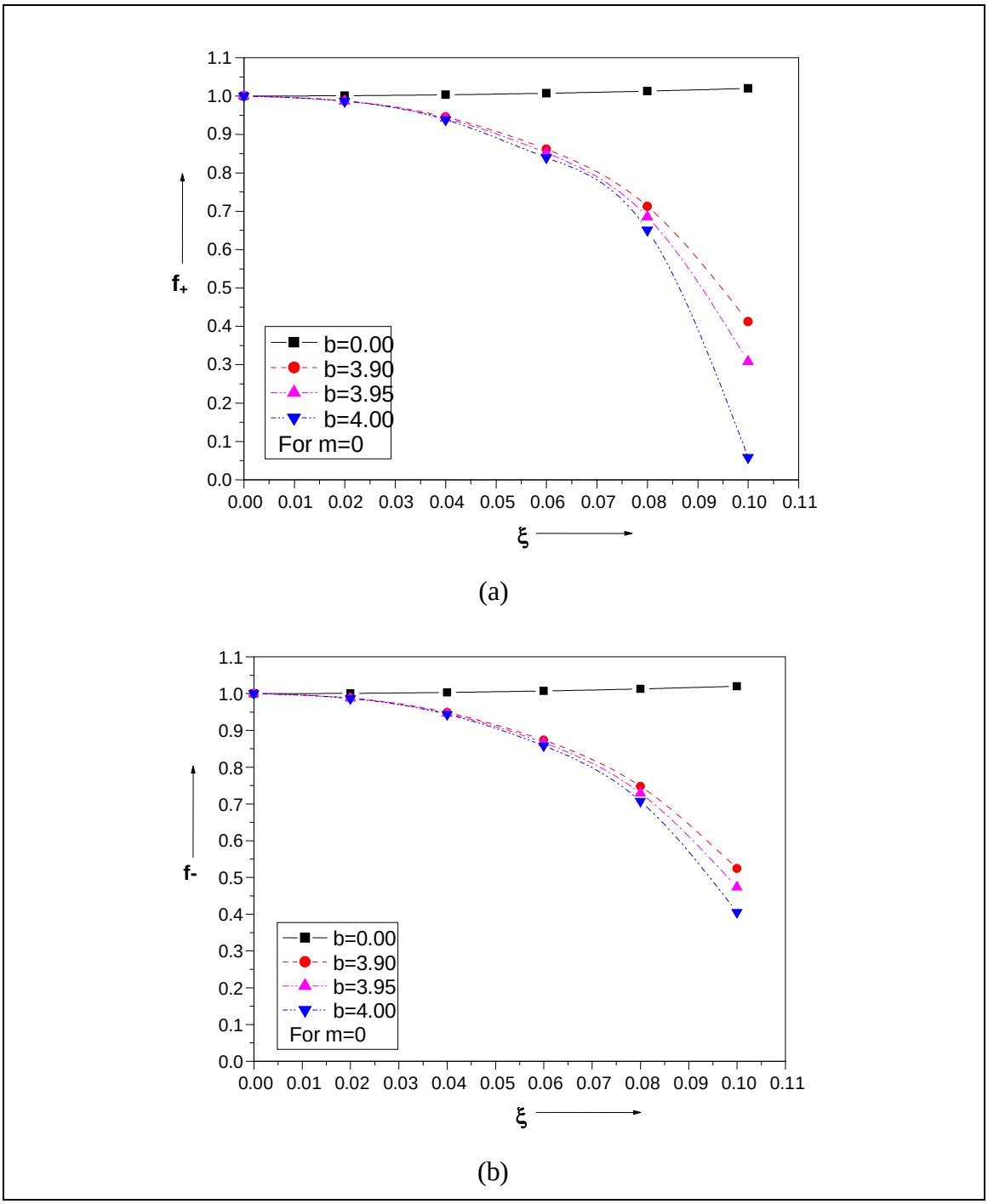

Figure 4.1: Variation of beam width parameter with normalised propagation distance for (a) extraordinary and (b) ordinary mode for different values of decentered parameter. The other various values are taken as $m=0, d=5,$ $\omega r_0/c=150$ $\alpha E_0^2=0.01,$ $\omega_c/\omega=0.10, \omega_{P0}/\omega=0.45$ **and** $m_0/M=0.01.$

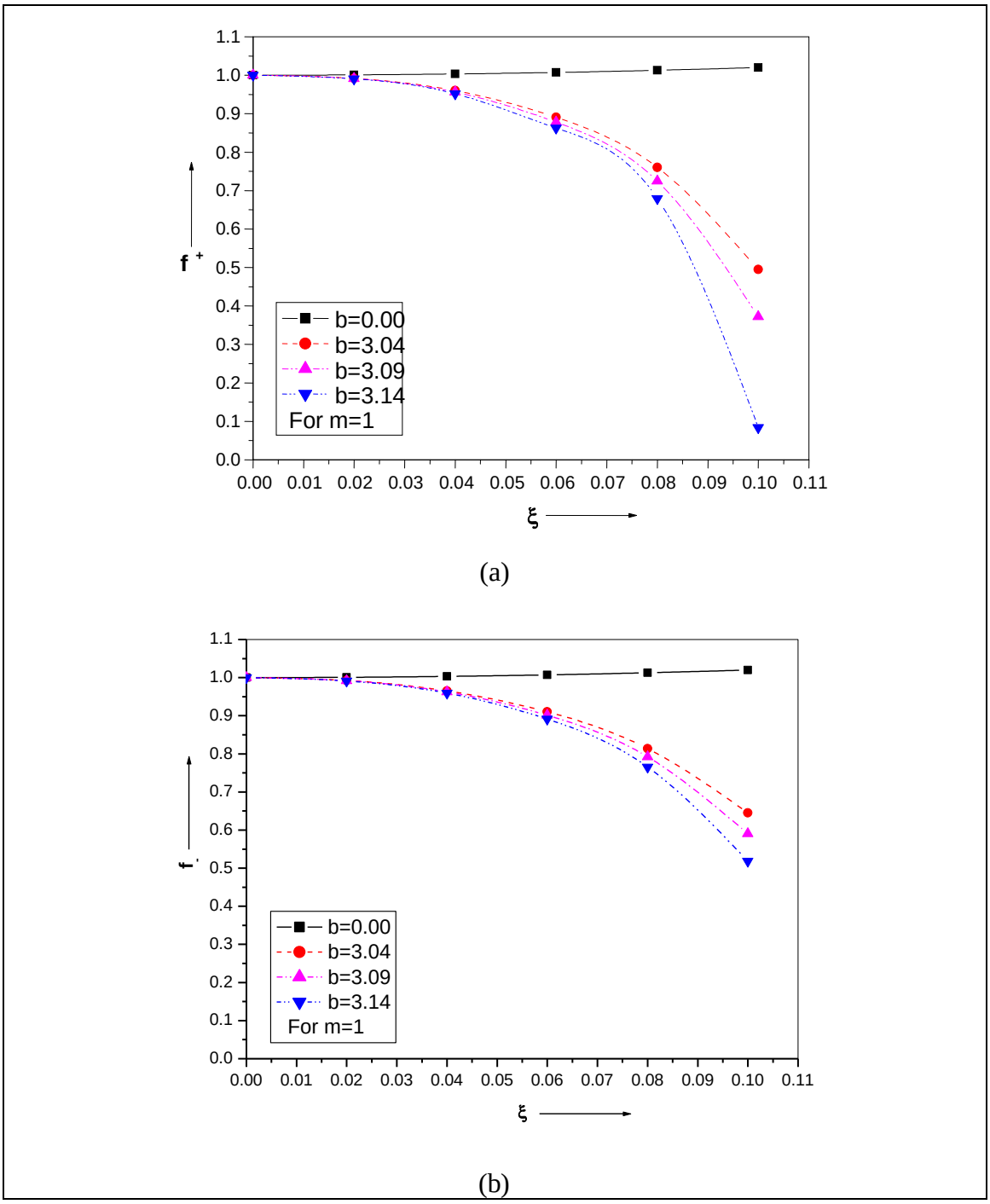

Figure 4.2: Variation of beam width parameter with normalised propagation distance for (a) extraordinary and (b) ordinary mode for different values of decentered parameter. The other various values are taken as $m=1, d=5,$ $\omega r_0/c=150$ $\alpha E_0^2=0.01,$ $\omega_c/\omega=0.10, \omega_{P0}/\omega=0.45$ **and** $m_0/M=0.01.$

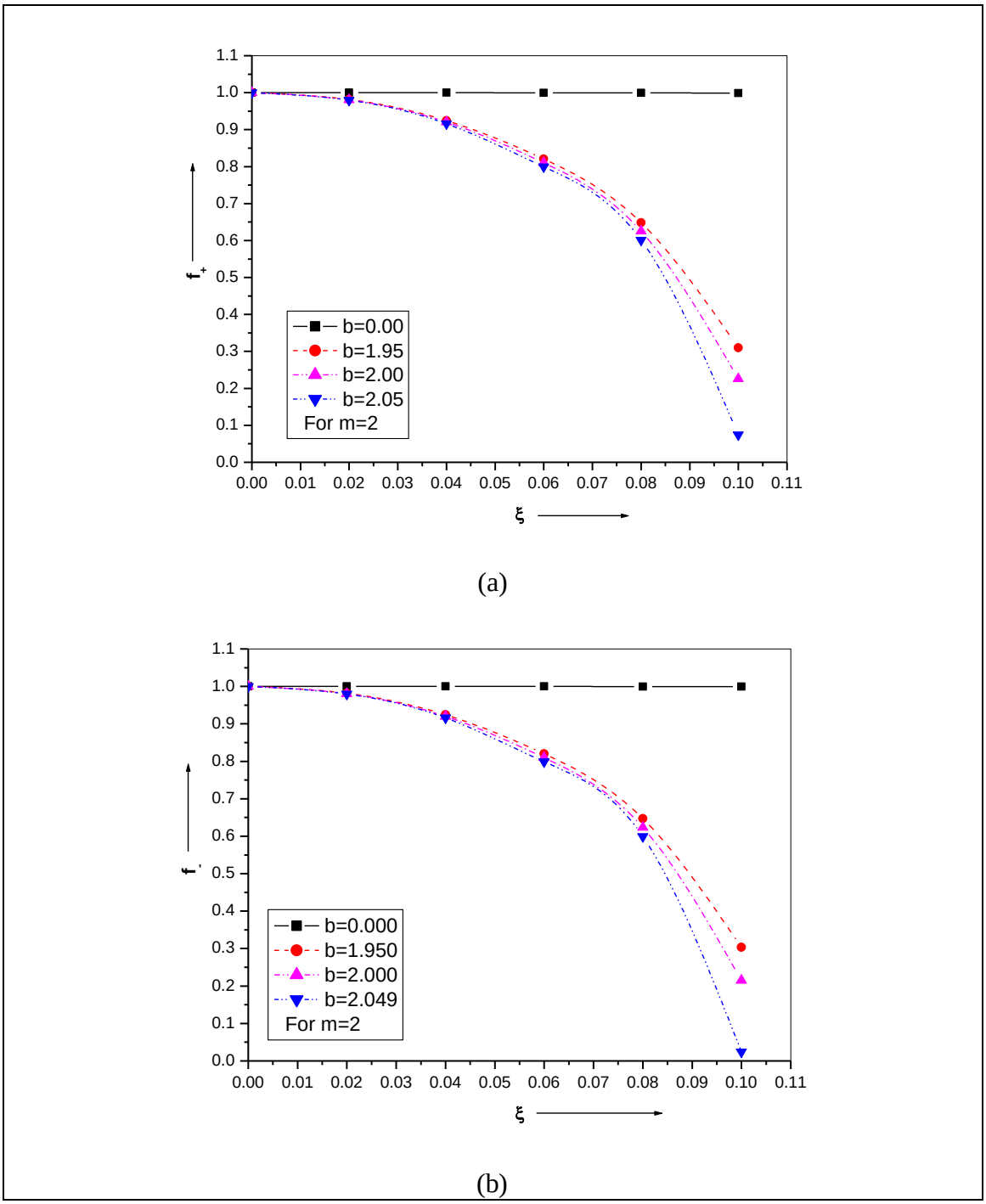

Figure 4.3: Variation of beam width parameter with normalised propagation distance for (a) extraordinary and (b) ordinary mode for different values of decentered parameter. The other various values are taken as $m=2, d=5,$ $\omega r_0/c=150$ $\alpha E_0^2=0.01,$ $\omega_c/\omega=0.10, \omega_{p0}/\omega=0.45$ **and** $m_0/M=0.01.$

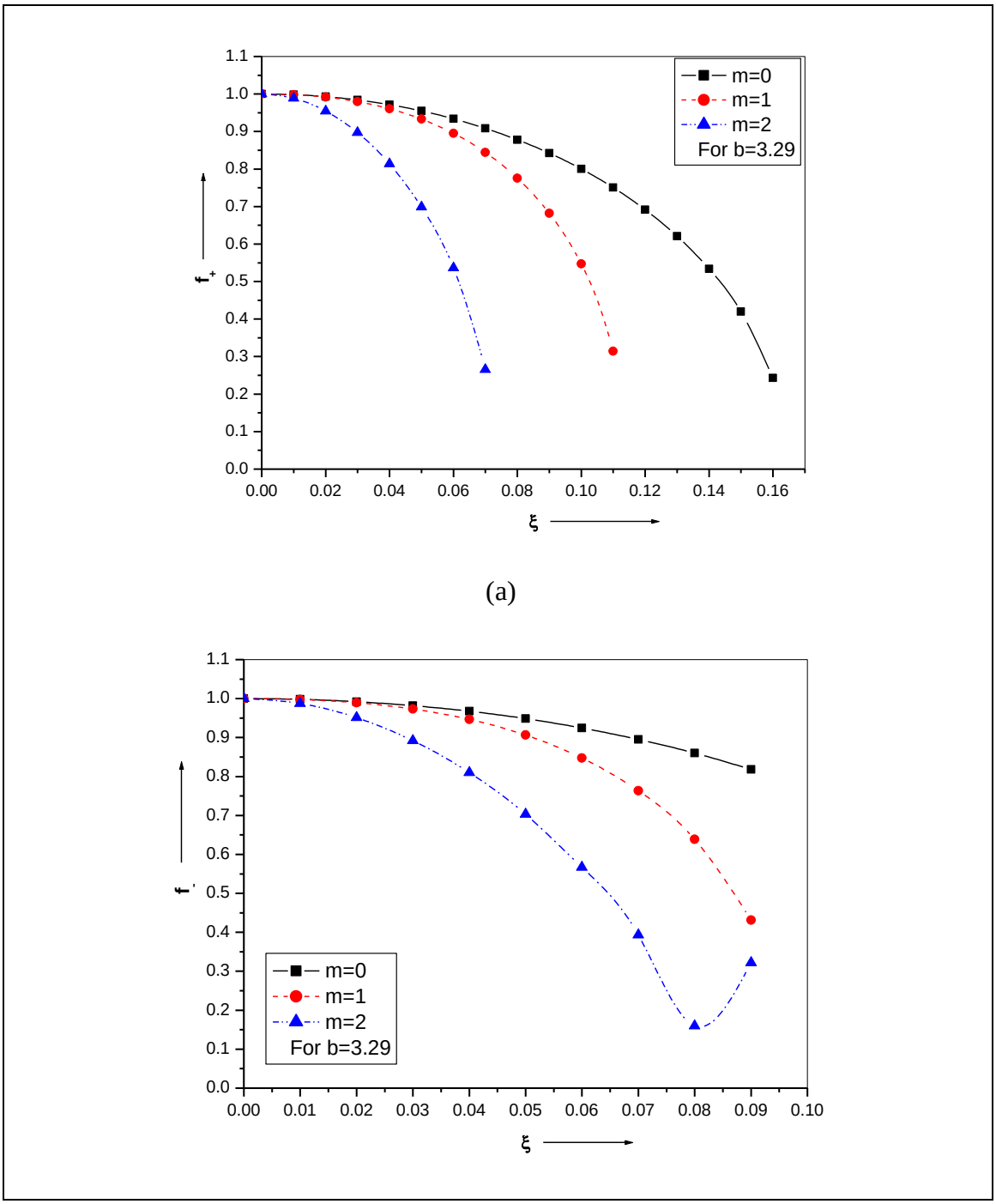

Figure 4.4: Variation of beam width parameter with normalised propagation distance for (a) extraordinary and (b) ordinary mode for mode indices $m = 0, 1$ and 2. **The other various values are taken as** $b = 3.29$, $d = 5$, $\omega r_0 / c = 150$ $\alpha E_0^2 = 0.01$, $\omega_c / \omega = 0.10$, $\omega_{P0} / \omega = 0.45$ **and** $m_0 / M = 0.01$.

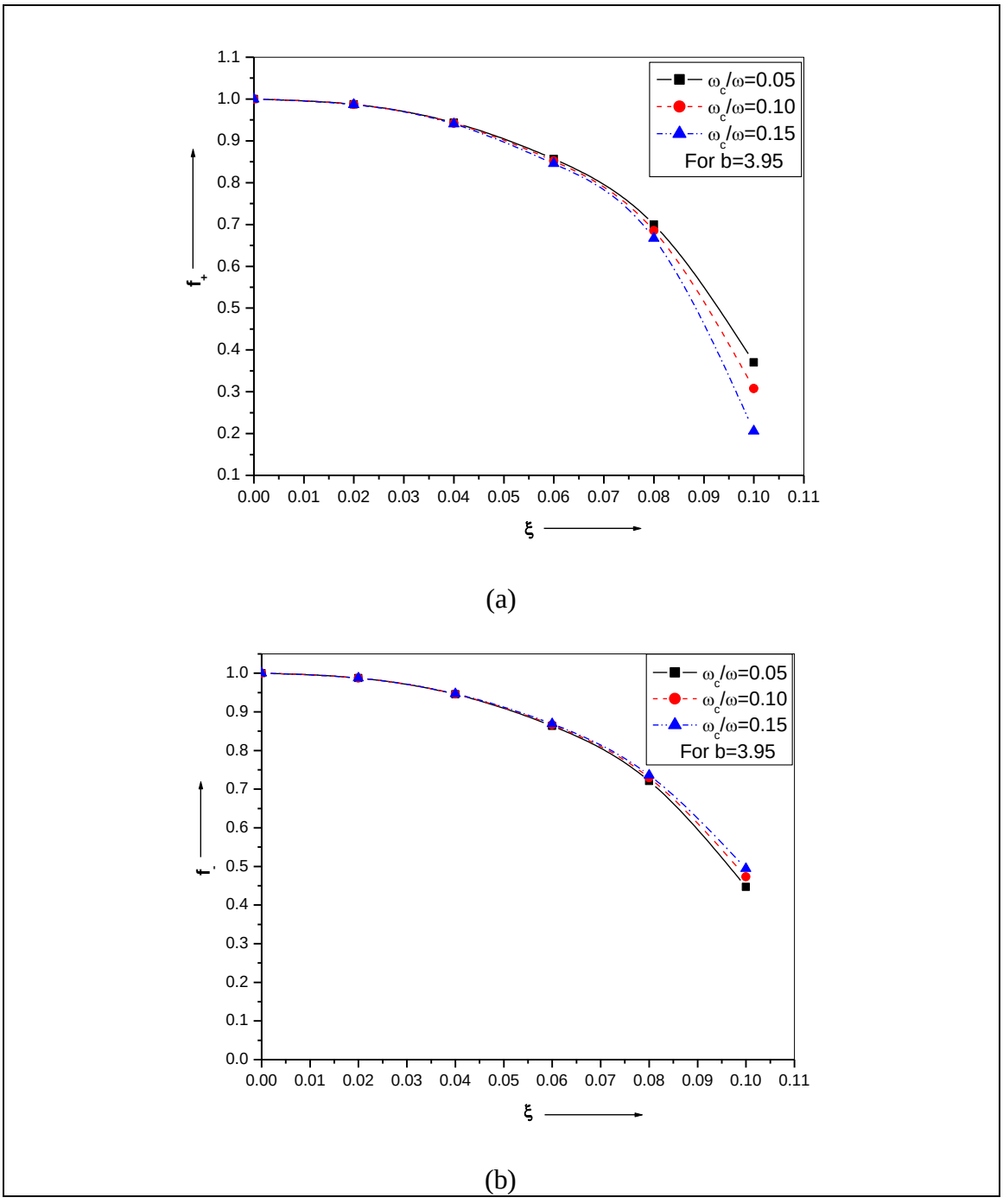

4.5: Variation of beam width parameter with normalised propagation distance for (a) extraordinary and (b) ordinary mode of propagation for different values of ω_c / ω**. The other various values are taken as** $m = 0, b = 3.95, d = 5,$ $\omega r_0 / c = 150$ $\alpha E_0^2 = 0.01,$ $\omega_{P0} / \omega = 0.45$ **and** $m_0 / M = 0.01.$

CHAPTER-5

ENHANCED RELATIVISTIC SELF-FOCUSING OF HERMITE-COSH-GAUSSIAN LASER BEAM IN PLASMA UNDER DENSITY TRANSITION

5.1 INTRODUCTION

After the discovery of the self-focusing of light in 1962 by Askar'yan [1], self-focusing of light becomes the most fascinating and interesting field of research. The propagation of Gaussian beam [2-4], Hermite-Gaussian beam [87], Cosh-Gaussian beam [14], Hermite cosh-Gaussian beam [16-18] etc. are widely studied by researchers for several decades due to its socially useful applications like generation of inertial fusion energy driven by lasers [9-11], the production of quasi mono-energetic electron bunches [12], optical harmonic generation [13], x-rays lasers and laser driven accelerators [8] arising due to self-focusing effect [1-4, 61, 87]. These applications need the laser pulse to propagate over several Rayleigh lengths in the plasmas without loss of energy. Today, extremely high intensity of the order of 10^{20} W/cm^2 produced by short pulse laser technology enabled various high energy related experiments.

As the laser pulse propagates through the plasma, the dielectric constant of plasma changes significantly with the increase in intensity of the laser beam and it leads to the self-focusing of the laser beam [85, 87] which may be relativistic or ponderomotive or thermal self-focusing in nature. The combined effect of relativistic self-focusing and axial nonlinear force results in the acceleration of tin ions up to 5 GeV energy [89]. The high intensity laser pulses provide sufficient energy to the constituents like electrons of the plasma which cause an electron oscillatory velocity comparable to the velocity of light. Thus the mass of electron, oscillating at relativistic velocities in laser field, increases by a factor given by $\gamma = 1/\sqrt{1-v^2/c^2}$ and give rise to non-linearity due to which the relativistic self-focusing effect occurs. Earlier, the relativistic self-focusing of laser beam in plasma has been studied by Hora [88]. Relativistic self-focusing and self-channeling of an intense laser pulse in an underdense plasma has been experimentally studied by Gibbon *et al.* [57]. Relativistic self-focusing of an intense laser under plasma density ramp has been theoretically investigated by Gupta *et al.* [77]. Self-focusing in a plasma due to ponderomotive forces and relativistic effects has been studied by Siegrist

[3], Relativistic self-focusing and self-channeling of Gaussian laser beam has been studied by Singh *et al.* [88]. Relativistic focusing and ponderomotive channelling of intense laser beam has been investigated theoretically by Hafizi *et al.* [59].

In the present study, propagation of Hermite cosh-Gaussian beam in plasma under density transition has been studied. Hermite-cosh-Gaussian beam is one of the solutions of paraxial wave equation and such HChG beam can be obtained in the laboratory by the superposition of two decentered Hermite-Gaussian beams as Cosh-Gaussian ones. Propagation of Hermite-cosh-Gaussian beam in plasma [16-18] and in magneto-plasma [81, 95, 96] has been studied earlier.

In the present work, enhanced relativistic self-focusing of Hermite-cosh-Gaussian laser beam in plasma under density transition has been reported theoretically. Application of plasma density ramp profile to the medium is not new to researcher as earlier it has been applied by Kant *et al.* [85, 87], Gupta *et al.* [77] etc. under various beam profiles and conditions. We develop the equations for beam width parameter for HChG beam in the presence of plasmas density ramp and solve them numerically by applying Wentzel-Kramers-Brillouin (WKB) approximation and Paraxial approximation [4, 90] for mode indices $m = 0, 1 \text{ and } 2,$ and observed the enhancement of self-focusing of the laser beam. In this work, for the sake of simplicity, we have not assumed the longitudinal components of laser field and only the transversal components of laser field are evaluated, but for exact formulation, one should consider the longitudinal components during dealing with non linearity [52].

5.2 EVOLUTION OF BEAM WIDTH PARAMETER

The field distribution of HChG laser beam propagating in the plasma along z-axis is of the following form:

$$E(r,z) = \frac{E_0}{f(z)}\left[H_m\left(\frac{\sqrt{2}r}{r_0 f(z)}\right)\right]e^{\frac{b^2}{4}}\left(Exp\left[-\left(\frac{r}{r_0 f(z)}+\frac{b}{2}\right)^2\right]+Exp\left[-\left(\frac{r}{r_0 f(z)}-\frac{b}{2}\right)^2\right]\right) \quad \ldots (5.1)$$

here E_0 is the amplitude of HChG laser beam for the central position at $r = z = 0$, '$f(z)$' is the dimensionless beam width parameters, 'H_m' is the Hermite polynomial of 'm^{th}' order, 'r_0' is the spot size of the beam and 'b' is the decentered parameter of the beam. This propagating beam imparts an oscillatory velocity, $v = eE/m_0\omega\gamma$, to the electrons. Here e, m_0 and ω are the charge on electron, rest mass of electron and angular frequency of incident laser beam respectively, and $\gamma = \sqrt{1+\alpha EE^*}$, is the intensity dependent relativistic factor with $\alpha = e^2/m_0^2\omega^2c^2$, here c is the speed of light in vacuum. The intensity dependent dielectric constant for the non-linear medium is obtained by applying the approach given by Sodha *et al.* [4]:

$$\varepsilon = \varepsilon_0 + \phi(EE^*) \qquad \ldots (5.2)$$

where $\varepsilon_0 = 1-\omega_P^2/\omega^2$, is linear part of the dielectric constant with ω_P is plasma frequency. In the absence of density transition and considering relativistic mass of electron $m_e = m_0\gamma$, therefore, dielectric constant of the plasma is modified to the form, $\varepsilon_{\text{rel}} = 1-\omega_{P0}^2/\gamma\omega^2$ with $\omega_{P0} = \left(4\pi e^2 n_0/m_0\right)^{1/2}$ is the equilibrium plasma frequency.

The intensity dependent non-linear part of the dielectric constant is given by

$$\phi(EE^*) = \left(\frac{\omega_{P0}^2}{\omega^2}\right)\left[1-\frac{1}{(1+\alpha EE^*)^{1/2}}\right] \qquad \ldots (5.3a)$$

Now, in the presence of plasma density ramp given by relation, $n(\xi) = n_0 + n_0\tan(\xi/d)$, and using $m_e = m_0\gamma$, the dielectric constant of the plasma is modified to the form given by $\varepsilon(z) = 1-\left(\omega_{P0}^2/\gamma\omega^2 + \omega_{P0}^2\tan(\xi/d)/\gamma\omega^2\right)$, where $\xi = z/R_d$, is the normalized propagation distance, R_d is the diffraction length and d is adjustable constant.

Thus, intensity dependent non-linear part of the dielectric constant is given by

$$\phi(EE^*) = \left(\frac{\omega_{P0}^2}{\omega^2} + \frac{\omega_{P0}^2\tan(\xi/d)}{\omega^2}\right)\left[1-\frac{1}{(1+\alpha EE^*)^{1/2}}\right] \qquad \ldots (5.3b)$$

The value of $\phi(EE^*)$ is obtained by applying Taylor expansion in terms of r^2 and neglecting terms containing higher powers of r.

For isotropic, non conducting and non absorbing medium (for set of values $J=0,\ \rho=0$) with $\mu=1$, Maxwell's equations give the following wave equation

$$\nabla^2\vec{E}-\frac{\varepsilon}{c^2}\frac{\partial^2\vec{E}}{\partial t^2}+\vec{\nabla}\left(\vec{E}\frac{\vec{\nabla}(\varepsilon)}{\varepsilon}\right)=0 \qquad \ldots (5.4)$$

For $(1/K^2)\nabla^2(\ln\varepsilon)<<1$, we get,

$$\frac{\partial^2\vec{E}}{\partial z^2}+\frac{\partial^2\vec{E}}{\partial r^2}+\frac{1}{r}\frac{\partial\vec{E}}{\partial r}+\frac{\varepsilon\omega^2}{c^2}\vec{E}=0 \qquad \ldots (5.5)$$

We know that the solution of Eq. (5.5) is of the form,

$$\vec{E}=A(r,z)\exp\left[i(\omega t-kz)\right] \qquad \ldots (5.6)$$

where $k=(\varepsilon_{\text{rel}})^{1/2}\omega/c$, in the absence of density transition and $k=(\varepsilon(z))^{1/2}\omega/c$, in the presence of density transition. Substituting this value in Eq. (5) and neglecting $\partial^2 A/\partial z^2$, we get a complex differential equation with real and imaginary parts which are separated by introducing an additional eikonal $A(r,z)=A_0(r,z)\exp\left[-ikS(r,z)\right]$, here $'A_0'$ and $'S'$ are the real functions of $'r'$ and $'z'$ respectively. Following calculations are given, here, in the presence of density transition and by applying similar approach; we obtained the equations for beam width parameter in the absence of density transition.

Real part is

$$-2\frac{\partial S}{\partial z}+\frac{S\omega^2\sec^2(z/dR_d)}{c^2k^2dR_d}\frac{\omega_{P0}^2}{\gamma\omega^2}+\frac{z\omega^2\sec^2(z/dR_d)}{c^2k^2dR_d}\frac{\omega_{P0}^2}{\gamma\omega^2}\frac{\partial S}{\partial z}$$

$$-\frac{zS\omega^4\sec^4(z/dR_d)}{2c^4k^4d^2R_d^2}\left(\frac{\omega_{P0}^2}{\gamma\omega^2}\right)^2+\frac{z\omega^2\sec^2(z/dR_d)}{c^2k^2dR_d}\frac{\omega_{P0}^2}{\gamma\omega^2}$$

$$-\frac{z^2\omega^4\sec^4(z/dR_d)}{4c^4k^4d^2R_d^2}\left(\frac{\omega_{P0}^2}{\gamma\omega^2}\right)^2-\left(\frac{\partial S}{\partial r}\right)^2+\frac{1}{2A_0^2k^2}\frac{\partial^2A_0^2}{\partial r^2}-\frac{1}{4A_0^4k^2}\left(\frac{\partial A_0^2}{\partial r}\right)^2$$

$$+\frac{1}{2rA_0^2k^2}\left(\frac{\partial A_0^2}{\partial r}\right)+\frac{\phi(A_0^2)}{\varepsilon_0}=0 \qquad \ldots (5.7)$$

Imaginary part is

$$-\frac{1}{A_0^2}\left(\frac{\partial A_0^2}{\partial z}\right)+\frac{\omega^2\sec^2(z/dR_d)}{c^2k^2dR_d}\frac{\omega_{P0}^2}{\gamma\omega^2}+\frac{z\omega^2\sec^2(z/dR_d)\tan(z/dR_d)}{c^2k^2d^2R_d^2}\frac{\omega_{P0}^2}{\gamma\omega^2}$$

$$+\frac{z\omega^4\sec^4(z/dR_d)}{4c^4k^4d^2R_d^2}\frac{\omega_{P0}^2}{\gamma\omega^2}-\frac{z\omega^2\sec^2(z/dR_d)}{2c^2k^2dR_dA_0^2}\frac{\omega_{P0}^2}{\gamma\omega^2}\frac{\partial A_0^2}{\partial z}-\frac{\partial^2 S}{\partial r^2}$$

$$-\frac{1}{A_0^2}\frac{\partial S}{\partial r}\frac{\partial A_0^2}{\partial r}-\frac{1}{r}\frac{\partial S}{\partial r}=0 \qquad \text{... (5.8)}$$

The solution of equation (7) & (8) are of the form,

$$A_0^2=\frac{E_0^2}{f^2(z)}\left[H_m\left(\frac{\sqrt{2}r}{r_0 f}\right)\right]^2 e^{\frac{b^2}{2}}$$

$$\left(Exp\left[-2\left(\frac{r}{r_0 f(z)}+\frac{b}{2}\right)^2\right]+Exp\left[-2\left(\frac{r}{r_0 f(z)}-\frac{b}{2}\right)^2\right]+2Exp\left[-\left(\frac{2r^2}{r_0^2 f^2(z)}+\frac{b^2}{2}\right)\right]\right)$$

… (5.9)

And

$$S=\frac{r^2}{2}\beta(z)+\varphi(z) \qquad \text{… (5.10)}$$

with, $\beta(z)=(1/f(z))df/dz.$ where '$\varphi(z)$' is an arbitrary function of 'z'.

Using these values in Eq. (5.7), we obtain the equation governing the evolution of beam with parameter,

For m=0

$$\left[H_0\left(\frac{\sqrt{2}r}{r_0 f(z)}\right)\right]^2=1$$

Thus

$$A_0^2=\frac{E_0^2}{f^2(z)}e^{\frac{b^2}{2}}$$

$$\left(Exp\left[-2\left(\frac{r}{r_0 f(z)}+\frac{b}{2}\right)^2\right]+Exp\left[-2\left(\frac{r}{r_0 f(z)}-\frac{b}{2}\right)^2\right]+2Exp\left[-\left(\frac{2r^2}{r_0^2 f^2(z)}+\frac{b^2}{2}\right)\right]\right)$$

In the presence of density transition

$$\left[\frac{\xi\sec^2(\xi/d)}{2d\left\{1-\frac{\omega_{P0}^2}{\gamma\omega^2}-\frac{\omega_{P0}^2\tan(\xi/d)}{\gamma\omega^2}\right\}}\left(\frac{\omega_{P0}^2}{\gamma\omega^2}\right)-1\right]\frac{d^2f}{d\xi^2}$$

$$-\frac{\xi\sec^2(\xi/d)}{2d\left\{1-\frac{\omega_{P0}^2}{\gamma\omega^2}-\frac{\omega_{P0}^2\tan(\xi/d)}{\gamma\omega^2}\right\}}\left(\frac{\omega_{P0}^2}{\gamma\omega^2}\right)\frac{1}{f}\left(\frac{df}{d\xi}\right)^2+\frac{\left(4-4b^2\right)}{f^3}$$

$$-\frac{4\alpha E_0^2}{f^3}\left(\frac{\omega_{P0}^2}{\omega^2}+\frac{\omega_{P0}^2\tan(\xi/d)}{\omega^2}\right)\left(\frac{\omega r_0}{c}\right)^2\left(1+\frac{4\alpha E_0^2}{f^2}\right)^{-\frac{3}{2}}e^{\frac{b^2}{2}}=0 \qquad \ldots(5.11a)$$

Similarly, in the absence of density transition

$$\frac{d^2f}{d\xi^2}=\frac{\left(4-4b^2\right)}{f^3}-\frac{4\alpha E_0^2}{f^3}\left(\frac{\omega_{P0}^2}{\omega^2}\right)\left(\frac{\omega r_0}{c}\right)^2\left(1+\frac{4\alpha E_0^2}{f^2}\right)^{-\frac{3}{2}}e^{\frac{b^2}{2}} \qquad \ldots(5.11b)$$

For m=1

$$\left[H_1\left(\frac{\sqrt{2}r}{r_0f(z)}\right)\right]^2=\frac{8r^2}{f^2(z)r_0^2}$$

$$A_0^2=\frac{E_0^2}{f^2(z)}e^{\frac{b^2}{2}}\left(\frac{8r^2}{f^2(z)r_0^2}\right)$$

$$\left(Exp\left[-2\left(\frac{r}{r_0f(z)}+\frac{b}{2}\right)^2\right]+Exp\left[-2\left(\frac{r}{r_0f(z)}-\frac{b}{2}\right)^2\right]+2Exp\left[-\left(\frac{2r^2}{r_0^2f^2(z)}+\frac{b^2}{2}\right)\right]\right)$$

In the presence of density transition

$$\left[\frac{\xi\sec^2(\xi/d)}{2d\left\{1-\frac{\omega_{P0}^2}{\gamma\omega^2}-\frac{\omega_{P0}^2\tan(\xi/d)}{\gamma\omega^2}\right\}}\left(\frac{\omega_{P0}^2}{\gamma\omega^2}\right)-1\right]\frac{d^2f}{d\xi^2}-\frac{\xi\sec^2(\xi/d)}{2d\left\{1-\frac{\omega_{P0}^2}{\gamma\omega^2}-\frac{\omega_{P0}^2\tan(\xi/d)}{\gamma\omega^2}\right\}}\left(\frac{\omega_{P0}^2}{\gamma\omega^2}\right)\frac{1}{f}\left(\frac{df}{d\xi}\right)^2$$

$$+\frac{\left(4-4b^2\right)}{f^3}-\frac{8\alpha E_0^2}{f^3}\left(\frac{\omega_{P0}^2}{\omega^2}+\frac{\omega_{P0}^2\tan(\xi/d)}{\omega^2}\right)\left(\frac{\omega r_0}{c}\right)^2e^{\frac{b^2}{2}}\left(b^2-2\right)=0 \qquad \ldots(5.12a)$$

Similarly, in the absence of density transition

$$\frac{d^2 f}{d\xi^2} = \frac{\left(4-4b^2\right)}{f^3} - \frac{8\alpha E_0^2}{f^3}\left(\frac{\omega_{P0}^2}{\omega^2}\right)\left(\frac{\omega r_0}{c}\right)^2 e^{\frac{b^2}{2}}\left(b^2-2\right) \qquad \ldots (5.12b)$$

For m=2

$$\left[H_2\left(\frac{\sqrt{2}r}{r_0 f(z)}\right)\right]^2 = \frac{64r^4}{f^4(z)r_0^4} - \frac{32r^2}{f^2(z)r_0^2} + 4$$

$$A_0^2 = \frac{E_0^2}{f^2(z)} e^{\frac{b^2}{2}}\left(\frac{64r^4}{f^4(z)r_0^4} - \frac{32r^2}{f^2(z)r_0^2} + 4\right)$$

$$\left(Exp\left[-2\left(\frac{r}{r_0 f(z)} + \frac{b}{2}\right)^2\right] + Exp\left[-2\left(\frac{r}{r_0 f(z)} - \frac{b}{2}\right)^2\right] + 2Exp\left[-\left(\frac{2r^2}{r_0^2 f^2(z)} + \frac{b^2}{2}\right)\right]\right)$$

In the presence of density transition

$$\left[\frac{\xi \sec^2(\xi/d)}{2d\left\{1-\frac{\omega_{P0}^2}{\gamma\omega^2} - \frac{\omega_{P0}^2 \tan(\xi/d)}{\gamma\omega^2}\right\}}\left(\frac{\omega_{P0}^2}{\gamma\omega^2}\right) - 1\right]\frac{d^2 f}{d\xi^2} + \frac{\left(4-4b^2\right)}{f^3}$$

$$- \frac{\xi \sec^2(\xi/d)}{2d\left\{1-\frac{\omega_{P0}^2}{\gamma\omega^2} - \frac{\omega_{P0}^2 \tan(\xi/d)}{\gamma\omega^2}\right\}}\left(\frac{\omega_{P0}^2}{\gamma\omega^2}\right)\frac{1}{f}\left(\frac{df}{d\xi}\right)^2$$

$$- \frac{16\alpha E_0^2}{f^3}\left(\frac{\omega_{P0}^2}{\omega^2} + \frac{\omega_{P0}^2 \tan(\xi/d)}{\omega^2}\right)\left(\frac{\omega r_0}{c}\right)^2\left(1+\frac{16\alpha E_0^2}{f^2}\right)^{-\frac{3}{2}} e^{\frac{b^2}{2}}\left(5-2b^2\right) = 0$$

$$\ldots (5.13a)$$

Similarly, in the absence of density transition

$$\frac{d^2 f}{d\xi^2} = \frac{\left(4-4b^2\right)}{f^3} - \frac{16\alpha E_0^2}{f^3}\left(\frac{\omega_{P0}^2}{\omega^2}\right)\left(\frac{\omega r_0}{c}\right)^2\left(1+\frac{16\alpha E_0^2}{f^2}\right)^{-\frac{3}{2}} e^{\frac{b^2}{2}}\left(5-2b^2\right) \qquad \ldots (5.13b)$$

Similarly Eq. (5.8) gives the boundary conditions, $\xi = 0,\ f = 1$ and $df/d\xi = 0$.

5.3 RESULTS AND DISCUSSION

Numerical simulation has been done by taking the frequency and spot size of incident laser beam as $\omega = 1.778 \times 10^{15}\,\text{rad/}s$ and $r_0 = 80.82\mu\text{m}$ respectively. Equations (5.11a, 5.11b), (5.12a, 5.12b) and (5.13a, 5.13b) have been solved numerically using above mentioned values of physical quantities to analyze the effect of density transition and decentered parameter on self-focusing of HChG beam for mode indices $m = 0, 1 \text{ and } 2$. In the present study, we assume the plasmas density ramp profile given by the relation $n(\xi) = (n_0 + n_0 \tan(\xi / d_0))$ with initial electron density $n_0 = 0.503 \times 10^{21} cm^{-3}$ and $d = 0.05$. Figure 1 depicts the comparative study of variation of beam width parameter (*f*) with the normalized propagation distance (ξ) for mode indices $m = 0, 1 \text{ and } 2$ in the presence and absence of density transition and the intensity of incident laser beam is taken to be $I = 1.23 \times 10^{17} W / cm^2$. For $m = 0,$ from figure 5.1(a), one can, clearly see the influence of density transition on the propagating HChG beam through the plasma as the beam propagates deep into the plasma, its converging tendency shifted towards lower value of normalized propagation distance. In the absence of density transition self-focusing of beam occurs at higher values of normalized propagation distance; however, initially two curves follows the same track. This happens because, initially, there is infinitesimal change in the density of the medium at smaller values of normalized propagation distance. But as the normalized propagation distance increase, the density of the medium rises and beam propagating through it converge earlier than a beam propagating in plasma of uniform density. Plasma density ramp for relativistic self-focusing of an intense laser has been studied by Gupta *et al.* [77] and reported strong self-focusing which occurs nearly at $\xi = 0.5.$ In the present case, strong self-focusing of HChG beam occurs at $\xi = 0.005$ Similarly for $m = 1,$ figure 5.1(b), it is observable that beam propagating in the plasma with and without density transition gets diffracted. In case of $m = 2,$ figure 5.1(c), beam converges strongly and hence self-focusing effect becomes stronger. It is observable that presence of density transition enhances the self-focusing tendency of the laser beam. It is noticed that for $m = 0 \,\&\, 2,$ HChG beam converges strongly due to the dominance of focusing term over diffraction term in equations (5.11a) and (5.13a) respectively. Previously, Kant *et al.* [85] have studied ponderomotive self-

focusing of a short laser pulse under plasma density ramp and reported strong self-focusing for $\omega_{p0}^2/\omega^2 = 0.08,$ which occurs nearly at $\xi = 0.5.$ In the present case, enhancement in self-focusing is observed for smaller values of normalized propagation distance.

Figure 5.2 depicts the variation of the beam width parameter (*f*) with the normalized propagation distance (ξ) at different values of decentered parameters in the presence of density transition for mode index $m = 0, 1 \text{ and } 2.$ For $m = 0 \text{ and } b = 1.8,$ figure 5.2(a), stronger self-focusing of beams is observed at $\xi = 0.003.$ It is clear from the figure 5.2(a) that with the increase in the value of decentered parameter 'b', self-focusing of HChG beam enhanced and shifted towards lower values of normalized propagation distance. Patil *et al.* [81] has studied focusing of Hermite-cosh-Gaussian laser beams in collisionless magnetoplasma and reported strong self-focusing. In the present case, HChG beam converges earlier than results reported by Patil *et al.* [81]. Figure 5.2(b) depicts that for $m = 1 \text{and } b = 0 \& 0.9,$ diffraction term dominates over focusing term; however, for $b = 1.8,$ strong self-focusing is observed. The trends followed by curves supports the previous work of Patil *et al.* [81] in which strong self-focusing is reported nearly at $\xi = 0.002,$ for $b = 2;$ however, in the present case self-focusing occurs at $\xi = 0.001$ for $b = 1.8.$ This happens due to the plasmas density transition. From figure 5.2(c), it is clear that for $m = 2,$ self-focusing is observed for $b = 0 \text{ and } 0.9;$ however, for higher values of decentered parameter diffraction term in equation (5.13a) becomes dominant. Similar plot trends are followed in the present case for $b = 1.8 \& 2.7,$ as that reported by Patil *et al.* [81]. In another works Patil *et al.* [17, 18] reported the similar behavior of HChG beam at different values of decentered parameter for $m = 0, 1 \text{ and } 2.$ A comparative study between the results reported by Patil *et al.* [17, 18] and the results reported in the present case at different values of decentered parameter for $m = 0, 1 \text{ and } 2,$ indicates the enhancement in the self-focusing which occur at smaller values of normalized propagation distance. Thus, we report that the spot size of the HChG beam shrinks as it propagates deeper inside the non linear medium with density transition in order to avoid the violation of basic laws of physics.

5.4 CONCLUSION

In the present investigation we have studied the relativistic self-focusing of HChG laser beam in plasma under density transition. We have derived the equation of beam width parameter using WKB approximation and paraxial ray approach and reported enhancement of self-focusing of HChG beam. The self-focusing of HChG laser beam in plasma for mode indices $m = 0, 1 \text{ and } 2$ is investigated and it is observed that as the beam propagates deeper inside the plasma under density transition, the self-focusing ability of the beam enhances and occurs earlier than the beam propagating in the plasma with uniform density. Moreover, self-focusing becomes stronger with the increase in values of the decentered parameter at a particular intensity for mode indices $m = 0 \text{ and } 1$. We conclude that spot size of the HChG beam shrinks greatly as it propagates deeper inside the plasma with density transition. The present study may help the investigators to choose the intensity parameter as per their requirement by the proper selection of the decentered parameter leads to substantial improvement in the focusing quality which may be useful in inertial fusion energy driven by lasers.

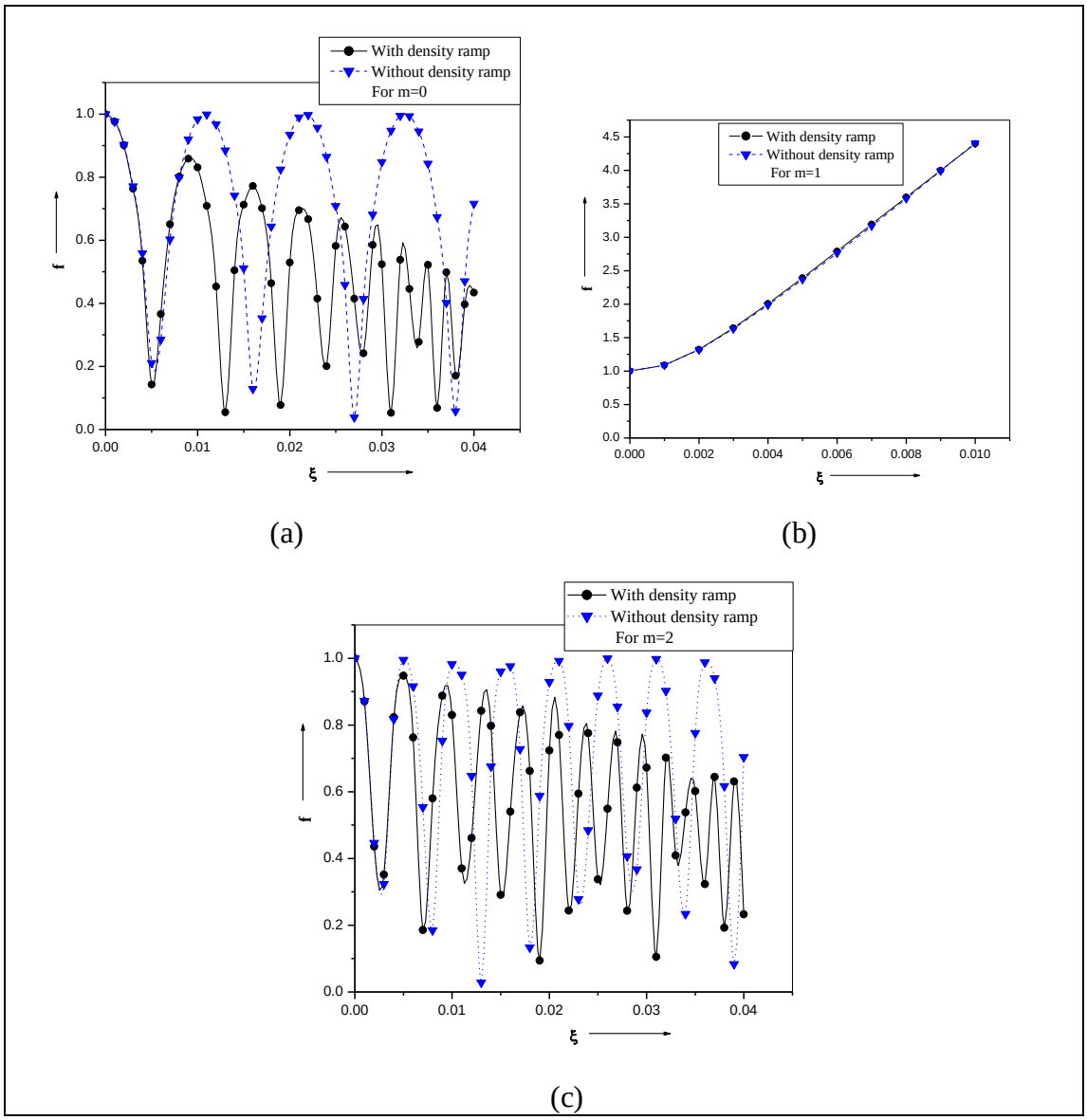

Figure 5.1: Variation of beam width parameter (f) with normalized propagation distance (ξ) for $m=0$, (a), $m=1$, (b) and $m=2$, (c) with and without density ramp. The various parameters are taken as $\alpha E_0^2 = 0.1$, $\omega_{P0}/\omega = 0.75$, $b = 0.9$, $\omega r_0/c = 479$, $d = 0.05$.

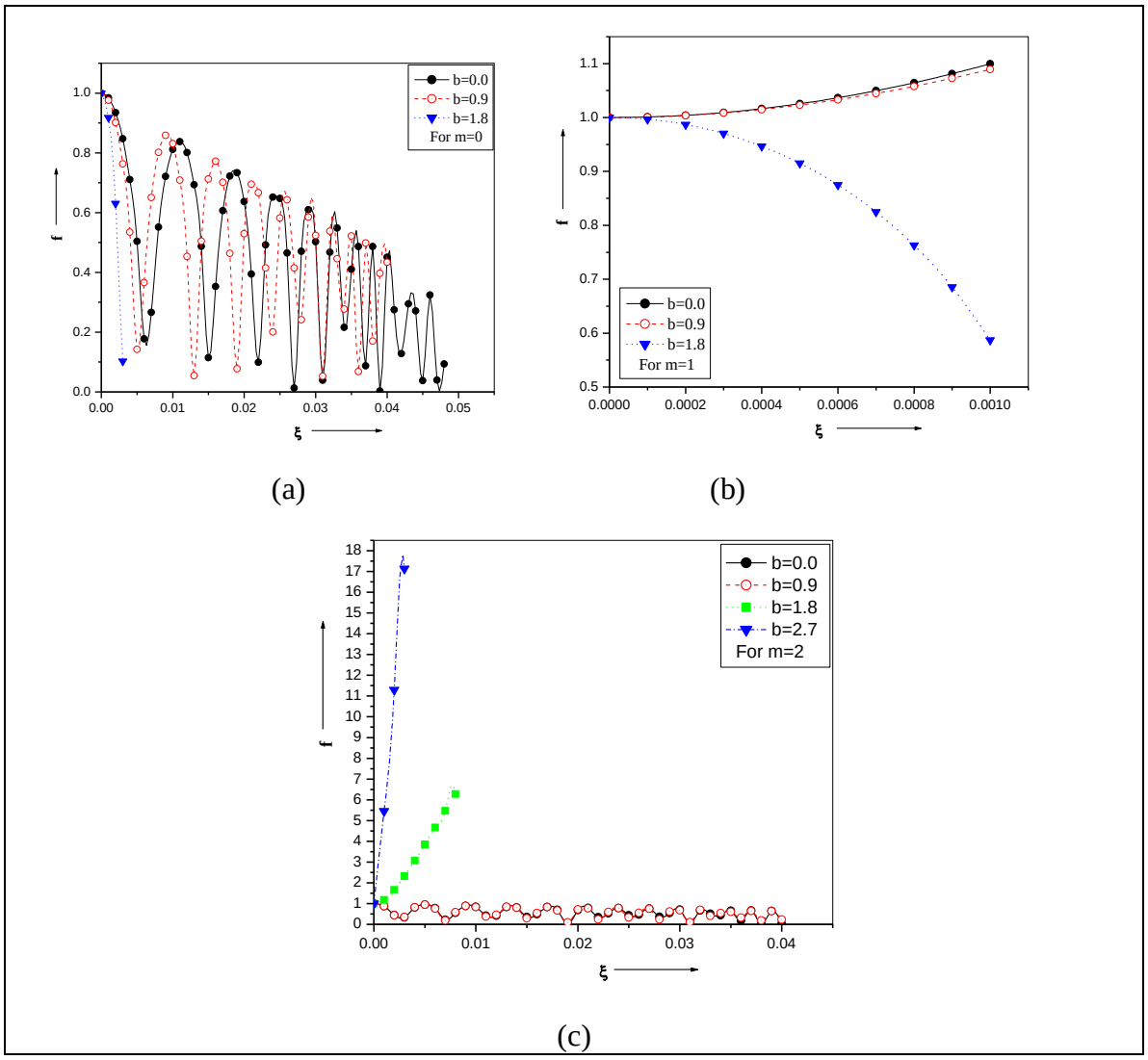

Figure 5.2: Variation of beam width parameter (f) with normalized propagation distance (ξ) at different values of decentered parameter for $m = 0$, (a), $m = 1$, (b) and $m = 2$, (c) in the presence of density transition. The other parameters are taken as $\alpha E_0^2 = 0.1$, $\omega_{P0} / \omega = 0.75$, $\omega r_0 / c = 479$ and $d = 0.05$.

CHAPTER-6

STRONG SELF-FOCUSING OF A COSH-GAUSSIAN LASER BEAM IN COLLISIONLESS MAGNETO-PLASMA UNDER PLASMA DENSITY RAMP

6.1 INTRODUCTION

The nonlinear interactions of laser beams with plasmas have been studied intensively for over more than 40 years. Short-pulse high intensity lasers of the order of $10^{20} W/cm^2$ make it possible to investigate the nonlinear interaction of strong electromagnetic waves with plasmas. The various applications of self-focusing of laser beam in plasmas [2, 3] like optical harmonic generation [13], laser driven fusion [11], x-ray lasers and the laser driven accelerators [8], the production of quasi mono-energetic electron bunches [12], the generation of inertial fusion energy driven by lasers [97] etc. attract the attention of researchers and make self-focusing of laser beams in plasmas as most interesting and fascinating field of research for several decades. These applications need the laser beams to propagate over several Rayleigh lengths in the plasmas without loss of the energy. Investigators chooses the propagation of different kind of laser beams profile like Gaussian beams [4], cosh-Gaussian beams [84, 91], Hermite-cosh-Gaussian beams [16] etc. in the plasmas. Recently, theoretical investigators focus their attention on paraxial wave family of laser beams. Propagation of Hermite-cosh-Gaussian beams in plasmas has been studied theoretically earlier by Belafhal *et al.* [16], Nanda *et al.* [95, 98] and Patil *et al.* [17, 18]. The focusing of HChG laser beam in magneto-plasma by considering ponderomotive nonlinearity has been theoretically examined by Patil *et al.* [81] and reported the effect of mode index and decentered parameter on the self-focusing of the beams.

In collisionless plasmas, ponderomotive force on electrons acting in an inhomogeneous electromagnetic field causes self-focusing. This force arises due to the drift of electrons in an inhomogeneous field and the interaction of drift velocity of electron with magnetic field. The ponderomotive force of the incident laser beam pushes the electron out of the region of high intensity and reduces the local concentration of electrons density in plasma. It increases the plasma dielectric function and laser beams

become more self-focused in plasma. Gill *et al.* [84] have recently studied the relativistic self-focusing and self-phase modulation of cosh-Gaussian laser beam in magnetoplasma in the absence of plasma density ramp and reported strong self-focusing of the laser beams. Gupta *et al.* [78] have investigated the additional focusing of a high intensity laser beams in a plasma with a density ramp and a magnetic field and reported the strong self-focusing of the laser beams. Again plasma density ramp has also been applied by Kant *et al.* [85, 87] to study the Ponderomotive self-focusing of a short laser pulse and self-focusing of Hermite-Gaussian laser beams in plasma. In both the cases Kant *et al.* [85, 87] reported strong self-focusing of the laser beams in the presence of plasma density ramp profile.

The present work is dedicated to the study of self focusing of cosh-Gaussian laser beams in collisionless magneto-plasma under plasma density ramp in applied magnetic field. The cosh-Gaussian beam has the ability to focus earlier than Gaussian beam as it is obvious from figure 2. Moreover, a cosh-Gaussian laser beam possesses more power than that of Gaussian laser beams having high intensity near the axis of propagation and hence, generates flat top beam profiles [99] which is useful for scribing type of applications in electronics where same intensity of laser beams for long time is required. On the basis of superposition of beams, a group of virtual sources that generate a cosh-Gaussian wave is identified by Zhang *et al.* [100]. Belafhal *et al.* [16] have investigated that for $b = 0$, the intensity profile of the HChG beam is similar to a Hermite-Gaussian distribution and with increasing b, the cosh function acts to concentrate the energy in the outer lobes of the beam. Moreover, previous works by Gupta *et al.* [78] and Kant *et al.* [85, 87] indicates the enhancement of self-focusing of laser beams due to the presence of plasmas density ramp profile. So, it is quite interested to apply plasmas density ramp profile in the medium in which cosh-Gaussian laser beam is propagating.

In the present paper we investigate the self-focusing of a cosh-Gaussian laser beam in collisionless magneto-plasma under plasma density ramp. We derive the equations for beam width parameter for cosh-Gaussian beam profile propagating in the plasmas in the presence of magnetic field and plasma density ramp, by applying WKB and paraxial approximation [4, 90] and solve them numerically by applying initial conditions. We observe the enhancement in the self-focusing of the laser beam as the

beam width parameter decreases with the normalized distance for the change in various parameters like intensity of laser beam, relative plasma density, decentered parameter and magnetic field. The presence of plasma density ramp plays a vital role to affect the self-focusing nature of propagating laser beams in the plasmas. To make the mathematical calculation simpler, only the transversal components of laser field are evaluated and longitudinal components are not taken in to consideration in the present paper. However, while dealing with nonlinear phenomenon, longitudinal components should be considered for an exact formulation [52].

6.2 BASIC FORMULATION

The field distribution of cosh-Gaussian laser beam propagating in the plasma along z-axis is of the following form:

$$E(r,z)=\frac{E_0}{f_{\pm}(z)}e^{\frac{b^2}{4}}\left(Exp\left[-\left(\frac{r}{r_0 f_{\pm}(z)}+\frac{b}{2}\right)^2\right]\right)+Exp\left[-\left(\frac{r}{r_0 f_{\pm}(z)}-\frac{b}{2}\right)^2\right] \quad \ldots (6.1)$$

here E_0 is the amplitude of cosh-Gaussian laser beam for the central position at $r=z=0$, $f_{\pm}(z)$ is the dimensionless beam width parameters for extraordinary (+ sign) and ordinary (- sign) mode of propagation of magnetoplasma, r_0 is the spot size of the beam and b is the decentered parameter of the beam.

The dielectric constant for the non-linear medium due to ponderomotive non-linearity (collision-less magnetoplasma) is obtained by applying the approach as applied by Sodha *et al.* [4]:

$$\varepsilon_{\pm}=\varepsilon_{\pm 0}+\phi_{\pm}(EE^*) \quad \ldots (6.2)$$

As relative displacements between ions and electrons of plasma set up a restoring electric field $E=4\pi n_0 ed$, which returns the electrons to equilibrium position and hence in this fashion, motion of each electron becomes simple harmonic with plasma frequency $\omega_P^2=4\pi e^2 n_0/m$. Here n_0, e, d and m are the electron density, electronic charge, displacement of charge layer from original position and rest mass of electron respectively. Figure 6.1 shows a layer of negative charge per unit area on one side of the

plasma slab with the stationary ions producing a layer of positive charge on the other side for (a) constant electron density and (b) varying electron density respectively.

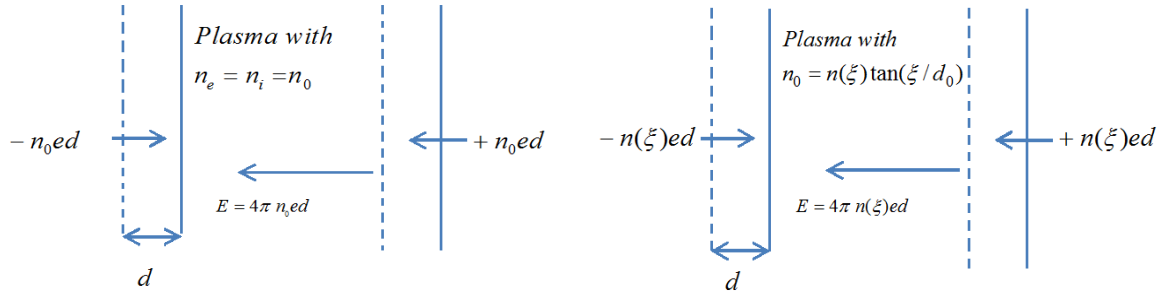

(a) (b)

Figure 6.1: Generation of restoring electric field inside the plasma due to relative displacements between ions and electrons for (a) constant electron density and (b) varying electron density.

In figure 6.1(a), each electron experiences electric force $F = -4\pi n_o e^2 d$, in the direction of its equilibrium position. The equation of motion of electron is of the form, $m\ddot{d} = \left(-4\pi n_0 e^2\right)d$, with index of refraction given by $\left(1-\omega_P^2/\omega^2\right)$. If the value of $'\omega'$ is less than plasma frequency $'\omega_P'$, then the refractive index is purely imaginary which gives rise to attenuation and if the value of $'\omega'$ is greater than $'\omega_P'$, then the refractive index is real. We consider the plasma density ramp profile $n(\xi) = n_0 \tan(\xi/d_0)$, as previously taken by various authors [78, 85, 87, 96], where $\xi = z/R_d$ is the normalized propagation distance, d_0 is a dimensionless adjustable parameter and R_d is the diffraction length. Now, each electron experiences an electric force $F = -4\pi n(\xi)e^2 d$, in the direction of its equilibrium position as depicted in figure 6.1(b). The equation of motion of electron, in this case, is of the form, $m\ddot{d} = \left(-4\pi n(\xi)e^2\right)d$. So, in the present study, application of plasma density ramp and external static magnetic field modify the index of refraction to, $\varepsilon_{\pm 0} = 1-\omega_P^2(\xi)/\omega(\omega \mp \omega_c)$, where $\omega_c = eB_0/mc$, is the electron cyclotron frequency, $\omega_P(\xi) = \left(4\pi e^2 n(\xi)/m\right)^{1/2}$ is the plasma frequency which varies

along z-axis. This Plasma frequency can also be written in terms of ω_{P0} as $\omega_P^2(\xi) = 4\pi e^2 n_0 \tan(\xi/d_0)/m = \omega_{P0}^2 \tan(\xi/d_0)$.

The non-linear part of dielectric constant is given by $\phi_\pm(EE^*) = \varepsilon_{\pm 2} A_0^2 / (1 \mp \omega_c/\omega)^2$ with $\varepsilon_{\pm 2} = 3m\alpha\omega_P^2(1 \mp (\omega_c/2\omega))/8M\omega(\omega \mp \omega_c)$ and $\alpha = e^2 M/6m^2\omega^2 k_B T_0$, here M is the mass of scatterer in the plasma, ω is the frequency of incident laser, k_B is the Boltzmann constant and T_0 is the equilibrium plasma temperature. 'A_0^2' will be defined later on in equation (6.13).

The general form of wave equation for exponentially varying field obtained from Maxwell's equation by applying the approach as applied by Sodha *et al.* [4] and is given by

$$\nabla^2 \vec{E} - \nabla(\nabla.\vec{E}) = -\frac{\omega^2}{c^2} \varepsilon.\vec{E} \qquad \ldots (6.3)$$

In components form this equation can be written as

$$\frac{\partial^2 E_x}{\partial z^2} + \frac{\partial^2 E_x}{\partial y^2} - \frac{\partial}{\partial x}\left(\frac{\partial E_y}{\partial y} + \frac{\partial E_z}{\partial z}\right) = -\frac{\omega^2}{c^2}\left(\varepsilon.\vec{E}\right)_x \qquad \ldots (6.4a)$$

$$\frac{\partial^2 E_y}{\partial z^2} + \frac{\partial^2 E_y}{\partial x^2} - \frac{\partial}{\partial y}\left(\frac{\partial E_x}{\partial x} + \frac{\partial E_z}{\partial z}\right) = -\frac{\omega^2}{c^2}\left(\varepsilon.\vec{E}\right)_y \qquad \ldots (6.4b)$$

$$\frac{\partial^2 E_z}{\partial x^2} + \frac{\partial^2 E_z}{\partial y^2} - \frac{\partial}{\partial z}\left(\frac{\partial E_x}{\partial x} + \frac{\partial E_y}{\partial y}\right) = -\frac{\omega^2}{c^2}\left(\varepsilon.\vec{E}\right)_z \qquad \ldots (6.4c)$$

In the present case, the variation of magnetic field is assumed to be very strong along z-direction of the co-ordinate system than x-y plane. This gives the condition $\nabla.\vec{D} = 0$.

or,

$$\frac{\partial E_z}{\partial z} \approx -\frac{1}{\varepsilon_{zz}}\left(\varepsilon_{xx}\frac{\partial E_x}{\partial x} + \varepsilon_{xy}\frac{\partial E_y}{\partial x} + \varepsilon_{yx}\frac{\partial E_x}{\partial y} + \varepsilon_{yy}\frac{\partial E_y}{\partial y}\right) \qquad \ldots (6.5)$$

The equations (6.4a), (6.4b) & (6.4c) are coupled and one cannot define the propagation vectors which describe the independent propagation of E_x, E_y and E_z.

To investigate the independent modes of propagation, we multiply equation (6.4b) by '*i*' and adding so obtained equation to equation (6.4a), we get,

$$\frac{\partial^2 E_x}{\partial z^2}+\frac{\partial^2 E_x}{\partial y^2}-\frac{\partial}{\partial x}\left(\frac{\partial E_y}{\partial y}+\frac{\partial E_z}{\partial z}\right)+i\left(\frac{\partial^2 E_y}{\partial z^2}+\frac{\partial^2 E_y}{\partial x^2}-\frac{\partial}{\partial y}\left(\frac{\partial E_x}{\partial x}+\frac{\partial E_z}{\partial z}\right)\right)$$
$$=-\frac{\omega^2}{c^2}\left(\varepsilon.\vec{E}\right)_x-i\frac{\omega^2}{c^2}\left(\varepsilon.\vec{E}\right)_y$$

Using the value of $\frac{\partial E_z}{\partial z}$, $A_1=E_x+iE_y$ and $A_2=E_x-iE_y$, we get

$$\frac{\partial^2 A_1}{\partial z^2}+\frac{\partial^2 E_x}{\partial y^2}+i\frac{\partial^2 E_y}{\partial x^2}-i\frac{\partial^2 A_2}{\partial x\partial y}-\frac{\partial}{\partial x}\left[-\frac{1}{\varepsilon_{zz}}\left(\varepsilon_{xx}\frac{\partial E_x}{\partial x}+\varepsilon_{xy}\frac{\partial E_y}{\partial x}+\varepsilon_{yx}\frac{\partial E_x}{\partial y}+\varepsilon_{yy}\frac{\partial E_y}{\partial y}\right)\right]$$
$$-i\frac{\partial}{\partial y}\left[-\frac{1}{\varepsilon_{zz}}\left(\varepsilon_{xx}\frac{\partial E_x}{\partial x}+\varepsilon_{xy}\frac{\partial E_y}{\partial x}+\varepsilon_{yx}\frac{\partial E_x}{\partial y}+\varepsilon_{yy}\frac{\partial E_y}{\partial y}\right)\right]=-\frac{\omega^2}{c^2}\left[\left(\varepsilon.\vec{E}\right)_x+i\left(\varepsilon.\vec{E}\right)_y\right]$$

Solving this equation and using $\varepsilon_{xx}=\varepsilon_{yy}$ and $\varepsilon_{yx}=-\varepsilon_{xy}$, we get,

$$\frac{\partial^2 A_1}{\partial z^2}+\frac{1}{2}\left(1+\frac{\varepsilon_{+0}}{\varepsilon_{0zz}}\right)\left(\frac{\partial^2 A_1}{\partial x^2}+\frac{\partial^2 A_1}{\partial y^2}\right)+\frac{1}{2}\left(\frac{\varepsilon_{-0}}{\varepsilon_{0zz}}-1\right)\left(\frac{\partial^2 A_2}{\partial x^2}-\frac{\partial^2 A_2}{\partial y^2}\right)-i\left(1-\frac{\varepsilon_{-0}}{\varepsilon_{0zz}}\right)\frac{\partial^2 A_2}{\partial x\partial y}$$
$$+\frac{\omega^2}{c^2}\left[\varepsilon_{+0}+\varepsilon_{+2}\left\{\frac{A_1A_1^*}{\left(1-\frac{\omega_c}{\omega}\right)^2}+\frac{A_2A_2^*}{\left(1+\frac{\omega_c}{\omega}\right)^2}\right\}\right]A_1=0$$

… (6.6)

Similarly for ordinary mode of propagation,

$$\frac{\partial^2 A_2}{\partial z^2}+\frac{1}{2}\left(1+\frac{\varepsilon_{-0}}{\varepsilon_{0zz}}\right)\left(\frac{\partial^2 A_2}{\partial x^2}+\frac{\partial^2 A_2}{\partial y^2}\right)+\frac{1}{2}\left(\frac{\varepsilon_{+0}}{\varepsilon_{0zz}}-1\right)\left(\frac{\partial^2 A_1}{\partial x^2}-\frac{\partial^2 A_1}{\partial y^2}\right)+i\left(1-\frac{\varepsilon_{+0}}{\varepsilon_{0zz}}\right)\frac{\partial^2 A_1}{\partial x\partial y}$$
$$+\frac{\omega^2}{c^2}\left[\varepsilon_{-0}+\varepsilon_{-2}\left\{\frac{A_1A_1^*}{\left(1-\frac{\omega_c}{\omega}\right)^2}+\frac{A_2A_2^*}{\left(1+\frac{\omega_c}{\omega}\right)^2}\right\}\right]A_2=0 \qquad \text{... (6.7)}$$

with, $\varepsilon_{0zz}=1-\omega_P^2/\omega^2$

The functions A_1 and A_2, having propagation vectors k_+ and k_- respectively, represent the extraordinary and ordinary modes of propagation of a magnetoplasma. The variation of equation (6.6) and (6.7) is very slow along x and y-direction as compared to z-direction. It indicates the weak coupling of these two equations. In order to study the

behaviour of one of the mode other mode can be considered to be zero. Let us assume $A_2 \approx 0$, then equation (6.6) becomes,

$$\frac{\partial^2 A_1}{\partial z^2} + \frac{1}{2}\left(1+\frac{\varepsilon_{+0}}{\varepsilon_{0zz}}\right)\left(\frac{\partial^2 A_1}{\partial x^2}+\frac{\partial^2 A_1}{\partial y^2}\right)+\frac{\omega^2}{c^2}\left[\varepsilon_{+0}+\varepsilon_{+2}\left\{\frac{A_1 A_1^*}{\left(1-\frac{\omega_c}{\omega}\right)^2}\right\}\right]A_1 = 0 \qquad \ldots (6.8a)$$

Similarly for considering $A_1 \approx 0$, equation (6.7) becomes,

$$\frac{\partial^2 A_2}{\partial z^2} + \frac{1}{2}\left(1+\frac{\varepsilon_{-0}}{\varepsilon_{0zz}}\right)\left(\frac{\partial^2 A_2}{\partial x^2}+\frac{\partial^2 A_2}{\partial y^2}\right)+\frac{\omega^2}{c^2}\left[\varepsilon_{-0}+\varepsilon_{-2}\left\{\frac{A_2 A_2^*}{\left(1+\frac{\omega_c}{\omega}\right)^2}\right\}\right]A_2 = 0 \qquad \ldots (6.8b)$$

The solution of equation (6.8a) is of the form

$$A_1 = AExp\left[i(\omega t - k_+ z)\right] \qquad \ldots(6.9)$$

with $k_+ = (\omega/c)\varepsilon_{+0}^{1/2}(z)$, where $'A'$ is a complex function of x, y and z.

Differentiating this eq. twice w. r. t. x, we get,

$$\frac{\partial A_1}{\partial x} = \exp[i(\omega t - k_+ z)]\frac{\partial A}{\partial x}$$

$$\frac{\partial^2 A_1}{\partial x^2} = \exp[i(\omega t - k_+ z)]\frac{\partial^2 A}{\partial x^2}$$

Similarly, differentiating eq. (6.9) twice w. r. t. y, we get,

$$\frac{\partial A_1}{\partial y} = \exp[i(\omega t - k_+ z)]\frac{\partial A}{\partial y}$$

$$\frac{\partial^2 A_1}{\partial y^2} = \exp[i(\omega t - k_+ z)]\frac{\partial^2 A}{\partial y^2}$$

Now, differentiating eq. (6.9) twice w. r. t. z, we get,

$$\frac{\partial A_1}{\partial z} = -iA\exp[i(\omega t - k_+ z)]k_+ - iAZ\exp[i(\omega t - k_+ z)]\frac{\partial k_+}{\partial z} + \exp[i(\omega t - k_+ z)]\frac{\partial A}{\partial z}$$

$$\frac{\partial^2 A_1}{\partial z^2} = -2iA\exp[i(\omega t - k_+ z)]\frac{\partial k_+}{\partial z} - ik_+\frac{\partial A_1}{\partial z} - iAZ\exp[i(\omega t - k_+ z)]\frac{\partial^2 k_+}{\partial z^2} - iz\frac{\partial A_1}{\partial z}\frac{\partial k_+}{\partial z}$$

$$+\exp[i(\omega t - k_+ z)]\frac{\partial^2 A}{\partial z^2} - ik_+\exp[i(\omega t - k_+ z)]\frac{\partial A}{\partial z} - iz\exp[i(\omega t - k_+ z)]\frac{\partial A}{\partial z}\frac{\partial k_+}{\partial z}$$

Substituting these values in equation (6.8a) and neglecting $\partial^2 A/\partial z^2 = 0$, we get

$$\frac{iA\omega^2\omega_s Sec^2\left(\frac{z}{dR_d}\right)}{k_+ c^2 dR_d} - Ak_+^2 + \frac{Az\omega^2\omega_s Sec^2\left(\frac{z}{dR_d}\right)}{2c^2 dR_d} - ik_+\frac{\partial A}{\partial z}$$

$$+\frac{iAz\omega^2\omega_s Sec^2\left(\frac{z}{dR_d}\right)\tan\left(\frac{z}{dR_d}\right)}{k_+ c^2 d^2 R_d^2} + \frac{iAz\omega^4\omega_s^2 Sec^4\left(\frac{z}{dR_d}\right)}{4k_+^3 c^4 d^2 R_d^2}$$

$$+\frac{Az\omega^2\omega_s Sec^2\left(\frac{z}{dR_d}\right)}{2c^2 dR_d} - \frac{Az\omega^4\omega_s^2 Sec^4\left(\frac{z}{dR_d}\right)}{4k_+^3 c^4 d^2 R_d^2} + \frac{iz\omega^2\omega_s Sec^2\left(\frac{z}{dR_d}\right)}{2k_+ c^2 dR_d}\frac{\partial A}{\partial z}$$

$$+\frac{\partial^2 A}{\partial z^2} - ik_+\frac{\partial A}{\partial z} + \frac{iz\omega^2\omega_s Sec^2\left(\frac{z}{dR_d}\right)}{2k_+ c^2 dR_d}\frac{\partial A}{\partial z} + \frac{1}{2}\left(1+\frac{\varepsilon_{+0}}{\varepsilon_{0zz}}\right)\left(\frac{\partial^2 A}{\partial x^2} + \frac{\partial^2 A}{\partial y^2}\right)$$

$$+Ak_+^2 + \frac{\omega^2}{c^2}\varepsilon_{+2}\left(\frac{AA^*}{\left(1-\frac{\omega_c}{\omega}\right)^2}\right)A = 0$$

$$i\frac{A\omega^2\omega_s Sec^2\left(\frac{z}{dR_d}\right)}{k_+c^2dR_d}-2ik_+\frac{\partial A}{\partial z}+i\frac{Az\omega^2\omega_s Sec^2\left(\frac{z}{dR_d}\right)\tan\left(\frac{z}{dR_d}\right)}{k_+c^2d^2R_d^2}$$

$$+i\frac{Az\omega^4\omega_s^2 Sec^4\left(\frac{z}{dR_d}\right)}{4k_+^3c^4d^2R_d^2}+i\frac{z\omega^2\omega_s Sec^2\left(\frac{z}{dR_d}\right)}{k_+c^2dR_d}\frac{\partial A}{\partial z}$$

$$+\frac{Az\omega^2\omega_s Sec^2\left(\frac{z}{dR_d}\right)}{c^2dR_d}-\frac{Az\omega^4\omega_s^2 Sec^4\left(\frac{z}{dR_d}\right)}{4k_+^3c^4d^2R_d^2}$$

$$+\frac{1}{2}\left(1+\frac{\varepsilon_{+0}}{\varepsilon_{0zz}}\right)\left(\frac{\partial^2 A}{\partial x^2}+\frac{\partial^2 A}{\partial y^2}\right)+\frac{\omega^2}{c^2}\varepsilon_{+2}\left(\frac{AA^*}{\left(1-\frac{\omega_c}{\omega}\right)^2}\right)A=0$$

where $\omega_s=\omega_{P0}^2/\omega(\omega-\omega_c)$

The solution of this equation is of the form

$$A=A_0(x,y,z)\exp[-ik_+(z)S(x,y,z)] \quad \ldots (6.10)$$

Substituting this value in equation, we get

$$i\frac{A_0\omega^2\omega_s Sec^2\left(\frac{z}{dR_d}\right)}{k_+c^2dR_d}-2ik_+\frac{\partial A_0}{\partial z}+i\frac{A_0z\omega^2\omega_s Sec^2\left(\frac{z}{dR_d}\right)\tan\left(\frac{z}{dR_d}\right)}{k_+c^2d^2R_d^2}$$

$$+i\frac{A_0z\omega^4\omega_s^2 Sec^4\left(\frac{z}{dR_d}\right)}{4k_+^3c^4d^2R_d^2}+i\frac{z\omega^2\omega_s Sec^2\left(\frac{z}{dR_d}\right)}{k_+c^2dR_d}\frac{\partial A_0}{\partial z}-2A_0k_+^2\frac{\partial S}{\partial z}$$

$$-\frac{i}{2}\left(1+\frac{\varepsilon_{+0}}{\varepsilon_{0zz}}\right)\left[A_0k_+\frac{\partial^2 S}{\partial x^2}+2k_+\frac{\partial S}{\partial x}\frac{\partial A_0}{\partial x}+A_0k_+\frac{\partial^2 S}{\partial y^2}+2k_+\frac{\partial S}{\partial y}\frac{\partial A_0}{\partial y}\right]$$

$$+\frac{A_0S\omega^2\omega_s Sec^2\left(\frac{z}{dR_d}\right)}{c^2dR_d}+\frac{A_0z\omega^2\omega_s Sec^2\left(\frac{z}{dR_d}\right)}{c^2dR_d}\frac{\partial S}{\partial z}$$

$$-\frac{A_0Sz\omega^4\omega_s^2 Sec^4\left(\frac{z}{dR_d}\right)}{2k_+^3c^4d^2R_d^2}+\frac{A_0z\omega^2\omega_s Sec^2\left(\frac{z}{dR_d}\right)}{c^2dR_d}-\frac{A_0z^2\omega^4\omega_s^2 Sec^4\left(\frac{z}{dR_d}\right)}{4k_+^2c^4d^2R_d^2}$$

$$-\frac{1}{2}\left(1+\frac{\varepsilon_{+0}}{\varepsilon_{0zz}}\right)\left[A_0k_+^2\left(\frac{\partial S}{\partial x}\right)^2-\frac{\partial^2 A_0}{\partial x^2}+A_0k_+^2\left(\frac{\partial S}{\partial y}\right)^2-\frac{\partial^2 A_0}{\partial y^2}\right]$$

$$+\frac{\omega^2}{c^2}\varepsilon_{+2}\left(\frac{A_0^2}{\left(1-\frac{\omega_c}{\omega}\right)^2}\right)A_0=0$$

Separating real and imaginary parts,

Real part is

$$\left[\frac{z\omega^2\omega_s\sec^2\left(\frac{z}{d_0R_d}\right)}{k_+^2c^2d_0R_d}-2\right]\frac{\partial S}{\partial z}-\frac{1}{2}\left(1+\frac{\varepsilon_{+0}}{\varepsilon_{0zz}}\right)\left[\left(\frac{\partial S}{\partial x}\right)^2+\left(\frac{\partial S}{\partial y}\right)^2\right]+\frac{1}{4A_0^2k_+^2}\left(1+\frac{\varepsilon_{+0}}{\varepsilon_{0zz}}\right)$$

$$\left[\left(\frac{\partial^2A_0^2}{\partial x^2}+\frac{\partial^2A_0^2}{\partial y^2}\right)-\frac{1}{2A_0^2}\left\{\left(\frac{\partial A_0^2}{\partial x}\right)^2+\left(\frac{\partial A_0^2}{\partial y}\right)^2\right\}\right]-\frac{S\omega^2\omega_s\sec^2\left(\frac{z}{d_0R_d}\right)}{k_+^2c^2d_0R_d}-\frac{Sz\omega^4\omega_s^2\sec^4\left(\frac{z}{d_0R_d}\right)}{2k_+^4c^4d_0^2R_d^2}$$

$$+\frac{z\omega^2\omega_s\sec^2\left(\frac{z}{d_0R_d}\right)}{k_+^2c^2d_0R_d}-\frac{z^2\omega^4\omega_s^2\sec^4\left(\frac{z}{d_0R_d}\right)}{4k_+^4c^4d_0^2R_d^2}+\frac{\omega^2}{k_+^2c^2}\varepsilon_{+2}\left(\frac{A_0^2}{\left(1-\frac{\omega_c}{\omega}\right)^2}\right)=0 \qquad \text{... (6.11)}$$

Imaginary part is

$$\frac{\omega^2\omega_s\sec^2\left(\frac{z}{d_0R_d}\right)}{k_+^3c^2d_0R_d}+\frac{z\omega^2\omega_s\sec^2\left(\frac{z}{d_0R_d}\right)\tan\left(\frac{z}{d_0R_d}\right)}{k_+^3c^2d_0R_d}+\frac{z\omega^4\omega_s^2\sec^4\left(\frac{z}{d_0R_d}\right)}{4k_+^5c^4d_0^2R_d^2}$$

$$+\left(\frac{z\omega^2\omega_s\sec^2\left(\frac{z}{d_0R_d}\right)}{2A_0^2k_+^3c^2d_0R_d}-\frac{1}{k_+A_0^2}\right)\frac{\partial A_0^2}{\partial z}-\frac{1}{2k_+}\left(1+\frac{\varepsilon_{+0}}{\varepsilon_{0zz}}\right)\left(\frac{\partial^2S}{\partial x^2}+\frac{\partial^2S}{\partial y^2}\right)$$

$$+\frac{1}{2k_+A_0^2}\left(1+\frac{\varepsilon_{+0}}{\varepsilon_{0zz}}\right)\left[\left(\frac{\partial S}{\partial x}\right)\left(\frac{\partial A_0^2}{\partial x}\right)+\left(\frac{\partial S}{\partial y}\right)\left(\frac{\partial A_0^2}{\partial y}\right)\right]=0 \qquad \text{... (6.12)}$$

with $\omega_s=\omega_{P0}^2/\omega(\omega-\omega_c)$

The solution of equation (6.11) & (6.12) for initially cosh-Gaussian beam are of the following form,

$$A_0^2=\frac{E_0^2}{f_+^2(z)}e^{\frac{b^2}{2}}$$

$$\left(Exp\left[-2\left(\frac{r}{r_0f(z)}+\frac{b}{2}\right)^2\right]+Exp\left[-2\left(\frac{r}{r_0f(z)}-\frac{b}{2}\right)^2\right]+2Exp\left[-\left(\frac{2r^2}{r_0^2f^2(z)}+\frac{b^2}{2}\right)\right]\right)$$

…(6.13)

$$S = \frac{r^2}{2}\beta(z) + \phi(z) \qquad \ldots(6.14)$$

where $\beta(z) = 2\left(\partial f_+(z)/\partial z\right)/\left\{f_+(z)\left(1+\varepsilon_{+0}/\varepsilon_{0zz}\right)\right\}$, is the curvature of the wave front, $\phi(z)$ is an arbitrary function of 'z' and $r^2 = x^2 + y^2$.

Thus equation (6.11) becomes,

$$\left\{\frac{\xi\omega_s \sec^2\left(\frac{\xi}{d_0}\right)}{d_0} - 2\left(1-\omega_s \tan\left(\frac{\xi}{d_0}\right)\right)\right\}\frac{\partial^2 f_+}{\partial\xi^2} - \frac{\xi\omega_s \sec^2\left(\frac{\xi}{d_0}\right)}{d_0}\frac{1}{f_+}\left(\frac{\partial f_+}{\partial\xi}\right)^2$$

$$-\frac{\xi\omega_s \sec^4\left(\frac{\xi}{d_0}\right)\omega_{P0}^2\varepsilon_{+0}}{d_0^2\omega^2\varepsilon_{0zz}^2\left(1+\frac{\varepsilon_{+0}}{\varepsilon_{0zz}}\right)}\frac{\partial f_+}{\partial\xi} + \frac{\xi\omega_s^2 \sec^4\left(\frac{\xi}{d_0}\right)}{d_0^2\varepsilon_{0zz}\left(1+\frac{\varepsilon_{+0}}{\varepsilon_{0zz}}\right)}\frac{\partial f_+}{\partial\xi}$$

$$+\frac{2\sec^2\left(\frac{\xi}{d_0}\right)\left(1-\omega_s \tan\left(\frac{\xi}{d_0}\right)\right)\omega_{P0}^2\varepsilon_{+0}}{d_0\omega^2\varepsilon_{0zz}^2\left(1+\frac{\varepsilon_{+0}}{\varepsilon_{0zz}}\right)}\frac{\partial f_+}{\partial\xi} - \frac{2\omega_s \sec^2\left(\frac{\xi}{d_0}\right)\left(1-\omega_s \tan\left(\frac{\xi}{d_0}\right)\right)}{d_0\varepsilon_{0zz}\left(1+\frac{\varepsilon_{+0}}{\varepsilon_{0zz}}\right)}\frac{\partial f_+}{\partial\xi}$$

$$+\frac{\left(1+\frac{\varepsilon_{+0}}{\varepsilon_{0zz}}\right)^2\left(1-\frac{\omega_{P0}^2}{\omega^2}\tan\left(\frac{\xi}{d_0}\right)\right)}{f_+^3}\left(2-2b^2\right)$$

$$-\frac{8R_{d1}^2 e^{\frac{b^2}{2}}\left(1-\frac{\omega_{P0}^2}{\omega^2}\tan\left(\frac{\xi}{d_0}\right)\right)}{R_{nl1}^2 f_+^3}\left(1+\frac{\varepsilon_{+0}}{\varepsilon_{0zz}}\right) = 0 \qquad \ldots(6.15)$$

where $R_{nl1}^2 = \left(1-\omega_c/\omega\right)^2 r_0^2\left(\varepsilon_{+0}/\varepsilon_{+2}\, E_0^2\right)$ and $R_{d1} = k_+ r_0^2$,

Equation (6.15) is the required equation for beam width parameter for extraordinary modes of propagation of magnetoplasma. Similarly equation for beam width parameter for ordinary mode can be obtained by replacing ω_c by $-\omega_c$ and + sign by – sign in the subscript of f.

However, for initially Gaussian beam, $A_0^2 = E_0^2 Exp\,(-r^2/f_+^2(z)r_0^2)/f_+^2(z)$, the beam width parameter comes out to be

$$\left\{\frac{\xi\omega_s \sec^2\left(\frac{\xi}{d_0}\right)}{d_0} - 2\left(1-\omega_s \tan\left(\frac{\xi}{d_0}\right)\right)\right\}\frac{\partial^2 f_+}{\partial\xi^2} - \frac{\xi\omega_s \sec^2\left(\frac{\xi}{d_0}\right)}{d_0}\frac{1}{f_+}\left(\frac{\partial f_+}{\partial\xi}\right)^2$$

$$-\frac{\xi\omega_s \sec^4\left(\frac{\xi}{d_0}\right)\omega_{P0}^2\varepsilon_{+0}}{d_0^2\omega^2\varepsilon_{0zz}^2\left(1+\frac{\varepsilon_{+0}}{\varepsilon_{0zz}}\right)}\frac{\partial f_+}{\partial\xi} + \frac{\xi\omega_s^2 \sec^4\left(\frac{\xi}{d_0}\right)}{d_0^2\varepsilon_{0zz}\left(1+\frac{\varepsilon_{+0}}{\varepsilon_{0zz}}\right)}\frac{\partial f_+}{\partial\xi}$$

$$+\frac{2\sec^2\left(\frac{\xi}{d_0}\right)\left(1-\omega_s \tan\left(\frac{\xi}{d_0}\right)\right)\omega_{P0}^2\varepsilon_{+0}}{d_0\omega^2\varepsilon_{0zz}^2\left(1+\frac{\varepsilon_{+0}}{\varepsilon_{0zz}}\right)}\frac{\partial f_+}{\partial\xi}$$

$$-\frac{2\omega_s \sec^2\left(\frac{\xi}{d_0}\right)\left(1-\omega_s \tan\left(\frac{\xi}{d_0}\right)\right)}{d_0\varepsilon_{0zz}\left(1+\frac{\varepsilon_{+0}}{\varepsilon_{0zz}}\right)}\frac{\partial f_+}{\partial\xi} + \frac{\left(1+\frac{\varepsilon_{+0}}{\varepsilon_{0zz}}\right)^2\left(1-\frac{\omega_{P0}^2}{\omega^2}\tan\left(\frac{\xi}{d_0}\right)\right)}{2f_+^3}$$

$$-\frac{R_{d1}^2\left(1-\frac{\omega_{P0}^2}{\omega^2}\tan\left(\frac{\xi}{d_0}\right)\right)}{R_{nl1}^2 f_+^3}\left(1+\frac{\varepsilon_{+0}}{\varepsilon_{0zz}}\right) = 0 \qquad \ldots (6.16)$$

The initial boundary conditions are $\xi = 0,\ f_{\pm}(z) = 1 \text{ and } df_{\pm}(z)/dz = 0$ for extraordinary and ordinary modes.

6.3 RESULTS AND DISCUSSION

In the present case, we assume the plasmas density ramp profile given by the relation $n(\xi) = n_0 \tan(\xi/d_0)$ with initial electron density $n_0 \approx 5\times10^{20} cm^{-3}$, angular frequency of incident laser $\omega = 1.778\times10^{15}$ rad/s, $r_0 = 49.44\mu m$. The variation of beam

width parameter *f* with normalized propagation distance (ξ) is depicted in figure 6.2 for the parameters taken as $\omega_c/\omega = 0.3,\ \omega r_0/c = 293,\ m_0/M = 0.0006$ and $\omega_{P0}/\omega = 0.77$ $\alpha E_0^2 = 0.5, d_0 = 0.9$. From figure 6.2(a), it is obvious that strong self-focusing occurs at normalized distance, $\xi = 0.12$ for cosh-Gaussian beam while for Gaussian beam, strong self-focusing occurs at $\xi = 0.5$ for extraordinary mode of propagation. Figure 6.2(b) depicts the diffraction tendency of Gaussian beam and converging tendency of cosh-Gaussian beam with normalized propagation distance for ordinary mode of propagation; however extraordinary mode is more prominent toward self-focusing than ordinary mode. The propensity of cosh-Gaussian beam to converge earlier than Gaussian beam leads us to choose the cosh-Gaussian laser beam profile.

Figure 6.3 represents the variation of beam width parameter $(f_{\pm})$ with the normalized propagation distance (ξ) for different values of decentered parameter, $b = 0, 1, 2$ and 2.12. It is clear from Fig 6.3(a), that for extraordinary mode, beam width parameter decreases earlier with increase in the values of decentered parameter. For $b = 2.12$, beam width parameter falls abruptly at normalized propagation distance, $\xi = 0.12$ and hence self-focusing becomes stronger. In the absence of decentered parameter, strong self-focusing effect is observed at certain higher value of normalized distance, $\xi = 0.3$. However, for other two values of decentered parameter, $b = 1$ and 2, strong self-focusing effect is reported at $\xi = 0.23$ and 0.13. Gill *et al.* [14] have studied self-focusing and self-phase modulation as well as self-trapping of cosh-Gaussian beam at various values of decentered parameter (b) and reported sharper self-focusing for $b = 2$ at $\xi = 1.45$ and the value of beam width parameter is nearly 0.91 (approximately). However, for $b = 1$, strong self-focusing occurs at nearly $\xi = 2.5$. In another work Gill *et al.* [84] reported strong self-focusing effect nearly at $\xi = 0.65$, however, for $b = 2$, they reported self-focusing which occur at $\xi = 0.07$, but the value of beam width parameter at this normalized distance is very less and is nearly $f = 0.995$. In the present work, strong converging of cosh-Gaussian beam occurs at $\xi = 0.12$ for $b = 2.12$ due to the presence of plasma density ramp. In case of ordinary mode, Fig 6.3(b), the self-focusing of laser

beam occurs for $b = 0, 1, 2 \text{ and } 2.12$ and in the absence of decentered parameter self-focusing effect occurs at longer normalized propagation distance. For $b = 2.12$, self-focusing effect is less strong in this case than in case of extraordinary mode.

Figure 6.4 represents the variation of beam width parameter with the normalized propagation distance for different values of intensity parameter, $\alpha E_0^2 = 0.1, 0.3 \text{ and } 0.5$ corresponding to intensity values $1.23 \times 10^{17} W/cm^2$, $3.67 \times 10^{17} W/cm^2$ and $6.12 \times 10^{17} W/cm^2$ respectively, for $b = 2.12$. It is obvious from figure 6.4(a), that with the increase in the value of intensity parameter, beam width parameter decreases. For extraordinary mode, $\alpha E_0^2 = 0.5$, the beam width parameter decreases up to its minimum value $f = 0.09$ at $\xi = 0.12$. Hence self-focusing becomes very strong. This happens because at high intensities of incident laser beam, more electrons contribute to self-focusing. Gill *et al.* [84] have studied relativistic self-focusing and self-phase modulation of cosh-Gaussian laser beam in magnetoplasma in the absence of plasma density ramp and reported strong self-focusing, for $\alpha |A_{0+}|^2 = 0.5$ which occur nearly at $\xi = 0.3$. In the present work, the self-focusing of beam is strong and occurs earlier due to the presence of plasma density ramp than the results reported by Gill *et al.* [84] in uniform density profile of the plasma. In case of ordinary mode, figure 6.4(b), self-focusing occurs for all taken values of intensity parameter and is strong and occurs earlier for higher value of intensity parameter. However, for extraordinary mode self-focusing occurs earlier than that of ordinary mode for same values of intensity parameter.

Figure 6.5, represents the variation of beam width parameter with the normalized propagation distance for different values of magnetic field parameter (ω_c/ω) viz. 0.1, 0.2 and 0.3 for extraordinary mode, figure 6.5(a) and ordinary mode, figure 6.5(b) for $b = 2.12$. It is found that with the increase in the value of magnetic field parameter, (ω_c/ω), beam width parameter decreases and occurs earlier and hence self-focusing becomes strong. However, in case of ordinary mode, beam width parameter decreases with the increase in the value of magnetic field parameter but conversing tendency of cosh-Gaussian beam is shifted towards longer normalized propagation distance. Gill *et al.*[84] have studied relativistic self-focusing and self-phase modulation of cosh-Gaussian laser beam in

magnetoplasma in the absence of plasma density ramp and reported strong self-focusing, for $\omega_c/\omega = 0.06,$ which occur nearly at $\xi = 0.6$. In present case, strong self-focusing occurs at $\xi = 0.12$ for extraordinary mode at magnetic field parameter, ω_c/ω=0.3 for $b = 2.12$, in the presence of plasma density ramp. Hence present results in the presence of plasma density ramp may be more useful.

Figure 6.6, represents the variation of beam width parameter with the normalized propagation distance for different values of relative plasma densities, ω_{P0}/ω = 0.65, 0.70, 0.75 and 0.77 at $b = 2.12$ for extraordinary mode, figure 6.6(a) and ordinary mode, figure 6.6(b). It is obvious that for higher value of relative plasma density, the beam width parameter reaches its minimum value $f = 0.09$ at $\xi = 0.12$ and hence self-focusing effect enhanced. However, for ordinary mode, self-focusing trends are similar to extraordinary mode but occurs at higher value of normalized propagation distance. Singh *et al.* [82] have studied the self-focusing of a laser beam in relativistic plasma and reported the strong self-focusing for relative plasma density, $\omega_{P0}/\omega = 0.7$ at $\xi = 0.7$ (approximately). In another work, Kant *et al.* [85], analyzed the ponderomotive self-focusing of a short pulse laser in an underdense plasma under density ramp and reported strong self-focusing for $\omega_{P0}^2/\omega^2 = 0.08$ at $\xi = 0.5$. In our case, the strong self-focusing of beam occurs earlier than the results reported by [14, 81] due to the presence of plasma density ramp and cosh-Gaussian beam profile.

6.4 CONCLUSION

From the above results, we conclude that with the increase in the value of magnetic field for decentered parameter $b = 2.12$, self-focusing of cosh-Gaussian laser beam becomes stronger for extraordinary mode while for ordinary mode, it becomes somewhat weaker and occurs at higher values of normalized propagation distance. Decentered parameter also plays a significant role to decide the early and strong focusing ability of cosh-Gaussian beam as for $b = 0$, focusing of beam occurs at higher value of 'ξ' for extraordinary and ordinary modes. The self-focusing of the cosh-Gaussian laser beam is found to be very strong and occurs earlier at $\xi = 0.12$. This happens due to the presence

of plasma density ramp and chosen beam profile. Thus plasma density ramp plays a very vital role to the self-focusing of the cosh-Gaussian laser beam. Also self-focusing becomes stronger with the increase in value of intensity and magnetic field parameter under the application of plasma density ramp. It is concluded that extraordinary mode is more prominent toward self-focusing rather than ordinary mode of propagation and density ramp enhances the self-focusing effect. Our investigation may be useful for laser induced fusion as well as for scribing type of applications in electronics.

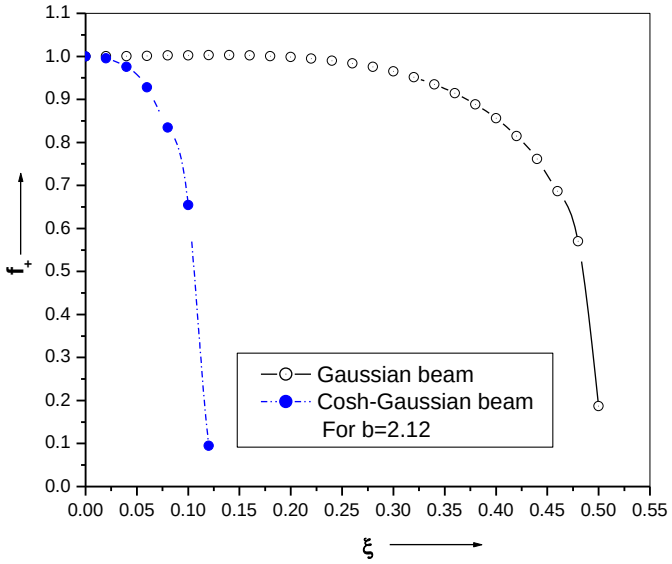

Fig.6.2(a)

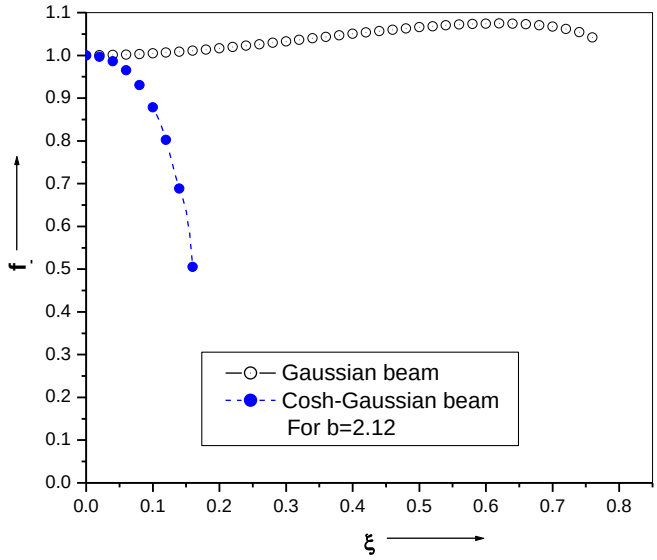

Fig. 6.2(b)

Figure 6.2: Variation of beam width parameter $(f_{\pm})$ with normalized propagation distance (ξ) for cosh-Gaussian and Gaussian beam for (a) extraordinary and (b) ordinary mode of propagation. The various parameters are taken as $\alpha E_0^2 = 0.5, d_0 = 0.9, \omega_c/\omega = 0.3, \omega r_0/c = 293, m_0/M = 0.0006$ and $\omega_{P0}/\omega = 0.77$.

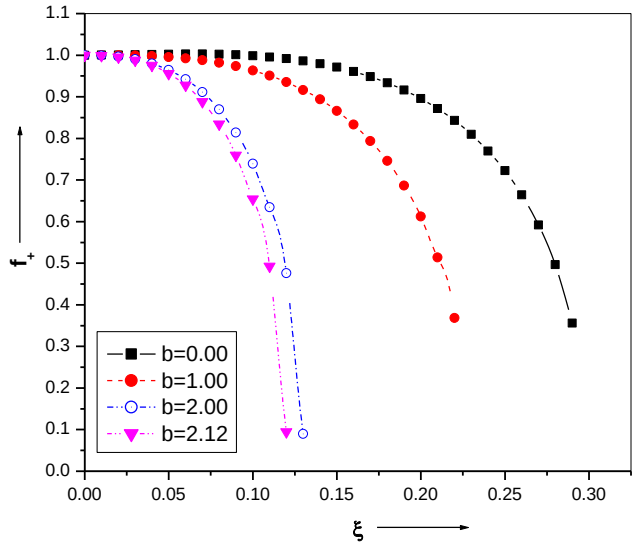

Fig. 6.3(a)

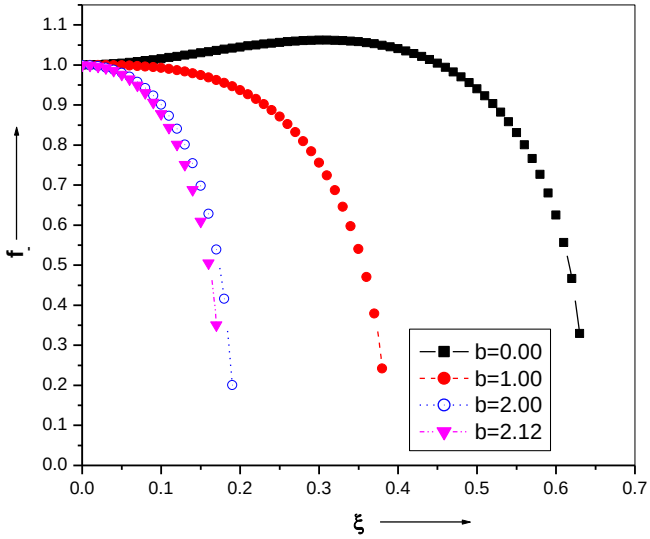

Fig. 6.3(b)

Figure 6.3: Variation of beam width parameter $(f_{\pm})$ with normalized propagation distance (ξ) for different values of decentered parameter for (a) extraordinary and (b) ordinary mode of propagation. The other parameters are taken as $\alpha E_0^2 = 0.5,\ d_0 = 0.9,\ \omega_c/\omega = 0.3,\ \omega r_0/c = 293,\ m_0/M = 0.0006$ and $\omega_{P0}/\omega = 0.77$.

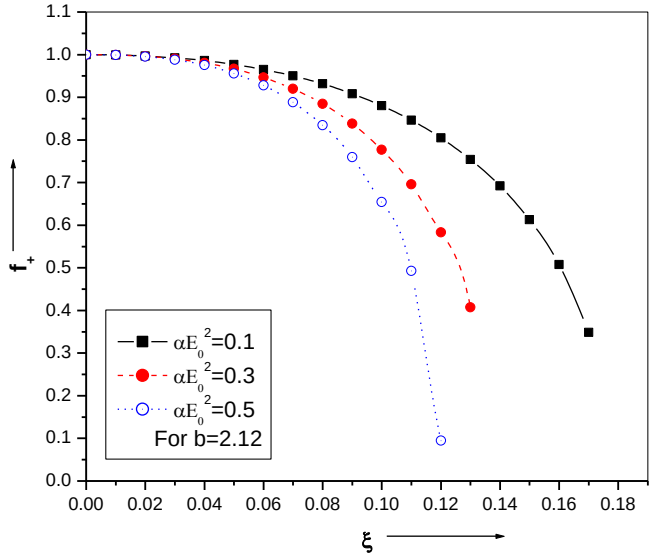

Fig. 6.4(a)

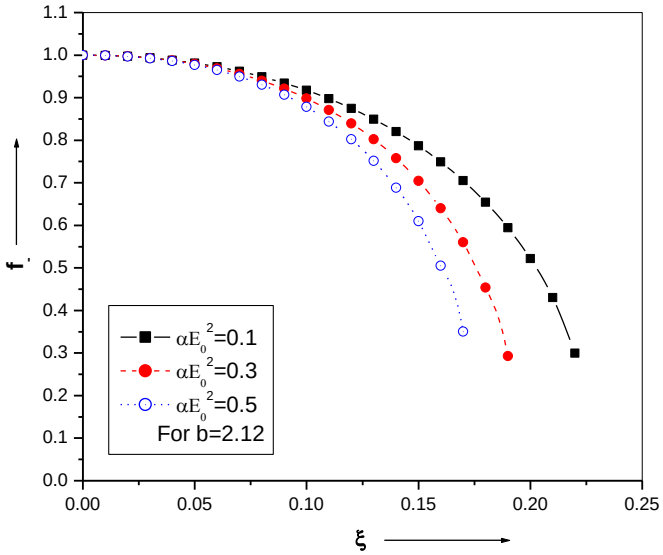

Fig. 6.4(b)

Figure 6.4: Variation of beam width parameter $(f_{\pm})$ with normalized propagation distance (ξ) for different values of intensity parameter for (a) extraordinary and (b) ordinary mode of propagation. The other parameters are taken as $d_0 = 0.9, \omega_c/\omega = 0.3, \omega r_0/c = 293, m_0/M = 0.0006$ and $\omega_{P0}/\omega = 0.77.$

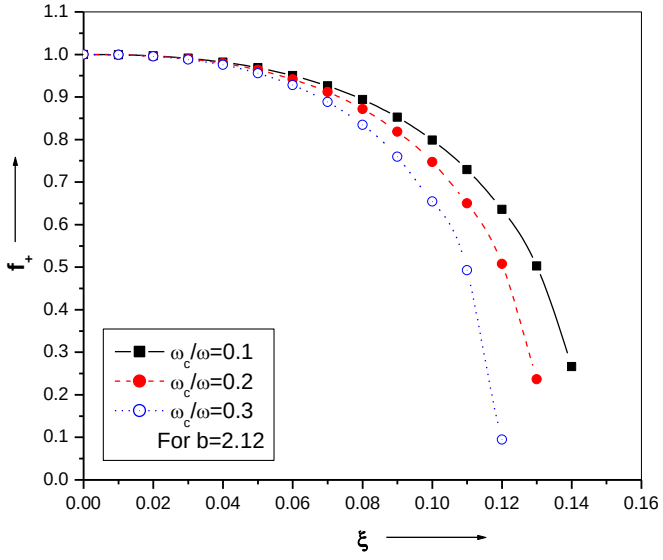

Fig. 6.5(a)

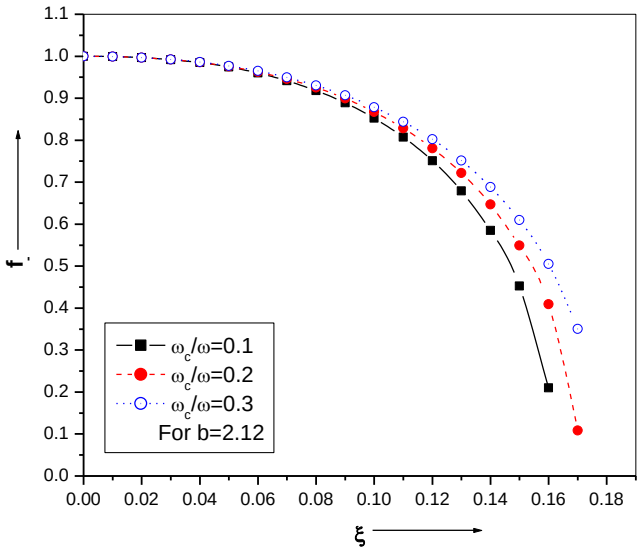

Fig. 6.5(b)

Figure 6.5: Variation of beam width parameter $(f_{\pm})$ with normalized propagation distance (ξ) for different values of magnetic field parameter for (a) extraordinary and (b) ordinary mode of propagation. The other parameters are taken as $\alpha E_0^2 = 0.5, d_0 = 0.9, \omega r_0 / c = 293, m_0 / M = 0.0006$ and $\omega_{P0} / \omega = 0.77$.

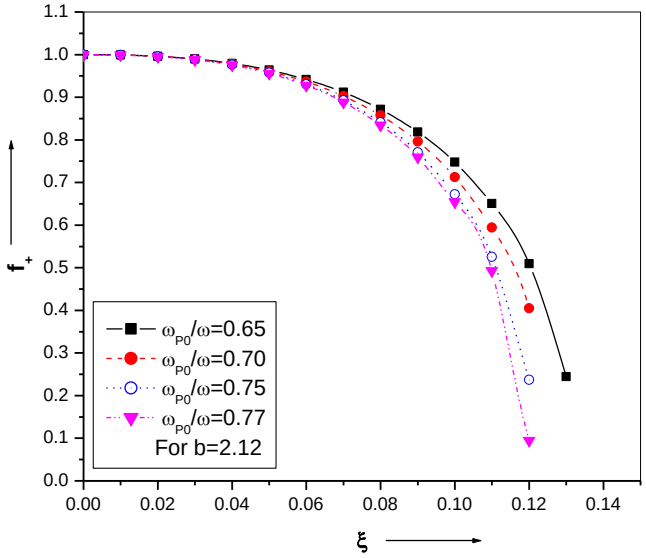

Fig. 6.6(a)

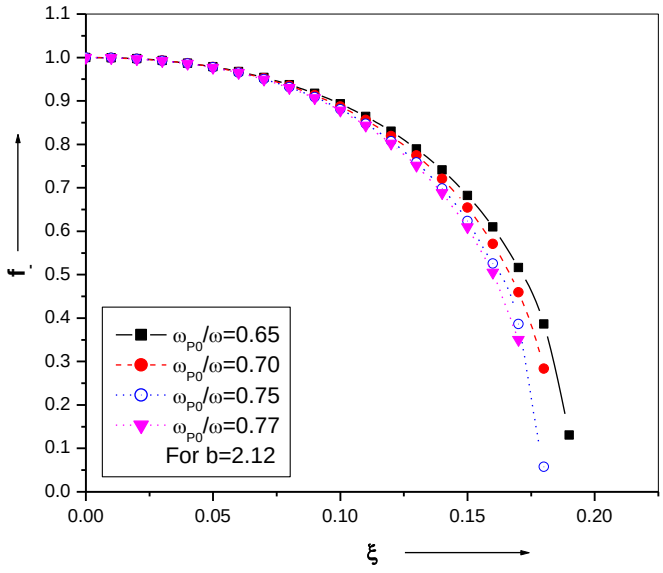

Fig. 6.6(b)

Figure 6.6: Variation of beam width parameter ($f_{\pm}$) with normalized propagation distance (ξ) for different values of relative plasma density parameter for (a) extraordinary and (b) ordinary mode of propagation. The other parameters are taken as $\alpha E_0^2 = 0.5,\ d_0 = 0.9,\ \omega_c/\omega = 0.3,\ \omega r_0/c = 293$ and $m_0/M = 0.0006.$

CHAPTER 7

OBSERVATION OF EARLY AND STRONG RELATIVISTIC SELF-FOCUSING OF COSH-GAUSSIAN LASER BEAM IN COLD QUANTUM PLASMA

7.1 INTRODUCTION

In the year 1962, Askar'yan [1] discovered the self-focusing effect of light. Hora [2], Siegrist [3] etc. have the remarkable contribution in the field of relativistic self-focusing of light. Thereafter, it attracts the attention of researcher and turn out to be most charming field of research. Lot of work has been done on self-focusing of laser beam in plasma[2-4], cluster[5, 6], liquid [7] etc. using various beam profiles like Gaussian beam [4], Hermite-Gaussian beam [15], cosh-Gaussian beam [14], Hermite-cosh-Gaussian beam [16-18, 95, 96, 98] etc. Self-focusing of light has many socially useful applications like x-ray lasers and the laser driven accelerators [8], the generation of inertial fusion energy driven by lasers [9-11] etc. which makes the life of human being quite easier. Short pulse laser having extremely high intensity of the order of $10^{17}-10^{20}\,W/cm^2$ enabled various high energy related experiments in the field of science and technology.

Self-focusing phenomenon in plasma arises as the laser light propagates through the plasma and modifies the dielectric constant of the plasma. It may be relativistic or ponderomotive or thermal self-focusing in nature. Now a day, propagation of laser beam through cold plasma is widely studied by researcher because the quantum plasma systems have many useful applications. Shukla [101], Misra [102], Bergamin [103] and many other researchers has studied nonlinear interaction in quantum plasma. Quantum plasma has high density and low temperature and now it is possible to produce plasmas with densities near to solid state density. Moreover, quantum plasma systems become more significant because of their relevance to laser-solid interactions, quantum dots [104], astrophysical and cosmological environments [105, 106], nanotechnology [107-109] and fusion-science [110, 111]. In classical plasmas, Boltzmann-Maxwell statistical distribution is widely used while in the quantum plasmas, Fermi-Dirac statistical distribution is used and Wigner formalism is employed rather than classical Vlasov equation [112]. In classical regimes, the de-Broglie wavelength is very small and all

particles are considered as point-like particles, however; if the de-Broglie wavelength becomes of the order of the average interparticle distance, then quantum effect can be considered [113].

In the present case, relativistic self-focusing effect in cold plasma is analyzed. The high intensity laser pulses provide sufficient energy to the constituents like electrons of the plasma which cause an electron oscillatory velocity comparable to the velocity of light. Thus the mass of electron, oscillating at relativistic velocities in laser field, increases by a factor given by $\gamma = 1/\left(1 - v^2/c^2\right)^{1/2}$ and give rise to non-linearity due to which the relativistic self-focusing effect occurs. Earlier, self-focusing in cold plasma has been studied by Jung *et al.* [79]. The self-focusing of Gaussian laser beam in relativistic cold quantum plasma has been studied by Patil *et al.* [114] and reported strong self-focusing of the beam with the increase in the value of intensity parameter and relative density parameter due to the generation of quasi-stationary magnetic field. Habibi *et al.* [115] has studied stationary self-focusing of intense laser beam in cold quantum plasma using ramp density profile.

In the present work, propagation of cosh-Gaussian beam in cold plasma has been studied. We have choose the cosh-Gaussian laser beam profile as cosh-Gaussian laser beam possesses more power than that of Gaussian laser beams having high intensity near the axis of propagation and hence, generates flat top beam profiles [99] which is useful for scribing type of applications in electronics where same intensity of laser beams for long time is required. Zhang *et al.* [100] has identified a group of virtual sources that generate a cosh-Gaussian wave. Previously, cosh-Gaussian profile has been studied by various authors viz. Gill *et al*. [14], Nanda *et al.* [116] etc. We develop the equations for beam width parameter for cosh-Gaussian beam and solve them numerically by applying Wentzel-Kramers-Brillouin (WKB) approximation and Paraxial approximation [4, 90] and observed the early enhancement of self-focusing of the laser beam with normalized propagation distance. This paper is planned as follows: we find the beam width parameter equation in section II, result is discussed in section III and a brief conclusion is given in section IV.

7.2 EVOLUTION OF BEAM WIDTH PARAMETER

The field distribution of cosh-Gaussian laser beam propagating in the plasma along z-axis is of the following form:

$$E(r,z)=\frac{E_0}{f(z)}e^{\frac{b^2}{4}}\left\{e^{-\left(\frac{r}{r_0 f(z)}+\frac{b}{2}\right)^2}+e^{-\left(\frac{r}{r_0 f(z)}-\frac{b}{2}\right)^2}\right\} \quad \ldots (7.1)$$

here E_0 is the amplitude of cosh-Gaussian laser beam for the central position at $r=z=0$, $'f(z)'$ is the dimensionless beam width parameters, $'r_0'$ is the spot size of the beam and $'b'$ is the decentered parameter of the beam.

The propagating beam imparts an oscillatory velocity, $v=eE/m_0\omega\gamma$, to the electrons. Here e, m_0 and ω are the charge on electron, rest mass of electron and angular frequency of incident laser beam respectively, and $\gamma=\left(1+\alpha EE^*\right)^{1/2}$ is the intensity dependent relativistic factor with $\alpha=e^2/m_0^2\omega^2c^2$, here c is the speed of light in vacuum. The intensity dependent dielectric constant for the non-linear medium is obtained by applying the approach given by Sodha *et al.* [4]:

$$\varepsilon=\varepsilon_0+\phi(EE^*) \quad \ldots (7.2)$$

where $\varepsilon_0=1-\omega_{P0}^2/\omega^2$, is linear part of the dielectric constant with ω_{P0} as plasma frequency. For cold plasma the dielectric constant is obtained by applying the approach as applied by Jung and Murakami [79],

$$\varepsilon_{rel}=1-\frac{\omega_{P0}^2}{\gamma\omega^2}\left(1-\frac{\delta q}{\gamma}\right)^{-1} \quad \ldots (7.3)$$

with $\delta q=4\pi^4h^2/m^2\omega^2\lambda^4$, where h is Planck's constant, λ is the wavelength of incident laser beam. The classical relativistic dielectric constant can be obtained easily by ignoring the quantum effect by setting the value of δq as zero.

For isotropic, non-conducting and non absorbing medium, Maxwell's equations give the following wave equation

$$\nabla^2\vec{E}-\frac{\varepsilon}{c^2}\frac{\partial^2\vec{E}}{\partial t^2}+\vec{\nabla}\left(\vec{E}\frac{\vec{\nabla}(\varepsilon)}{\varepsilon}\right)=0 \quad \ldots (7.4)$$

For $(1/K^2)\nabla^2(\ln\varepsilon) << 1$, we get,

$$\frac{\partial^2\vec{E}}{\partial z^2}+\frac{\partial^2\vec{E}}{\partial r^2}+\frac{1}{r}\frac{\partial\vec{E}}{\partial r}+\frac{\varepsilon\omega^2}{c^2}\vec{E}=0 \qquad \ldots (7.5)$$

The solution of Eq. (7.5) is of the form $\vec{E}=A(r,z)\exp\left[i(\omega t-kz)\right]$, with $k=\left(\varepsilon_{\text{rel}}\right)^{1/2}\omega/c$. Substituting this value in Eq. (7.5) and neglecting $\partial^2 A/\partial z^2$, we get a complex differential equation with real and imaginary parts. The real and imaginary parts of this equation are separated by introducing an additional eikonal $A(r,z)=A_0(r,z)\exp\left[-ikS(r,z)\right]$, here $'A_0'$ and $'S'$ are the real functions of $'r'$ and $'z'$ respectively.

Real part is

$$2\frac{\partial S}{\partial z}+\left(\frac{\partial S}{\partial r}\right)^2=\frac{1}{2A_0^2k^2}\frac{\partial^2A_0^2}{\partial r^2}-\frac{1}{4A_0^4K^2}\left(\frac{\partial A_0^2}{\partial r}\right)^2+\frac{1}{2A_0^2k^2r}\frac{\partial A_0^2}{\partial r}+\frac{\phi(A_0^2)}{\varepsilon_0} \qquad \ldots (7.6)$$

Imaginary part is

$$\frac{\partial A_0^2}{\partial z}+\frac{A_0^2}{r}\frac{\partial S}{\partial r}+A_0^2\frac{\partial^2S}{\partial r^2}+\frac{\partial S}{\partial r}\frac{\partial A_0^2}{\partial r}=0 \qquad \ldots (7.7)$$

The solution of equation (7.6) & (7.7) are of the form,

$$A_0^2=\frac{E_0^2}{f^2(z)}e^{\frac{b^2}{2}}\left\{e^{-2\left(\frac{r}{r_0f(z)}+\frac{b}{2}\right)^2}+e^{-2\left(\frac{r}{r_0f(z)}-\frac{b}{2}\right)^2}+2e^{-\left(\frac{2r^2}{r_0^2f^2(z)}+\frac{b^2}{2}\right)}\right\} \qquad \ldots (7.8)$$

And

$$S=\frac{r^2}{2}\beta(z)+\varphi(z) \qquad \ldots (7.9)$$

with $\beta(z)=\left(1/f(z)\right)df/dz$ where $'\varphi(z)'$ is an arbitrary function of $'z'$.

Using these values in Eq. (7.6), we obtain the equation governing the evolution of beam width parameter,

$$\frac{d^2f}{d\xi^2}=\frac{\left(4-4b^2\right)}{f^3}-\frac{4\alpha E_0^2}{f^3}\left(\frac{\omega_{P0}^2}{\omega^2}\right)\left(\frac{\omega r_0}{c}\right)^2\left(1+\frac{4\alpha E_0^2}{f^2}\right)^{-\frac{1}{2}}\left[\left(1+\frac{4\alpha E_0^2}{f^2}\right)^{\frac{1}{2}}-\delta q\right]^{-2}e^{\frac{b^2}{2}} \qquad \ldots (7.10)$$

Similarly Eq. (7.7) gives the boundary conditions, $\xi = 0,\ f = 1$ and $df/d\xi = 0$.

7.3 RESULTS AND DISCUSSION

In the present study numerical calculations has been done by taking the frequency, plasma electron density and spot size of incident laser beam similar as taken by Patil *et. al.*[114] and are given by $\omega = 1.778 \times 10^{20}\, rad/s$, $n_e = 4 \times 10^{19}\, cm^{-3}$ and $r_0 = 20\mu m$ respectively. In order to study classical relativistic case, we assume that $\delta q \to 0$.

Figure 7.1 depicts the variation of beam width parameter (f) with the normalized propagation distance (ξ) for classical relativistic and cold quantum cases for decentered parameter $b = 0$. From the figure, it is observed that in classical relativistic case the laser beam converges strongly at normalized propagation distance $\xi = 0.2$ while in case of cold quantum plasma, it converges strongly earlier at normalized propagation distance $\xi = 0.12$. Thus, the focusing length decreases greatly in case of cold quantum plasma than classical relativistic case and hence converging tendency of the laser beam, in the cold quantum case, shifted towards lower value of normalized propagation distance as compared to classical relativistic case. This happens because the quantum contribution adds additional self-focusing effect which is missing in classical relativistic case. The results observed in the present study are in agreement with the previously reported results by Patil e*t. al.*[114].

Figure 7.2 depicts the variation of the beam width parameter (f) with the normalized propagation distance (ξ) at different values of relative density parameter for $b = 0$. For relative density parameter, $\omega_{P0}/\omega = 1 \times 10^{-6}$, the laser beam converses strongly at normalized propagation distance $\xi = 0.12$. However; the conversing tendency of the laser beam shifted towards lower value of normalized propagation distance with the increase in the value of relative density parameter. At higher value of relative density parameter, $\omega_{P0}/\omega = 2 \times 10^{-6}$, earlier and strong self-focusing of laser beam is observed at normalized propagation distance $\xi = 0.06$. Further, at certain higher value of relative density parameter, $\omega_{P0}/\omega = 3 \times 10^{-6}$ strong self-focusing of laser beam is observed at normalized propagation distance $\xi = 0.04$. It is obvious from the figure 2 that with the

increase in the value of relative density parameter (ω_{P0}/ω), self-focusing of cosh-Gaussian beam enhanced and shifted towards lower values of normalized propagation distance. The basic physics behind this is that as the density of the medium enhances, the propagating laser beam in the medium creates more and more relativistic electrons and which results stronger self-focusing effect. Patil *et al.*[114] has reported strong self-focusing of Gaussian beam at $\xi = 0.05$ for $\omega_P / \omega = 3 \times 10^{-6}$. We have reported strong self-focusing of the laser beam at $\xi = 0.04$ for $\omega_{P0} / \omega = 3 \times 10^{-6}$. In the present study, we observe early and strong self-focusing of cosh-Gaussian laser beam for higher values of relative density parameters.

Figure 7.3 depicts the variation of the beam width parameter (*f*) with the normalized propagation distance (ξ) at different values of decentered parameters. It is obvious from the plot that for decentered parameter $b = 0.0$, cosh-Gaussian laser beam converges strongly at normalized propagation distance $\xi = 0.12$. Similarly, for decentered parameter $b = 0.9$, cosh-Gaussian laser beam converges strongly at normalized propagation distance $\xi = 0.10$. The early and strong converging of laser beam is observed for decentered parameter $b = 1.8$, for which cosh-Gaussian laser beam converges strongly at normalized propagation distance $\xi = 0.05$. Thus it is quite obvious from the result obtained that the converging tendency of the cosh-Gaussian laser beam shifted towards lower values of normalized propagation distance for higher values of decentered parameter.

7.4 CONCLUSION

In the present investigation we have studied the relativistic self-focusing of cosh-Gaussian laser beam in cold quantum plasma. We have derived the equation for beam width parameter using WKB approximation and paraxial ray approach. We report early enhancement of self-focusing of cosh-Gaussian laser beam in cold quantum plasma. The comparative study between self-focusing of cosh-Gaussian laser beam in cold quantum case and classical relativistic case has been made for decentered parameter $b = 0$ and it is observed that as the beam propagates deeper inside the cold quantum plasma, the self-focusing ability of the laser beam enhances and occurs earlier with normalized

propagation distance due to quantum contribution. Moreover, early and strong self-focusing is observed with the increase in values of the relative density parameter. We conclude that spot size of the cosh-Gaussian laser beam contracts significantly as it propagates deeper inside the cold quantum plasma due to quantum contribution. Also early and strong self-focusing of the laser beam is observed for higher values of decentered parameter. The present study may be helpful to the researchers to select the value of relative density parameter as per their choice to obtained considerable improvement in the focusing quality which may be useful in inertial fusion energy driven by lasers, scribing type of applications in electronics etc.

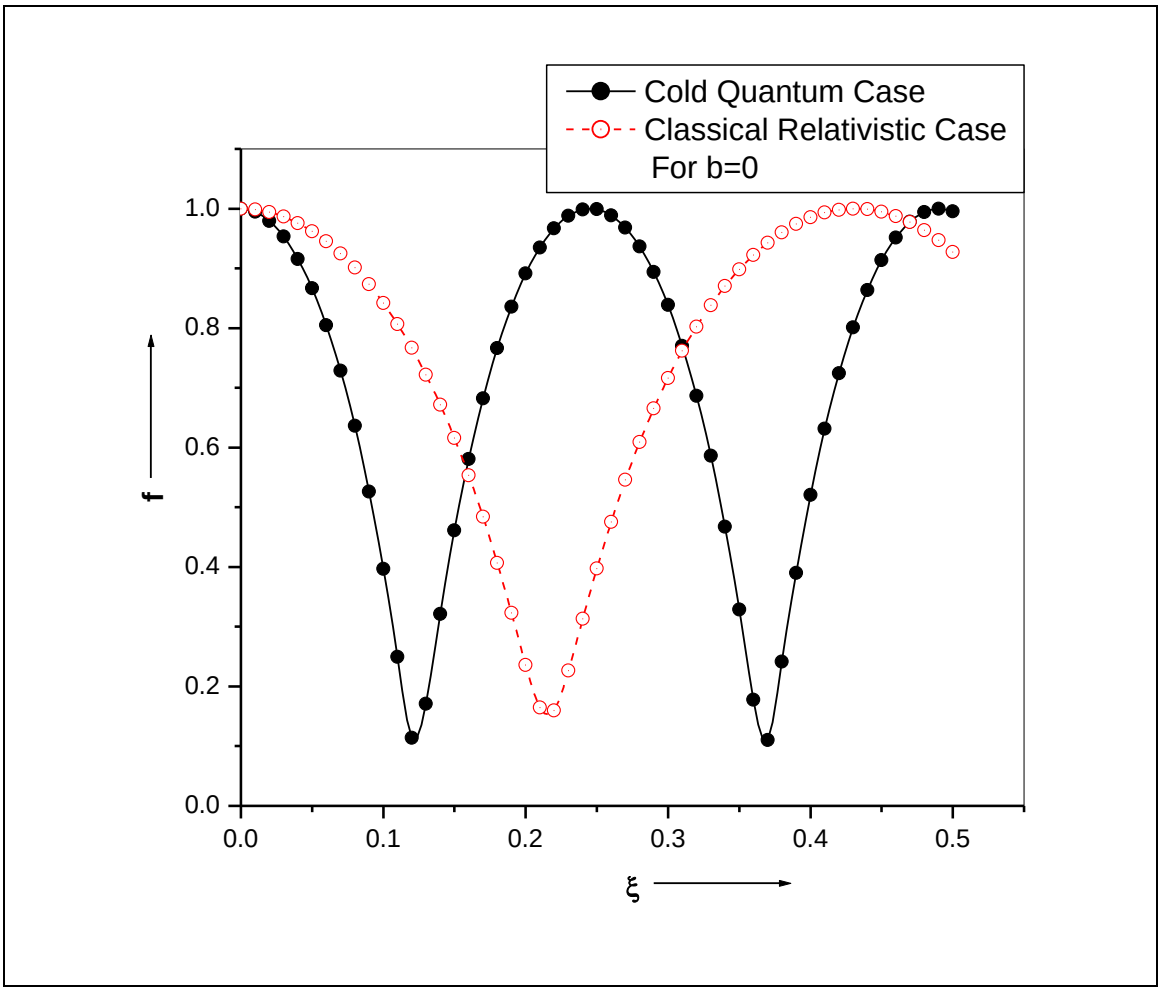

Figure 7.1: Variation of beam width parameter (f) with normalized propagation distance (ξ) for cold quantum case and classical relativistic case. The various parameters are taken as $\alpha E_0^2 = 0.1$, $\omega_{P0}/\omega = 1\times10^{-6}$, $\delta q = 0.00517\times10^2$ **and** $r_0 = 20\mu m$.

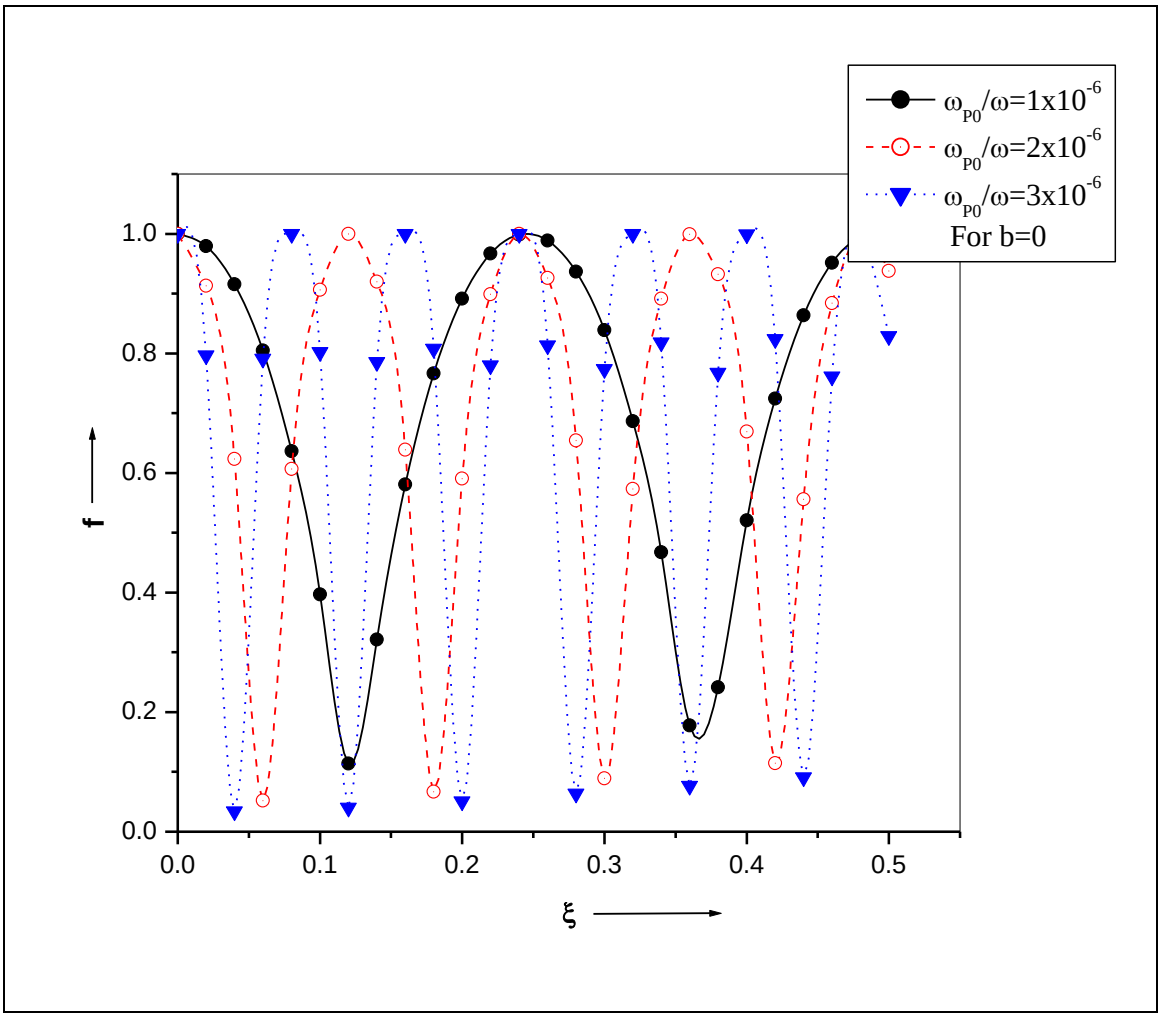

Figure 7.2: Variation of beam width parameter (f) with normalized propagation distance (ξ) at different values of relative density parameter for $b = 0$. **The other parameters are taken as** $\alpha E_0^2 = 0.1$, $\delta q = 0.00517 \times 10^2$ and $r_0 = 20 \mu m$.

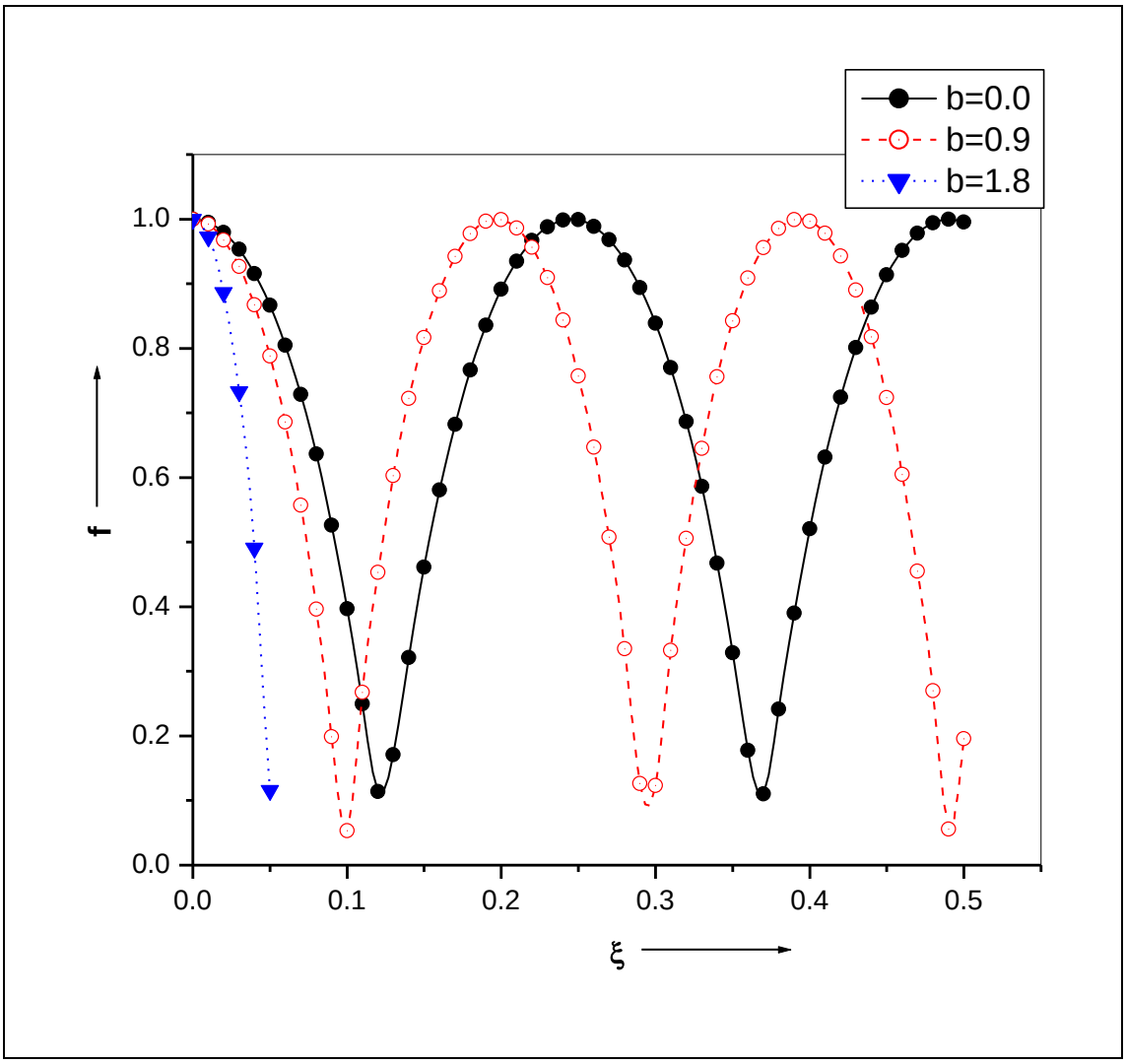

Figure 7.3: Variation of beam width parameter (f) with normalized propagation distance (ξ) at different values of decentered parameter. The other parameters are taken as $\alpha E_0^2 = 0.1$, $\delta q = 0.00517 \times 10^2$ and $r_0 = 20 \mu m$.

CHAPTER-8

SELF-FOCUSING OF COSH-GAUSSIAN LASER BEAM IN A CLUSTERED GAS

8.1 INTRODUCTION

The nonlinear interactions of laser beams with plasmas and clusters have been studied intensively for over more than four decades. Interaction of high power laser beams with the atomic cluster is one of the interesting areas of research and attracts the attention of the scientists and researchers. It is well known now that an intense short pulse laser quickly converts atomic clusters into plasma balls which expand rapidly under hydrodynamic expansion or Coulomb explosion [34, 35]. Due to this expansion the electron density inside the expanding cluster falls rapidly and approaches thrice the critical density. Thus electron response to the laser enhances which give rise to various phenomenon of great interest like strong absorption of laser energy [37], self-focusing of laser beam [6, 98, 116], production of energetic neutrons [38], generation of harmonics and x-rays [22] etc. This happens because under the action of intense laser pulse, the effective permittivity of the medium changes abruptly and thus gives rise to nonlinearity. The Coulomb explosion of the cluster produces energetic ions. Zweiback et al. [34] have developed a model for Coulomb explosion. Liu and Tripathi [35] have also developed a collsionless model of Coulomb explosion of clusters by the Gaussian laser beams. The first experimental and theoretical study of self-focusing of laser beams in cluster has been given by Alexeev et al. [33] They interacts $800nm, 3.5\times10^{16}Wcm^{-2}, 80\,fs-1.4\,ps$ laser pulse of spot size of the order of $10\mu m,$ with the argon cluster of average radius 300 Å. They have observed that after propagating a distance of $3mm$ through the gas jet, the beam radius decreases as pulse length varied from $80\,fs$ to $350\,fs$ and then rises mildly.

Liu et al. [119] have studied the self-focusing of laser beam and nonlinear absorption in expanding cluster and employed collisionless model of Coulomb explosion for small size clusters and hydrodynamic model for large size of clusters. They have studied self-focusing of laser beam with and without absorption and evaluated

transmission energy lose during the propagation of laser beam into the gas containing clusters. The effect of self-focusing on laser third harmonic generation in clustered gas has been studied by Parashar [117] by employing a $800\ nm$ laser of spot size $10\ \mu m$ in argon gas with $300\ \text{Å}$ clusters. Zharova et al. [118] studied analytically and numerically the self-focusing of laser radiation in plasma with ionized gaseous clusters and proposed an electro-dynamic model for cluster plasma in a field of ultra-short laser pulse. Further, it is shown that, for a laser power exceeding the self-focusing critical power, the wave-field self-compression occurs in a medium with dispersion of any type (normal, anomalous, or combined). In this work we have studied the self-focusing of cosh-Gaussian laser beam in clustered gas. In section II, the equation for beam width parameter has been developed by using WKB and paraxial approximation. In section III, results obtained have been discussed and in section IV, we have concluded the outcomings of the presented work.

8.2 EVOLUTION OF BEAM WIDTH PARAMETER

A cosh-Gaussian laser beam is propagating through a gas of atomic number Z_i comprising of n_c clusters per unit volume. Let r_{c0} is the initial radius of the cluster. This gas also contains free atoms outside the cluster and the density of these free atoms is n_0. The field distribution of the cosh-Gaussian beam is

$$E(r,z,t)=\frac{E_0(r,z,t)}{f(z,t)}e^{\frac{b^2}{4}}\left\{\exp\left[-\left(\frac{r}{r_0 f(z,t)}+\frac{b}{2}\right)^2\right]+\exp\left[-\left(\frac{r}{r_0 f(z,t)}-\frac{b}{2}\right)^2\right]\right\} \quad \ldots (8.1)$$

where $E_0(r,z,t)$ is the initial amplitude of cosh-Gaussian laser beam, $f(z,t)$ is the dimensionless beam width parameters, r_0 is the spot size of the laser beam and b is the decentered parameter of the beam. The laser beam quickly ionises the atoms of the clusters and converting them into plasma balls. In the present study these balls are considered as spherical and have uniform electron density n_e. Initially the electron density is $n_e = n_{e0}$, and as the cluster expands this electron density falls down with the radial location of the cluster as well as time. The electrons of each cluster undergo oscillatory displacement χ governed by the equation of motion

$\partial^2 x/\partial t^2 = -\left(\omega_{pe}^2/3\right)x - eE/m$, where e and m are the electronic charge and rest mass of the electron, $\omega_{pe} = \left(4\pi\, n_e e^2/m\right)^{1/2}$ is the plasma frequency inside the cluster.

The effective dielectric constant for the non-linear medium is obtained by applying the approach as applied by Liu *et al.* [119]:

$$\varepsilon_{eff} = 1 + \frac{4\pi}{3}\frac{n_c r_{c0}^3 \omega_{pe}^2}{\left(\frac{\omega_{pe}^2}{3} - \omega^2\right)} - \frac{\omega_{pp}^2}{\omega^2} \qquad \ldots (8.2)$$

where $\omega_{pp} = \left(4\pi\, n_{p0} e^2/m\right)^{1/2}$ is the plasma frequency outside the cluster and the term ω_{pp}^2/ω^2 is the dielectric constant contributed by the free electron provided by the free atoms outside the cluster. n_{p0} is the electron density provided by the free atoms outside the cluster and ω is the frequency of the incident laser beam. Initially at $r = 0$, the dielectric constant is maximum interior the cluster and as the radius of the cluster increases, the dielectric constant falls. The intensity of the laser beam affects the dielectric constant of the argon gas embedded with clusters and hence the free electrons outside the clusters vary with laser intensity. Thus the effective dielectric constant of the medium can be written as

$$\varepsilon_{eff} = \varepsilon_0 - \phi\frac{r^2}{r_0^2} \qquad \ldots (8.3)$$

where $\varepsilon_0 = 1 + (4\pi/3) n_c r_{c0}^3 \omega_{p1}^2/\left(\omega_{pe}^2/3 - \omega^2\right)$ and

$\phi = (4\pi/3) n_c r_c^3 \alpha \omega_{p1}^2/3\left(\omega_{p1}^2/\left(\omega_{p1}^2/3 - \omega^2\right)^2\right)$

The free electron reduces the value of ϕ and hence contributes for the defocusing of the laser beam. This means that initially self-focusing is strong. Applying hydrodynamic model of cluster expansion and following Liu et al. [35], we obtained

$$\omega_{p1}^2 = \frac{\omega_{pe0}^2}{\left(1 + \frac{\eta}{f}\right)^3} \qquad \ldots (8.4a)$$

And

$$\alpha = \frac{3}{2f^3}\frac{\eta}{\left(1+\frac{\eta}{f}\right)} \qquad \ldots (8.4b)$$

where η is the collision frequency and is given by

$$\eta = \sqrt{\frac{Z_i \nu \tau\, m}{2m_i}}\frac{eA_0\ t}{mf\omega\left(\frac{\omega_{pe0}^2}{3\omega^2}-1\right)^2 r_{c0}} \qquad \ldots (8.4c)$$

here τ is the pulse duration and m_i is the mass of the ion.

The general form of wave equation for exponentially varying field obtained from Maxwell's equation is given by

$$\nabla^2\vec{E} - \nabla(\nabla.\vec{E}) = -\frac{\omega^2}{c^2}\varepsilon.\vec{E} \qquad \ldots (8.5a)$$

For $\left(1/k^2\right)\nabla^2(\ln\varepsilon) << 1,$

$$\nabla^2\vec{E} + k^2\vec{E} = 0$$

In cylindrical co-ordinate system, we can write this equation as

$$\frac{\partial^2\vec{E}}{\partial z^2} + \frac{\partial^2\vec{E}}{\partial r^2} + \frac{1}{r}\frac{\partial\vec{E}}{\partial r} + \varepsilon\frac{\omega^2}{c^2}\vec{E} = 0 \qquad \ldots (8.5b)$$

For slowly converging or diverging cylindrically symmetric beam, the solution of equation (8.5b) is of the following form,

$$\vec{E} = A(r,z)Exp\left[i(\omega t - kz)\right] \qquad \ldots (8.6)$$

With $k^2 = \varepsilon_0\,\omega^2/c^2 = \omega^2/c^2\left(1-\omega_{P0}^2/\gamma\omega^2\right).$

Differentiating equation (8.6) twice w. r. t. 'r' and 'z', we get

$$\frac{\partial\vec{E}}{\partial r} = Exp\left[i(\omega t - kz)\right]\frac{\partial A(r,z)}{\partial r}$$

$$\frac{\partial^2\vec{E}}{\partial r^2} = Exp\left[i(\omega t - kz)\right]\frac{\partial^2 A(r,z)}{\partial r^2}$$

And

$$\frac{\partial \vec{E}}{\partial z} = -ikA(r,z)Exp\left[i(\omega t - kz)\right] + Exp\left[i(\omega t - kz)\right]\frac{\partial A(r,z)}{\partial z}$$

$$\frac{\partial^2 \vec{E}}{\partial z^2} = -k^2 A(r,z)Exp\left[i(\omega t - kz)\right] - 2ikExp\left[i(\omega t - kz)\right]\frac{\partial A(r,z)}{\partial z} + Exp\left[i(\omega t - kz)\right]\frac{\partial^2 A(r,z)}{\partial z^2}$$

Substituting these values in equation (8.5b), we get

$$-k^2 A(r,z)Exp\left[i(\omega t - kz)\right] - 2ikExp\left[i(\omega t - kz)\right]\frac{\partial A(r,z)}{\partial z} + Exp\left[i(\omega t - kz)\right]\frac{\partial^2 A(r,z)}{\partial z^2}$$

$$+ Exp\left[i(\omega t - kz)\right]\frac{\partial^2 A(r,z)}{\partial r^2} + \frac{1}{r}Exp\left[i(\omega t - kz)\right]\frac{\partial A(r,z)}{\partial r}$$

$$+ \left(\varepsilon_0 + \phi\left(AA^*\right)\right)\frac{\omega^2}{c^2}A(r,z)Exp\left[i(\omega t - kz)\right] = 0$$

$$-k^2 A(r,z) - 2ik\frac{\partial A(r,z)}{\partial z} + \frac{\partial^2 A(r,z)}{\partial z^2} + \frac{\partial^2 A(r,z)}{\partial r^2} + \frac{1}{r}\frac{\partial A(r,z)}{\partial r} + \varepsilon_0\frac{\omega^2}{c^2}A(r,z)$$

$$+ \phi\left(AA^*\right)\frac{\omega^2}{c^2}A(r,z) = 0$$

$$-k^2 A(r,z) - 2ik\frac{\partial A(r,z)}{\partial z} + \frac{\partial^2 A(r,z)}{\partial z^2} + \frac{\partial^2 A(r,z)}{\partial r^2} + \frac{1}{r}\frac{\partial A(r,z)}{\partial r} + k^2 A(r,z)$$

$$+ \phi\left(AA^*\right)\frac{\omega^2}{c^2}A(r,z) = 0$$

Neglecting $\frac{\partial^2 A(r,z)}{\partial z^2}$, we get

$$-2ik\frac{\partial A(r,z)}{\partial z} + \frac{\partial^2 A(r,z)}{\partial r^2} + \frac{1}{r}\frac{\partial A(r,z)}{\partial r} + \frac{\phi\left(AA^*\right)}{\varepsilon_0}k^2 A(r,z) = 0 \qquad \ldots (8.7)$$

To solve equation (8.7), we express

$$A(r,z) = A_{0p}(r,z)Exp\left[-ikS(r,z)\right] \qquad \ldots (8.8)$$

Here A_{0p} and S are the real functions of 'r' and 'z'.

Differentiating equation (8.8) twice, w. r. t. 'r', we get

$$\frac{\partial A(r,z)}{\partial r} = A_{0p}Exp\left[-ikS(r,z)\right](-ik)\frac{\partial S(r,z)}{\partial r} + Exp\left[-ikS(r,z)\right]\frac{\partial A_{0p}}{\partial r}$$

$$\frac{\partial^2 A(r,z)}{\partial r^2} = -ikA_{0p}Exp\left[-ikS(r,z)\right]\frac{\partial^2 S(r,z)}{\partial r^2} - k^2 A_{0p}Exp\left[-ikS(r,z)\right]\left(\frac{\partial S(r,z)}{\partial r}\right)^2 -$$

$$2ikExp\left[-ikS(r,z)\right]\frac{\partial S(r,z)}{\partial r}\frac{\partial A_{0p}}{\partial r} + Exp\left[-ikS(r,z)\right]\frac{\partial^2 A_{0p}}{\partial r^2}$$

Now differentiating equation (8.8) w. r. t. 'z',

$$\frac{\partial A(r,z)}{\partial z} = -ikA_{0p}Exp\left[-ikS(r,z)\right]\frac{\partial S(r,z)}{\partial z} + Exp\left[-ikS(r,z)\right]\frac{\partial A_{0p}}{\partial z}$$

Thus equation (8.7) becomes,

$$2ik\left(-ikA_{0p}Exp\left[-ikS(r,z)\right]\frac{\partial S(r,z)}{\partial z} + Exp\left[-ikS(r,z)\right]\frac{\partial A_{0p}}{\partial z}\right)$$

$$= -ikA_{0p}Exp\left[-ikS(r,z)\right]\frac{\partial^2 S(r,z)}{\partial r^2} - k^2 A_{0p}Exp\left[-ikS(r,z)\right]\left(\frac{\partial S(r,z)}{\partial r}\right)^2$$

$$-2ikExp\left[-ikS(r,z)\right]\frac{\partial S(r,z)}{\partial r}\frac{\partial A_{0p}}{\partial r} + Exp\left[-ikS(r,z)\right]\frac{\partial^2 A_{0p}}{\partial r^2}$$

$$-i\frac{kA_{0p}}{r}Exp\left[-ikS(r,z)\right]\frac{\partial S(r,z)}{\partial r} + Exp\left[-ikS(r,z)\right]\frac{1}{r}\frac{\partial A_{0p}}{\partial r}$$

$$+\frac{k^2 A_{0p}\phi\left(A_{0p}^2\right)}{\varepsilon_0}Exp\left[-ikS(r,z)\right]$$

$$2k^2 A_{0p}\frac{\partial S(r,z)}{\partial z} + 2ik\frac{\partial A_{0p}}{\partial z} = -ikA_{0p}\frac{\partial^2 S(r,z)}{\partial r^2} - k^2 A_{0p}\left(\frac{\partial S(r,z)}{\partial r}\right)^2$$

$$-2ik\frac{\partial S(r,z)}{\partial r}\frac{\partial A_{0p}}{\partial r} + \frac{\partial^2 A_{0p}}{\partial r^2} - i\frac{kA_{0p}}{r}\frac{\partial S(r,z)}{\partial r} + \frac{1}{r}\frac{\partial A_{0p}}{\partial r} + \frac{k^2 A_{0p}\phi\left(A_{0p}^2\right)}{\varepsilon_0}$$

$$\frac{\partial^2 A_{0p}}{\partial r^2} + \frac{k^2 A_{0p}\phi\left(A_{0p}^2\right)}{\varepsilon_0} - k^2 A_{0p}\left(\frac{\partial S(r,z)}{\partial r}\right)^2 - ik\left(A_{0p}\frac{\partial^2 S(r,z)}{\partial r^2} + 2\frac{\partial S(r,z)}{\partial r}\frac{\partial A_{0p}}{\partial r}\right) =$$

$$2k^2 A_{0p}\frac{\partial S(r,z)}{\partial z} + 2ik\frac{\partial A_{0p}}{\partial z} + i\frac{kA_{0p}}{r}\frac{\partial S(r,z)}{\partial r} - \frac{1}{r}\frac{\partial A_{0p}}{\partial r} \qquad \text{... (8.9)}$$

Comparing real and imaginary parts of equation (8.9), we get

Real part equation is

$$\frac{\partial^2 A_{0p}}{\partial r^2} + \frac{k^2 A_{0p}\phi\left(A_{0p}^2\right)}{\varepsilon_0} - k^2 A_{0p}\left(\frac{\partial S(r,z)}{\partial r}\right)^2 = 2k^2 A_{0p}\frac{\partial S(r,z)}{\partial z} - \frac{1}{r}\frac{\partial A_{0p}}{\partial r}$$

$$2\frac{\partial S(r,z)}{\partial z}+\left(\frac{\partial S(r,z)}{\partial r}\right)^2=\frac{1}{k^2}\left[\frac{1}{2A_{0p}^2}\frac{\partial^2 A_{0p}^2}{\partial r^2}-\frac{1}{4A_{0p}^4}\left(\frac{\partial A_{0p}^2}{\partial r}\right)^2+\frac{1}{2A_{0p}^2 r}\frac{\partial A_{0p}^2}{\partial r}\right]+\frac{\phi\left(A_{0p}^2\right)}{\varepsilon_0}$$

… (8.10)

Imaginary part equation is

$$-k\left(A_{0p}\frac{\partial^2 S(r,z)}{\partial r^2}-2\frac{\partial S(r,z)}{\partial r}\frac{\partial A_{0p}}{\partial r}\right)=2k\frac{\partial A_{0p}}{\partial z}+\frac{kA_{0p}}{r}\frac{\partial S(r,z)}{\partial r}$$

$$2\frac{\partial A_{0p}}{\partial z}+\frac{A_{0p}}{r}\frac{\partial S(r,z)}{\partial r}+A_{0p}\frac{\partial^2 S(r,z)}{\partial r^2}+2\frac{\partial S(r,z)}{\partial r}\frac{\partial A_{0p}}{\partial r}=0$$

Multiplying by A_{0p}

$$2A_{0p}\frac{\partial A_{0p}}{\partial z}+\frac{A_{0p}^2}{r}\frac{\partial S(r,z)}{\partial r}+A_{0p}^2\frac{\partial^2 S(r,z)}{\partial r^2}+2A_{0p}\frac{\partial S(r,z)}{\partial r}\frac{\partial A_{0p}}{\partial r}=0$$

$$\frac{\partial A_{0p}^2}{\partial z}+\frac{\partial S(r,z)}{\partial r}\frac{\partial A_{0p}^2}{\partial r}+A_{0p}^2\left[\frac{\partial^2 S(r,z)}{\partial r^2}+\frac{1}{r}\frac{\partial S(r,z)}{\partial r}\right]=0 \qquad \text{… (8.11)}$$

For initially cosh-Gaussian beam, the solution of equation (8.10) and (8.11) are of the form

$$A_{0p}^2=\frac{E_0^2}{f^2(z)}Exp\left[\frac{b^2}{2}\right]$$

$$\left\{Exp\left[-2\left(\frac{r}{r_0 f(z)}+\frac{b}{2}\right)\right]+Exp\left[-2\left(\frac{r}{r_0 f(z)}-\frac{b}{2}\right)\right]+2Exp\left[-\left(\frac{2r^2}{r_0^2 f^2(z)}+\frac{b^2}{2}\right)\right]\right\}$$

… (8.12)

And

$$S(r,z)=\frac{r^2}{2}\beta(z)+\varphi(z) \qquad \text{… (8.13)}$$

with, $\beta(z)=(1/f(z))df/dz.$ where $'\varphi(z)'$ is an arbitrary function of $'z'$.

Substituting these values in equation (8.10), we get the equation for beam width parameter given as,

$$\frac{d^2 f(z)}{d\xi^2}=\frac{\left(4-4b^2\right)}{f^3(z)}-\left(\frac{r_0\omega}{c}\right)^2\phi\frac{f}{\varepsilon_0} \qquad \text{… (8.14)}$$

Similarly Eq. (8.11) gives the boundary conditions, $\xi = 0,\ f = 1 \text{ and } \left(df/d\xi\right) = 0.$

8.3 RESULTS AND DISCUSSION

The numerical calculations has been done by assuming the following values of various parameters taken as $T = \left(Z_i m/m_i\right)^{1/2} \omega_{pe0} t$, $Z_i = 10$, $\delta = 5\times10^{-2}$, $(4\pi/3) n_c r_{c0}^3 \left(\omega r_0/c\right)^2 = 0.5\left(eA_0\right)/\left(m\omega^2 r_{c0}\sqrt{3\delta}\right) = 1$ and $\omega_{pe0}/\omega = 6$. Figure 8.1 represents the variation of beam width parameter with normalized propagation distance at different values of decentered parameter in clusters with normalized time $T = 60$ for argon clusters with $Z_i = 10$. From figure 8.1, it is clear that for higher values of decentered parameter the focusing ability of the laser beam is enhanced. For $b = 0,$ the cosh-Gaussian laser beam propagating through a gas embedded with clusters diverges at normalized time $T = 60,$ corresponds to $t = 400\ fs$. Thus cosh-Gaussian laser beam defocuses in the absence of decentered parameter. For $b = 1,$ the cosh-Gaussian laser beam propagating through a chosen medium converges at normalized time $T = 60$ and for $b = 2,$ there is strong and early self-focusing of cosh-Gaussian laser beam propagating through a gas embedded with clusters at normalized time $T = 60$. The result obtained indicates that early and strong self-focusing of laser beam occurs for $b = 2$ at normalized time $T = 60$.

Figure 8.2 represents the variation of beam width parameter with normalized propagation distance at decentered parameter $b = 1,$ for normalized time $T = 30,\ 45 \text{ and } 60$ corresponding to $t = 200\ fs,\ 300\ fs$ and $400\ fs$ respectively in clusters with other parameters taken as in Figure 8.1. It is clear from the plot that early in time the cosh-Gaussian beam converges feebly and later in time it converges strongly earlier with normalized propagation distance. For $t = 400\ fs,$ the beam width parameter (f) decreases due to dominance of self-focusing term over the diffraction term in Eq. (14). Previously, Liu and Parashar [119] and Parashar [117] have studied the variation of beam width parameter with normalized distance for $T = 0,\ 20 \text{ and } 60$. The result presented in this paper agrees the results reported earlier by Liu and Parashar [119] and Parashar [117].

Figure 8.3 depicts the variation of beam width parameter with normalized propagation distance for different values of relative density parameter (ω_{pe0}/ω) for decentered parameter $b=1$ at $T=60$. The other parameters are taken to be same as that in Figure 8.1. It is obvious from Figure 8.3 that for relative density parameter $\omega_{pe0}/\omega=5.0$, cosh-Gaussian beam converges at normalized propagation distance $\xi=0.24$, but in this case there is only about 10% reduction in the spot size of the incident laser beam. However, for $\omega_{pe0}/\omega=6.0$, cosh-Gaussian beam converges strongly at normalized propagation distance $\xi=1.12$ and in this case there is about 51% reduction in the spot size of the incident laser beam is seen. Thus with the increase in value of relative density parameter spot size shrinks and self-focusing becomes strong.

8.4 CONCLUSION

The cosh-Gaussian laser beam propagating through a gas embedded with clusters converts the clusters into plasma balls. These plasma balls expand rapidly under Coulomb explosion and hydrodynamic expansion and due to this expansion various processes occur like self-focusing of laser beam, production of energetic neutrons etc. We have studied the self-focusing effect by applying Wentzel-Kramers-Brillouin (WKB) approximation and Paraxial approximation. It is observed that cosh-Gaussian laser beam propagating into the selected medium converges strongly for $b=2,$ at normalized time $T=60$. However, in the absence of decentered parameter, laser beam diverges. Further, it is observed that for early in time diffraction term dominates over self-focusing at decentered parameter $b=1$. However, for $t=400\,fs,$ strong self- focusing of cosh-Gaussian laser beam has been observed due to dominance of self-focusing effect over diffraction. The present study might be very useful in the applications like the generation of inertial fusion energy driven by lasers, laser driven accelerators etc.

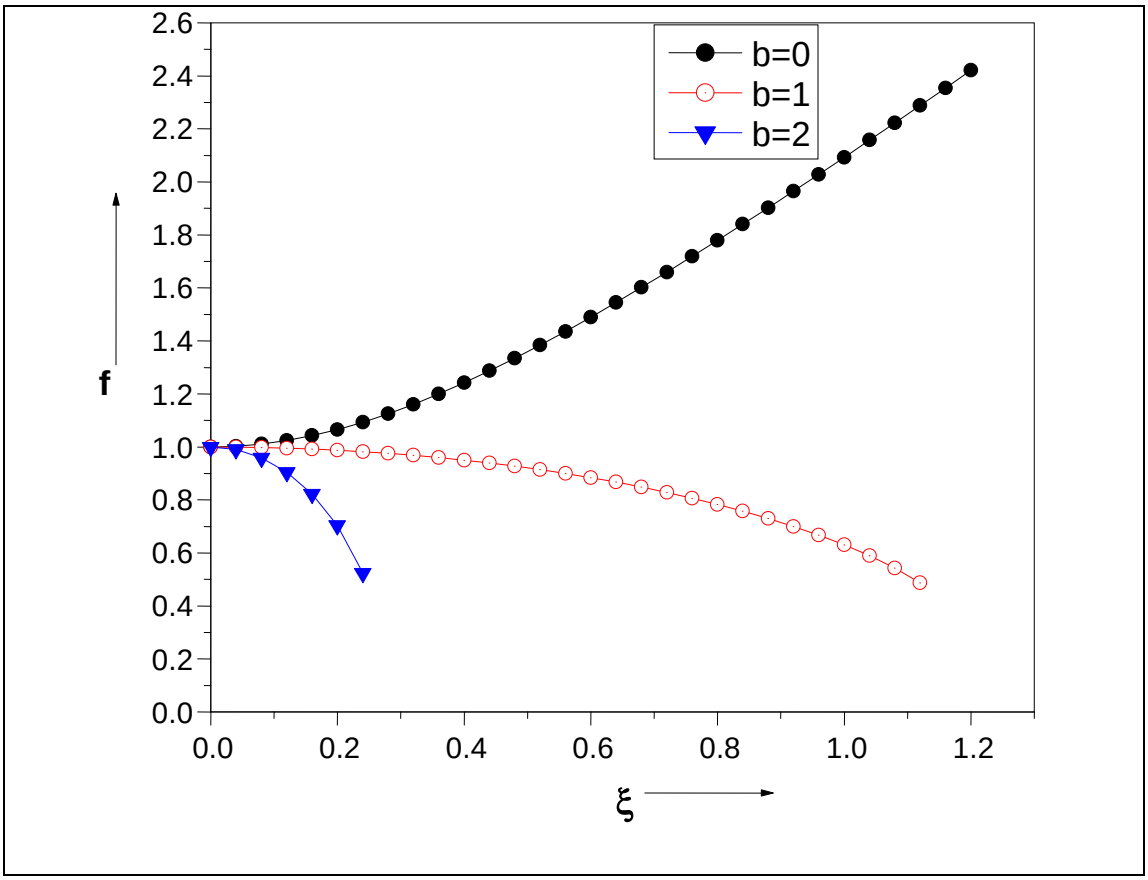

Figure 8.1: Variation of beam width parameter with normalized propagation distance at different values of decentered parameter. The other parameters are taken as $\omega_{pe0}/\omega = 6$, $\delta = 5\times10^{-2}$, $Z_i = 10$, $T = 60$, $(4\pi/3)n_c r_{c0}^3(\omega r_0/c)^2 = 0.5$, $(eA_0)/(m\omega^2 r_{c0}\sqrt{3\delta}) = 1$.

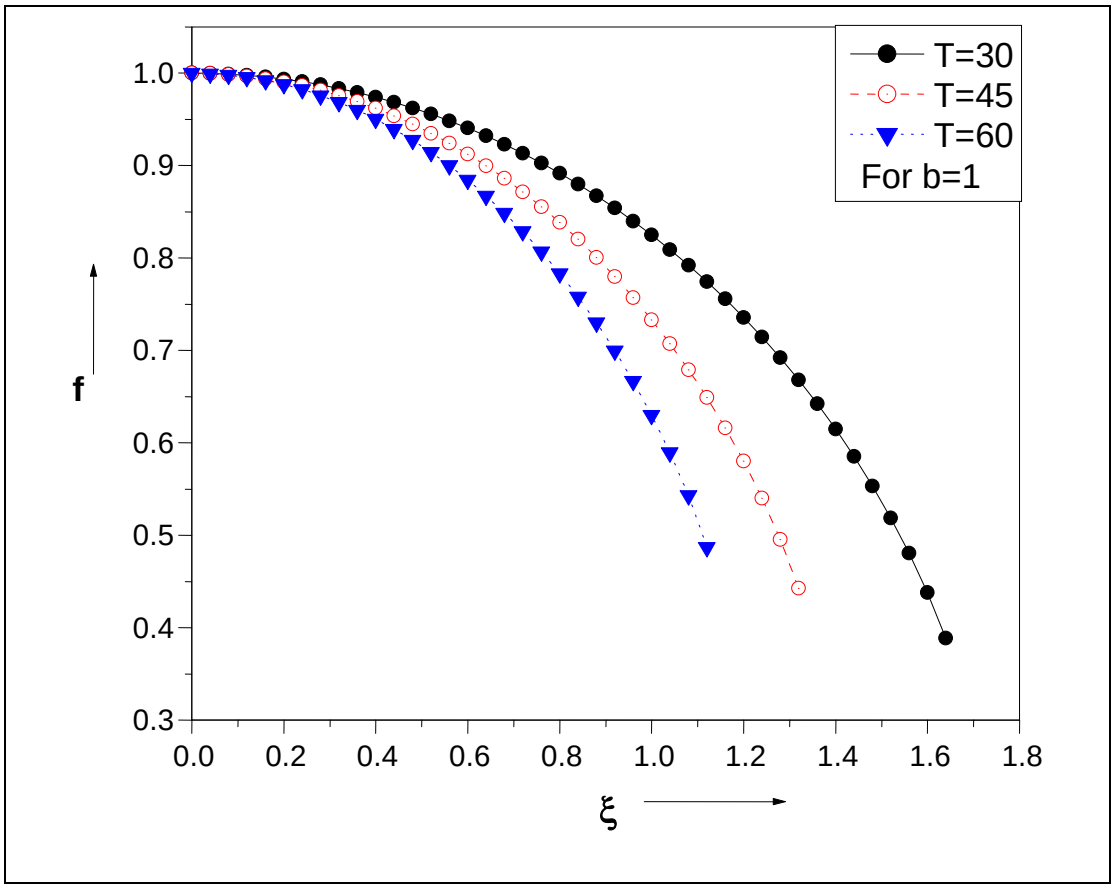

Figure 8.2: Variation of beam width parameter with normalized propagation distance at different values of normalized time T . The other parameters are taken as $\delta = 5\times10^{-2}$, $Z_i = 10$, $(4\pi/3)n_c r_{c0}^3(\omega r_0/c)^2 = 0.5$, $(eA_0)/\left(m\omega^2 r_{c0}\sqrt{3\delta}\right)=1$, $\omega_{pe0}/\omega = 6$.

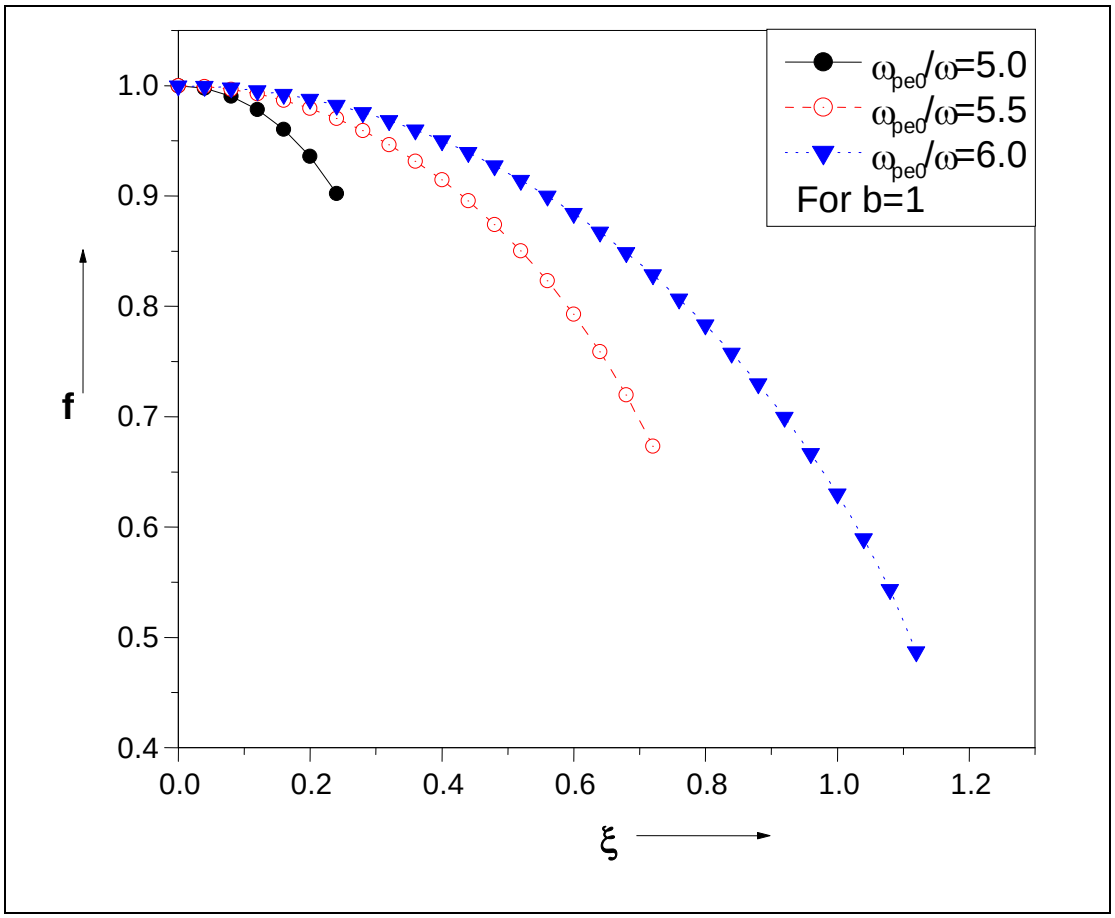

Figure 8.3: Variation of beam width parameter with normalized propagation distance at different values of relative density parameter (ω_{pe0}/ω). The other parameters are taken as T=60, $\delta = 5\times10^{-2}$, $Z_i = 10$, $(4\pi/3)n_c r_{c0}^3(\omega r_0/c)^2 = 0.5$ **and** $(eA_0)/\left(m\omega^2 r_{c0}\sqrt{3\delta}\right)=1$.

CHAPTER-9

BIBLIOGRAPHY

[1] Askaryan, G. A., (1962), "Effects of the gradient of strong electromagnetic beam on electrons and atoms", Sov. Phys. JETP, **15**, 1088-1090

[2] Hora, H., (1969), "Self-focusing of laser beams in a plasma by ponderomotive forces", Z. Physik. **226**, 156-159.

[3] Siegrist, M. R., (1976), "Self focusing in plasma due to ponderomotive forces and relativistic effects", Opt. Commun. **16**, 402-407.

[4] Sodha, M. S., Ghatak, A. K., Tripathi, V. K., "Self-focusing of laser beams", Tata-McGraw-Hill, New Delhi, 1974.

[5] Ditmire, T., Donnelly, T., Rubenchik, A. M., Falcone, R. W., Perry, M. D., (1996), "Interaction of intense laser pulses with atomic clusters", Phys. Rev. A **53**, 3379-3402.

[6] Alexeev, I., Antonsen, T. M., Kim, K. Y., Milchberg, H. M., (2003), "Self-focusing of intense laser pulses in a clustered gas", Phys Rev. Lett. **90**, 103402-1-4.

[7] Ashkin, A., Dziedzic, J. M., (1973), "Radiation pressure on a free liquid surface", Phys Rev. Lett. **30**, 139-142.

[8] Faure, J., Glinec, Y., Pukhov, A., Kiselev, S., Gordienko, S., Lefebvre, E., Rousseau, J. P., Burgy F., Malka, V., (2004), "A laser plasma accelerator producing mono energetic electron beams", Nature **431**, 541–544.

[9] Yang, X., Miley, G. H., Flippo, K. A., Hora, H., (2011), "Energy enhancement for deuteron beam fast ignition of a precompressed inertial confinement fusion target", Phys. Plasmas **18**, 032703-1-7.

[10] Yazdani, E., Cang, Y., Sadighi-Bonabi, R., Hora, H., Osman, F.,(2009), "Layers from initial rayleigh density profile by directed nonlinear force driven plasma blocks for alternative fast ignition", Laser Part. Beams **27**, 149-156.

[11] Brueckner, K. A., Jorna, S.,(1974), "Laser driven fusion", Rev. Mod. Phys. **46**, 325-367. [12]Sadighi-Bonabi, R., Navid, H. A., Zobdeh, P.,(2009), "Observation of quasi mono-energetic electron bunches in the new ellipsoid cavity model", Laser Part. Beams **27**, 223–231.

[13] Banerjee, S., Valenzuela, A. R., Shah, R. C., Maksimchuk, A., Umstadter, D., (2002) "High harmonic generation in relativistic laser plasma interaction," Phys. Plasmas **9**, 2393–2398.

[14] Gill, T. S., Mahajan R., Kaur, R., (2011), "Self-focusing of cosh-Gaussian laser beam in a plasma with weakly relativistic and ponderomotive regime", Phys. Plasmas, **18**, 033110-1-8.

[15] Kant, N., Wani, M. A., Kumar, A., (2012), "Self-focusing of Hermite-Gaussian laser beams in plasma under plasma density ramp", Optics Commun. **285**, 4483-4487

[16] Belafhal, A., Ibnchaikh,(2000), "Propagation properties of Hermite-cosh-Gaussian laser beams", Opt. Commun. **186**, 269-276.

[17] Patil, S. D., Takale, M. V., Dongare, M. B.,(2008), "Propagation of Hermite-cosh-Gaussian laser beams in n-InSb", Opt. Commun. **281**, 4776-4779.

[18] Patil, S., Takale, M., Fulari, V., Dongare, M.,(2008), "Propagation of Hermite-cosh-Gaussian laser beams in non-degenerate germanium having space charge neutrality", J. Mod. Opt. **55**, 3529-3535.

[19] Hagena, O.F., Obert, W., (1972), "Cluster formation in expanding supersonic jets effect of pressure, temperature, nozzle size, and test gas", J. Chem. Phys. **56**, 1793-1802.

[20] Ditmire, T., Smith, R. A., Tisch, J.W.G., (1997), "High intensity laser absorption by gases of atomic clusters", Phys. Rev. Letts., **78,** 3121-3124.

[21] Kim, K.Y., Alexeev, I., Kumarappan, V., Parra, E., Antonsen, T., Taguchi1, T., Gupta, A., Milchberg, H. M., (2004), "Gases of exploding laser-heated cluster nanoplasmas as a nonlinear optical medium", Phys. Plasmas, **11**, 2882-2889.

[22] Ditmire, T., Donnelly, T., Falcone, R. W., Perry, M. D., (1995), "Strong X-Ray-Emission from High-Temperature Plasmas Produced by Intense Irradiation of Clusters", Phys. Rev. Letts., **75**, 3122-3125.

[23] Feng, J., Richardson, C. M., Shimkaveg, G. M., (1995), "Characterization of a laser plasma water droplet EUV source", SPIE.

[24] Glenn, D. K., Luis, J. B., Kevin, D. K., Sweatt, W. C., (1999),"Scale-up of a cluster jet laser plasma source for extreme ultraviolet lithography", SPIE.

[25] Parra, E., Alexeev, I., Fan, J., Kim, K. Y., McNaught, S. J., Milchberg, H. M., (2000), "X- ray and extreme ultraviolet emission induced by variable pulse-width irradiation of Ar and Kr clusters and droplets", Phys. Rev. E **62**, 5931-5934.

[26] Mori, M., Shiraishi, T., Takahashi, E., Suzuki, H., Sharma, L. B., Miura, E., Kondo, K., (2001), "Extreme ultraviolet emission from Xe clusters excited by high-intensity lasers", J. Appl. Phys., **90**, 3595-3601.

[27] Ter-Avetisyan, S., Schnurer, M., Stiel, H., Vogt, U., Radloff, W., Karpov, W., Sandner, W., Nickles, P. V., (2001), "Absolute extreme ultraviolet yield from femtosecond-laser-excited Xe clusters", Phys. Rev. E **64**, 036404.

[28] Zachary, H.L., Andrew, R. K., Sean, P. F., Ian, M., Markus, K., (1999), "Tomographic reconstruction of an integrated circuit interconnect", Appl. Phys. Letts., **74**, 150-152.

[29] Ditmire, T., Zweiback, J., Yanovsky, V.P., (1999), "Nuclear fusion from explosions of femtosecond laser-heated deuterium clusters", Nature, **398**, 489-492.

[30] Shao, Y.L., Ditmire, T., Tisch, J. W. G., Springate, E., Marangos, J. P., Hutchinson, M. H. R., (1996), "Multi-keV electron generation in the interaction of intense laser pulses with Xe clusters", Phys. Rev. Letts., **77**, 3343-3346.

[31] Fourkal, E., Li, J.S., Xiong, W., Nahum, A., Ma, C. M., (2003), "Intensity modulated radiation therapy using laser accelerated protons: a Monte Carlo dosimetric study", Phys. Med. and Bio., **48**, 3977-4000.

[32] Donnelly, T. D., Ditmire, T., Neuman, K., Perry, M. D., Falcone, R. W., (1996), "High-order harmonic generation in atom clusters", Phys. Rev. Letts.", **76**, 2472-2475.

[33] Alexeev, I., Antonsen, T. M., Kim, K. Y., Milchberg, H. M., (2003), "Self-focusing of intense laser pulses in a clustered gas", Phys. Rev. Letts., **90**, 103402.

[34] Zweiback, J., Smith, R. A., Cowan, T. E., Hays, G., Wharton K. B., Yanovsky, V. P., Ditmire, T., (2000), "Nuclear fusion driven by Coulomb explosions of large deuterium clusters" Phys. Rev. Letts. **84**, 2634-2637.

[35] Liu, C. S., Tripathi, V. K., (2003), "Ion Coulomb explosion of clusters by a Gaussian laser beam" Phys. Plasmas **10**, 4085-4089.

[36] Zweiback J, Ditmire, T., Perry, M. D., (2000), "Resonance in scattering and absorption from large noble gas clusters", Opt. Express, **6**, 236-242.

[37] Zweiback, J., Ditmire, T., (2001), "Femtosecond laser energy deposition in strongly absorbing cluster gases diagnosed by blast wave trajectory analysis", phys. Plasmas **8**, 4545.

[38] Ditmire T., (1997), "Atomic clusters in ultrahigh intensity light fields", Contemp. Phys. **38**, 315-328.

[39] Litvak A. G., (1970), "Finite-amplitude wave beams in a magnetoactive plasma", Sov. Phys. JETP, **30**, 344-347.

[40] Sodha, M. S., Tewari, D. P., Ghatak, A. K., Kamal, J., Tripathi, V. K., (1971), "Self-focusing of laser beams in inhomogeneous dielectrics", Opto. Elect., **3**, 157-161.

[41] Askar'yan, G. A., (1973), "Self-focusing effect", Sov. Phys. Usp., **15**, 517-518.

[42] Sodha, M. S., Khanna, R. K., Tripathi, V. K., (1973), "Self-focusing of a laser beam in a strongly ionized plasma", Opto. Elect., **5**, 533-538.

[43] Sodha, M. S., Nayyar, V. P., Tripathi, V. K., (1974), "Asymmetric focusing of a laser beam in TEM_{01} doughnut mode in a nonlinear dielectric", Opt. Soc. Am. **64**, 941-943.

[44] Sodha, M. S., Prasad, S., Tripathi, V. K., (1974), "Nonstationary Self-focusing of a Gaussian pulse in a plasma", J. Appl. Phys. **46**, 637-642.

[45] Sodha, M. S., Nayyar, V. P., (1975), "Thermal self-focusing of TEM_{01} laser beams and ring-shape self-focusing of two specific mixtures of modes", Opt. Soc. Am. **65**, 1027-1030.

[46] Nayyar, V. P., (1978), "Self-focusing of a non-Gaussian laser mode in a dense plasma", J. Appl. Phys., **49**, 1114-1118.

[47] Nayyar, V. P., Soni, V. S., (1979), "Self-focusing and self-defocusing of elliptically shaped Gaussian laser beams in Plasmas", J. Phys. D: Appl. Phys. **12**, 239-247.

[48] Askar'yan, G. A, Mukhamadzhanov, M. A., (1981), "Nonlinear defocusing of a focused beam: a fine beam from the focus", JETP Letts. **33**, 44-48.

[49] Hagena O. F., (1981), "Nucleation and growth of clusters in expanding nozzle flows", Surf. Sci. **106**, 101-116.

[50] Mori, W. B., Joshi, C., Dawson, J. M., Forslund, D. W., Kindel, J. M., (1988), "Evolution of self-focusing of intense electromagnetic waves in plasma", Phys. Rev. Letts. **60**, 1298-1301.

[51] Kurki-Suonio, T., Morrison, P. J., Tajima, T. (1989), "Self-focusing of an optical beam in a plasma", Phys. Rev. A, **40**, 3230-3239.

[52] Cicchitelli, L., Hora, H., Postle, R., (1990), "Longitudinal field components for laser beams in Vacuum", Phys. Rev. A **41**, 3727-3732.

[53] Brandi, H. S., Manus, C., Mainfray, G., Lehner, T., Bonnaud, G., (1993), "Relativistic and Ponderomotive self-focusing of a laser beam in a radially inhomogeneous plasma I. Paraxial approximation", Phys. Fluids B, **5**, 3539-3550.

[54] Chen, X. L., Sudan, R. N., (1993), "Two dimensional self-focusing of short intense laser pulse in underdense plasma", Phys. Fluids B **5,** 1336-1348.

[55] Chen, X. L., Sudan, R. N., (1993), "Necessary and sufficient conditions for self-focusing of short ultra intense laser pulse in underdense plasma", Phys. Rev. Letts. **70**, 2082-2085.

[56] Bulanov, S. V., Pegoraro, F., Pukhov, A. M., (1995), "Two dimensional regimes of self-focusing, wake field generation and induced focusing of a short intense laser pulse in an underdense plasma", Phys. Rev. Letts.**74**, 710-713.

[57] Gibbon, P., Jakober, F., Monot, P., Auguste, T., (1996), "Experimental study of relativistic self-focusing and self-channeling of an intense laser pulse in an underdense plasma", IEEE Trans. Plasma Sci. **24**, 343-350.

[58] Asthana M. V., Vershney D., Sodha M. S. (2000), "Relativistic self-focusing of transmitted laser radiation in plasmas", Laser Part. Beams, **18**, 101-107.

[59] Hafizi, B., Ting, A., Sprangle, P., Hubbard, R. F., (2000), "Relativistic focusing and Ponderomotive channeling of intense laser beams," Phys. Rev. E, **62**, 4120-4125.

[60] Liu, C. S., Tripathi, V.K., (2000), "Laser frequency upshift, self-defocusing, and ring formation in tunnel ionizing gases and plasmas", Phys. Plasmas, **7**, 4360-4363.

[61] Osman, F., Castillo, R., Hora, H., (2000), "Numerical programming of self-focusing at laser-plasma interaction", Laser Part. Beams **18**, 59-72.

[62] Springate E., Hay N., Tisch J. W. G., Mason M. B., Ditmire T., Marangos J. P., Hutchinson, M. H. R.,(2000) "Enhanced explosion of atomic clusters irradiated by a sequence of two high-intensity laser pulses", Phys. Rev. A, **61**, 044101-1-4

[63] Feit, M. D., Komashko, A. M., Rubenchik, A. M., (2001), "Relativistic self-focusing in underdense plasma", Phys. D **152-153**,705-713.

[64] Krainov V. P., Smirnov, M. B., (2002), "Cluster beams in the super-intense femtosecond laser pulse", Phys. Reports **370**, 237-331.

[65] Zweiback, J., Cowan, T. E., Hartley, J. H., Howell, R., Wharton, K. B., Crane, J. K., Yanovsky, V. P., Hays, G., Smith, R. A., Ditmire, T., (2002), "Detailed study of nuclear fusion from femtosecond laser-driven explosions of deuterium clusters", Phys. Plasmas **9**, 3108-3120.

[66] Weaver, J. L., Feldman, U., Mostovych, A. N., Seely, J. F., Colombant, D., Holland, G., (2003), "Soft x-ray emission from postpulse expanding laser-produced plasmas", Rev. Scientific Instruments **74**, 5076-5083.

[67] Zharova, N. A., Litvak, A. G., Mironov, V. A., (2003), "Self-focusing of laser radiation in cluster plasma", JETP Letters **78,** 619-623.

[68] Issac, R. C., Vieux, G., Ersfeld, B., Brunetti, E., Jamison, S. P., Gallacher, J., Clark, D., Jaroszynski, D. A., (2004), "Ultra hard x rays from krypton clusters heated by intense laser fields", Phys. Plasmas **11**, 3491-3496.

[69] Jha, P., Wadhwani, N., Raj, G., Upadhyaya, A. K., (2004), "Relativistic and ponderomotive effects on laser plasma interaction dynamics", Phys. Plasmas, **11**, 1834-1839.

[70] Kant, N., Sharma, A. K., (2004), "Resonant second-harmonic generation of a short pulse laser in a plasma channel", J. Phys. D: Appl. Phys. **37**, 2395-2398.

[71] Sharma, A., Verma, M. P., Sodha, M. S., (2004), "Self-focusing of electromagnetic beams in collisional plasmas with nonlinear absorption", Phys. Plasmas, **11**, 4275-4279.

[72] Kant, N., Sharma, A. K., (2005), "Capillary plasma formation by a laser", Phys. Scripta. **71**, 402-405.

[73] Prakash, G., Sharma, A., Verma, M. P., Sodha, M. S., (2005), "Focusing of an intense Gaussian laser beam in a radially inhomogeneous medium", J. Opt. Soc. Am. B, **22**, 1268-1275.

[74] Varshney, M., Qureshi, K. A., Varshney, D., (2005), "Relativistic self-focusing of a laser beam in an inhomogeneous plasma", J. Plasma Phys. **72**, 195-203.

[75] Kumar, N., Tripathi, V. K., (2006), "Non-paraxial theory of self-focusing/defocusing of a laser pulse in a multiple-ionizing gas", Appl. Phys. B **82,** 53-58.

[76] Sodha, M. S., Sharma, A., (2006), "Mutual focusing/defocusing of Gaussian electromagnetic beams in collisional plasma", Phys. Plasmas, **13,** 053105-1

[77] Gupta, D. N., Hur, M. S., Hwang, I., Suk, H., Sharma, A. K., (2007), "Plasma density ramp for relativistic self-focusing of an intense laser", J. Opt. Soc. Am. B **24,** 1155-1159.

[78] Gupta, D. N., Hur, M. S., Suk, H., (2007), "Additional focusing of a high-intensity laser beam in a plasma with a density ramp and a magnetic field", Appl. Phys. Letts. **91,** 081505-1-3

[79] Jung, Y., Murakami, I., (2009), "Quantum effects on magnetization due to ponderomotive force in cold quantum plasmas", Phys. Lett. A **373,** 969-971.

[80] Patil, S.D., Navare, S.T., Takale, M.V., Dongare, M. B., (2009), "Self-focusing of Cosh-Gaussian laser beams in parabolic medium with linear absorption", Opt. Lasers Engg. **47**, 604-606.

[81] Patil, S. D., Takale, M. V., Navare, S. T., Dongare, M. B., (2010) "Focusing of Hermite-cosh-Gaussian laser beams in collisionless magnetoplasma", Laser Part. Beams **28**, 343-349.

[82] Singh, A., Walia, K., (2010), "Relativistic self-focusing and self-channeling of Gaussian laser beam in plasma", Appl. Phys. B **101**, 617-622.

[83] Xiong, H., Liu, S., Liao, J., Liu, X., (2010), "Self-focusing of laser pulse propagating in magnetized plasma", Optik Int. J. Light Electron Opt. **121**, 1680-1683.

[84] Gill, T. S., Kaur, R., Mahajan, R., (2011), "Relativistic self-focusing and self-phase modulation of cosh-Gaussian laser beam in magnetoplasma", Laser Part. Beams **29**, 183-191.

[85] Kant, N., Saralch, S., Singh, H.,(2011), "Ponderomotive self-focusing of a short laser pulse under a plasma density ramp", Nukleonika **56**, 149-153.

[86] Kim, J., Kim, G. J., Yoo S. H., (2011), "Energy enhancement using an upward density ramp in laser wakefield acceleration", J. Korean Phys. Soc. **59**, 3166-3170.

[87] Kant, N., Wani, M. A., Kumar, A., (2012), "Self-focusing of Hermite-Gaussian laser beams in plasma under plasma density ramp," Opt. Comm. **285**, 4483-4487.

[88] Hora, H., (1975), "Theory of relativistic self-focusing of laser radiation in plasmas", J. Opt. Soc. Am. **65**, 882-886.

[89] Jones, D. A., Kane, E. L., Lalousis, P., Wiles, P., Hora, H., (1982), "Density Modification and energeticion production at relativistic self-focusing of laser beam in plasmas", Phys. Fluids **25**, 2295.

[90] Akhmanov, S. A., Sukhorukov, A. P., Khokhlov, R. V., (1968), "Self-focusing and diffraction of light in a nonlinear medium", Sov. Phys. Usp. 10, 609-636.

[91] Patil, S. D., Takale, M. V., Navare, S. T., Fulari, V.J., Dongare, M. B.,(2011), "Relativistic self-focusing of cosh-Gaussian laser beams in a plasma", Opt. Laser Tech. **44**, 314-317.

[92] Gill, T. S., Saini, N.S., Kaul, S.S., Singh, A., (2004), "Propagation of ellipitic Gaussian laser beam in a higher order non-linear medium", Optik, **115**, 493-498.

[93] Johannisson, P., Anderson, D., Lisak, M., Marklund, M., (2003), "Nonlinear Bessel beams", Opt. Commun., **222**, 107-115.

[94] Thakur, A., Berakdar, J.,(2010), "Self-focusing and defocusing oftwisted light in non linear media", Opt Express, **18**, 27691-27696.

[95] Nanda, V., Kant, N., Wani, M. A., (2013), "Sensitiveness of decentered parameter for relativistic self-focusing of Hermite-cosh-Gaussian laser beam in plasma", IEEE Trans. Plasma Sci. **41**, 2251-2256.

[96] Nanda, V., Kant, N., Wani, M. A., (2013), "Self-focusing of a Hermite-cosh Gaussian laser beam in a magnetoplasma with ramp density profile", Phys. Plasma 20, 113109-1-7.

[97] Hora, H., (2007), "New aspects for fusion energy using inertial con- finement", Laser Part. Beams **25**, 37-45.

[98]Nanda, V., Kant, N., Wani, M. A., (2014), "Enhanced relativistic self-focusing of Hermite-cosh-Gaussian laser beam in plasma under density transition", Phys. Plasma **21**, 042101-1-6.

[99] Konar, S., Mishra, M., Jana, S., (2007), "Nonlinear evolution of cosh-Gaussian laser beams and generation of flat top spatial solitons in cubic quintic nonlinear media" Phys Lett. A, 362, 505-510.

[100] Zhang, Y., Song, Z., Chen, J. Ji, Shi, Z., (2007), "Virtual sources for a cosh-Gaussian beam" Opt. Lett. 32, 292-294.

[101] Shukla, P. K., Eliasson, B., (2010), "Nonlinear aspects of quantum plasma physics", Phys. Usp. 53**, 55-82.**

[102] Misra, A. P., Bhowmik, C., (2007), "Nonplanar ion-acoustic waves in a quantum plasma", Phys. Lett. A **369**, 530-532.

[103] Bergamin, L., Alitalo, P., Tretyakov, S., (2011), "Nonlinear transformation optics and engineering of the Kerr effect", Phys. Rev. B **84**, 205103.

[104] Shpatakovskaya, G., (2006), "Semiclassical model of a one-dimensional quantum dot", J. Exp. Theor. Phys. 102, 466.

[105] Lai, D., (2001), "Matter in strong magnetic fields", Rev. Mod. Phys. **73**, 629.

[106] Harding, A. K., Lai, D., (2006), "Physics of strongly magnetized neutron stars", Rep. Prog. Phys. **69**, 2631.

[107] Ozbay, E., (2006), "Plasmonics: Merging photonics and electronics at nanoscale dimensions", Science **311**, 189-192.

[108] Wei, L., Wang, Y., (2007), "Quantum ion-acoustic waves in single-walled carbon nanotubes studied with a quantum hydrodynamic model", Phys. Rev. B **75**, 193407.

[109] Crouseilles, N., Hervieux, P. A., Manfredi, G., (2008), "Quantum hydrodynamic model for the nonlinear electron dynamics in thin metal films", Phys. Rev. B **78**, 155412.

[110] Andreev, A. V., (2000), "Self-consistent equations for the interaction of an atom with an electromagnetic field of arbitrary intensity", J. Exp. Theor. Phys. Lett. **72**, 238-240.

[111] Chunyang, Z., Zhanjun, L., Shao-ping, Z., Xiantu, H., (2004), "Spontaneous Magnetic field and high harmonics in laser-dense plasma interaction", J. Plasma Fusion Res. Ser. **6**, 333.

[112] Manfredi, G., (2005), "How to model quantum plasmas", Fields. Inst. Commun. **46**, 263-287.

[113] Shukla, P. K., Ali, S., Stenflo, L. Marklund, M., (2006), "Nonlinear wave interactions in quantum magnetoplasmas", Phys. Plasmas 13, 112111.

[114] Patil, S. D., Takale, M. V., Navare, S. T., Dongare, M. B., Fulari, V. J., (2013), "Self-focusing of Gaussian laser beam in relativistic cold quantum plasma", J. Light Elec. Opt. **124**, 180-183.

[115] Habibi, M., Ghamari, F., (2012), "Stationary self-focusing of intense laser beam in cold quantum plasma using ramp density profile", Phys. Plasmas **19**, 103110.

[116] Nanda, V., Kant, N., (2014), "Strong self-focusing of a cosh-Gaussian laser beam in collisionless magneto-plasma under plasma density ramp", Phys. Plasmas **21**, 072111-1-8.

[117] Parashar, J., (2009), "Effect of self-focusing on laser third harmonic generation in a clustered gas", Phys. Scr. **79**, 015501-1-5.

[118] Zharova N. A., Litvak, A. G., Mironov, V. A., (2003), "Self-focusing of laser radiation in cluster plasma", JETP Lett. **78**, 619-623.

[119] Liu, C. S., Parashar, J., (2007), "Laser self-focusing and nonlinear absorption in expanding clusters", IEEE Trans. Plasma Sci. **35**, 1089-1097.

LIST OF PUBLICATIONS

1. Rajput J., Kant N., Singh H., **Nanda V.** (2009), " Resonant third harmonic generation of a short pulse laser in plasma by applying a wiggler magnetic field", *Opt. Comm.* **282**, 4614-4617.
2. **Nanda, V.**, Kant, N., Wani, M. A., (2013), "Sensitiveness of decentered parameter for
   relativistic self-focusing of Hermite-cosh-Gaussian laser beam in plasma", *IEEE Trans. Plasma Sci.* **41**, 2251-2256.
3. **Nanda, V.**, Kant, N., Wani, M. A., (2013), "Self-focusing of a Hermite-cosh Gaussian laser beam in a magnetoplasma with ramp density profile", *Phys. Plasma* 20, 113109-1-7.
4. **Nanda, V.**, Kant, N., Wani, M. A., (2014), "Enhanced relativistic self-focusing of Hermite-cosh-Gaussian laser beam in plasma under density transition", *Phys. Plasma* **21**, 042101-1-6.
5. **Nanda, V.**, Kant, N., (2014), "Strong self-focusing of a cosh-Gaussian laser beam in collisionless magneto-plasma under plasma density ramp", *Phys. Plasmas* **21**, 072111-1-8.
6. Kant N., **Nanda V.**, (2014), "Stronger Self-Focusing of Hermite-Cosh-Gaussian (HChG) Laser Beam in Plasma", *OALib Journal* **1:e681**, 1-8.

CONFERENCES ATTENDED

1. **Nanda V.**, "Effect of density ramp on self-focusing of a hermite-cosh-gaussian laser beam in plasma", QIP/CEP Topical Conference on Laser driven charged particle acceleration and applications, April 5-7, 2013, I.I.T. Delhi, India.
2. **Nanda V.**, "Density profile for relativistic self-focusing of cosh-gaussian laser beam in plasma", DAV National Congress on Science, Technology & Management, November 7-8, 2014, D.A.V.I.E.T. Jalandhar, Punjab, India.
3. **Nanda V**., "Relativistic self-focusing of cosh-gaussian laser beam in plasma" Conference on Exploring Basic and Applied Sciences for next generation frontiers, November 14-15, 2014, L.P.U., Phagwara, Punjab, India.